Collective dynamics in populations with microscopic variability

Silvia de Monte

COLLECTIVE DYNAMICS IN POPULATIONS WITH MICROSCOPIC VARIABILITY

Silvia De Monte

Ph.D. Thesis

Dept. of Physics, The Technical University of Denmark

April 2004

Supervisors:

Erik Mosekilde, Dept. of Physics, The Technical University of Denmark

Antonio Giorgilli, Dept. of Mathematics and Applications, University of Milano Bicocca, Italy

to Marilde Granero and Alfredo Porati
who created a door and left it open

Preface

> ... in an authentic commonplace there is certainly more humanity than in a new discovery.
>
> Robert Musil, *The man without qualities*

One of the characterising features of so-called "complex systems" is that the dynamics of the system is different depending on the level of observation one adopts. The dynamics of biological populations, for example, can be addressed by studying molecular processes, interaction among cells or among individuals. While the properties of one single cell in a population are known in progressively greater detail, the functional role of their ensemble transcends the single-element and is essentially related to the manner these elements communicate with each other. At the level of organisms, one would like the evolutionary dynamics of a population to be funded on some "microscopic" rules for the interaction among individuals.

This thesis approaches the problem of how to connect the single-element to the emergent macroscopic dynamics in the context of globally coupled dynamical systems. In particular, it deals with the effect of microscopic disorder, always present in non-ideal populations, on the regimes where the interaction among elements is strong. It proposes a method for systematically deriving the population dynamics from the microscopic features of the population. Starting from the regime of perfect synchronisation among identical units, disorder is introduced either in the form of parameter mismatch or in that of noise. This approach allows us to account for the observed collective regimes and provides a tool for a parsimonious description of systems with many degrees of freedom.

In the context of evolutionary game theory, this thesis addresses the dynamics of behavioural strategies based on the rules of public goods games. These games describe situations where the interest of the individual contrast with the interest of the group and therefore constitute a prototype for the study of how altruistic behaviour emerged in animal and human societies. Here, we show that allowing optional participation to the game solves the paradox and provides an alternative solution to that of economic stalemate. The analytical model predicts a periodic alternation of the different strategies and the long-term equivalence in the gains of cooperators and defectors.

In the course of my PhD studies I have been supported, helped and taken care by many people, to whom I am deeply grateful for their scientific and human generosity. Their teaching and their presence has been essential in my cultural development, as well as in my growth as a person and as a woman. I would like to be able to thank them properly, but finding appropriate words of acknowledgement goes beyond my literary skills. And since I cannot impose an order of importance in the different reasons why I feel close to these persons, I will thank them in (approximate) order of appearance, as in the movies. Starting from my grandmother Olga, who has gone smiling through a century and whose laughter has always made my thoughts lighter. I am grateful to my parents Laura and Giorgio, who have instilled in me curiosity and wonder, and a certain amount of stubbornness... Together with them, I thank for their constant support all my "extended family": Rita, Giulia and Sandro. I owe to Marilde Granero and Alfredo Porati my fist encounter with physics and mathematical models for biology. As teachers and as friends, they are always close to me. I am grateful to Antonio Giorgilli for having communicated to me his enthusiasm in the study of dynamical systems and for his support during his numerous co-supervisions. When I first followed a lecture by Karl Sigmund, I have been immediately captured by the elegance and synthetic power of evolutionary game theory. Later, I had the great luck of working with him. Together with Christoph Hauert, Joseph Hofbauer and the colleagues at the Institute of Mathematics, he has made my stay in Vienna scientifically enriching and enjoyable at the same time. I am in debt with Erik Mosekilde for the joyful time I spent in Denmark, first as a visitor and then as a PhD student. He has constantly stimulated the progress of my studies and encouraged an independent approach to the scientific problems. I am deeply grateful to him for having let me free of choosing how to organise my work and for guiding my studies without constraining them. I am greatly thankful to Preben Grae Sørensen and Sune Danø for having introduced me to the world of yeast. I have really enjoyed both the theoretical discussions and the bench experience. In particular, I acknowledge their patience in teaching me how to deal with pipettes, couvettes, dilutions and all the rest. The collaboration with Hugues Chaté has been extremely important for my scientific growth. I greatly enjoy working and discussing with him, as well as walking uphill in the morning and drinking a glass of good wine.

Out of the chronological order, I thank especially Francesco d'Ovidio, for his appreciation of my own stupidity, for believing in me also when I do not and for the many experiences we share.

To many friends and colleagues I owe the fact that the PhD experience has been very intense from a cultural and human point of view. Among those who have stand with admirable patience the intermittency of my presence and correspondence, I want to thank in particular: Barbara Trabucchi, my alter-ego in the human sciences; Marianna, Pia and Romolo d'Ovidio; Sergio Rinaldi, Fabio d'Ercole and Alessandra Gragnani at the Politecnico of Milano; Oscar De Feo; Vittorio, Maurizio, Germana, Gege, Elisa e Michele Sapienza; Vanessa Casagrande; Leonhard Shwartz; Anders Bisgård, for having seriously tried to introduce me to the Danish society, and Paddy Krishnaswamy; the collegues of the 'Biophysics

and Complex Systems group' at DTU, and in particular Anders Andersen, Haim Abitan, Olga Sosnovtseva and Victoria, Dan Luciani, Gunnar Cedersund, Sergej Senchenko and Irina Matskiv; Tomas Bohr, Carsten Knudsen and Mogens Samuelson; Gitte Schreier, my official translator from Danish; Netta Cohen and Annette Taylor in Leeds; the participants and lectures at the Complex Systems Summer School 2003 and in particular Mercedes Bleda, Hannelore Brandt, Ille Gebeshuber, Sara Dempster and Yogi Jaeger for the nice chatting in the desert; the people at SPEC in Saclay; François Taddei, his group and their bacteria; Irene Baudry for the life-tasting in Paris; Carolina Brito Carvalho do Santos and Leonardo Gregory Brunnet; the Dept. of Cross-Disciplinary Physics of IMEDEA and in particular Emilio Ernández-García for the kindest hospitality in Palma de Mallorca.

The PhD studies that led to the elaboration of this thesis have been conducted at the Department of Physics of the Technical University of Denmark. They have been financed for one third through a "Borsa di studio per corsi di specializzazione all'estero" (grant for following specialising courses abroad) of the Department of Mathematics, State University of Milano, Italy; for one third by DTU and for one third by the Graduate School in Nonlinear Science.

The PhD studies have been co-supervised by Erik Mosekilde, Department of Physics, DTU and by Antonio Giorgilli, Department of Mathematics and Applications, University of Milano Bicocca, Milano, Italy.

This thesis has led to the publication on international peer-reviewed journals of the following papers:

1. S. Danø, F. Hynne, S. De Monte, F. d'Ovidio, H. Westerhoff and P. G. Sørensen, "Synchronization of glycolitic oscillations in intact yeast cells" *Faraday Discuss.* **120**, 261-275, (2002).

2. S. De Monte and F. d'Ovidio, "Dynamics of order parameters for globally coupled oscillators" *Europhys. Lett.* **58**, 21-27 (2002).

3. C. Hauert, S. De Monte, J. Hofbauer and K. Sigmund "Volunteering as red queen mechanism for cooeration in public goods games" *Science* **296**, 1129-1132 (2002).

4. C. Hauert, S. De Monte, J. Hofbauer and K. Sigmund "Replicator dynamics for optional public good games" *J. Theor. Biol.* **218**, 187-194 (2002).

5. S. De Monte, F. d'Ovidio and E. Mosekilde, "Coherent regimes of globally coupled dynamical systems" *Phys. Rev. Lett.* **90**, 054102(1-4) (2003).

6. S. De Monte, F. d'Ovidio, H. Chaté and E. Mosekilde, "Noise-induced macroscopic bifurcations in globally coupled chaotic units'" *Phys. Rev. Lett.* to appear.

The following paper is in preparation:

7. S. De Monte, F. d'Ovidio, H. Chaté and E. Mosekilde, "Effects of microscopic disorder on the collective dynamics of globally coupled maps".

30 April 2004

Contents

Chapter 1

Introduction

The basic feature of a population is the existence of different levels to which it can be described: a microscopic level, relative to the behaviour of any of its components and a macroscopic level, where the population is considered as a whole and the observables are averaged quantities. The characterisation of how such two levels of description are connected is fundamental in the cases in which experimental measures can be performed only at one level, and the properties of the other have to be deduced. This question is particularly critical when nonlinearities come into play, since no general principle exists for determining how many degrees of freedom, each of which endowed with its own dynamics, give rise to a coordinated effect. In physics, such a problem is faced in statistical mechanics and in fluid dynamics and its solution relies on the existence of physical laws and symmetries that help to select the possible macroscopic outcomes.

In the case of biological populations, even models of the basic microscopic processes possess yet another degree of complexity with respect to physical systems. Indeed, one in general can not rely on first principles or conservation laws. Nonlinear dynamics and bifurcation theory provide with this respect a fundamental tool for studying the behaviour in time of dissipative systems. Indeed, by enquiring about the qualitative dynamical features of complex systems, one can infer important properties of their structure without the immediate need of an often overwhelmingly complicated model of biological detail.

In addressing the dynamics of ensembles of biological units, however, one is faced with the additional problem of the existence of several description levels whose time and space scales are often not neatly separated. This features, together with the approximations introduced in modelling the microscopic elements, result in a structural difficulty of assessing the degree of accuracy of any mathematical description of the units composing the population. From the modelling point of view, this can be interpreted as the presence of variability or disorder at the microscopic level.

The fact that a population consists of more than one, and often many, elements induces us to describe it it in terms of statistics -averaged variables, such as mean

value or relative frequencies- and thus to focus on the emergent collective dynamics rather than on the behaviour of each microscopic component.

The bottom-up connection between two such levels of description, that provides the high-level behaviour in terms of the single-element features is a central problem both from a theoretical point of view, in the definition of models for population dynamics, and from an empirical one, in their experimental validation. On the other hand, it frequently happens that measurements on a biological population are unfeasible at the level of a single individual, or that they require different and perhaps much more advanced techniques than the recording of an average value. In this case, a top-down approach might tell what classes of microscopic behaviour are compatible with an observed collective dynamics and what features of the bottom structure play the role of parameters at the macroscopic level.

Chapters 2 and 8 of this thesis present two modelling approaches to population dynamics and overview the main results so far established, providing some examples of populations for which the relation between single-element and collective behaviour is of theoretical and practical relevance.

Two commonly used mathematical approaches aimed at connecting "micro" to "macro" are either viewing the population as a set of interacting units possessing a defined dynamics, or group the elements into classes whose relations are derived according to some microscopic rule. Both viewpoints aim at providing a low-dimensional representation of the dynamics of a system that has inherently a large number of "natural" degrees of freedom. In the first approach, each element of the population (a cell, an organism) is modelled by means of a dynamical system and the collective behaviour is given by the time evolution of the average state variable (which, borrowed from the physics formalism, will be called the mean field). If the elements of the population are chosen perfectly identical, there are cases, e.g. the perfectly synchronous regime, in which the macroscopic dynamics is a perfect replica of the single-element behaviour. This can be used as a starting point for the study of the effect of microscopic variability.

This way of modelling a population is relevant for instance in the case when nonstationary biological processes interact and give rise to a macroscopically detectable signal. For instance, one system where such collective dynamics can be experimentally studied in a controlled setting is a suspension of yeast cells in a Continuous-flow Stirred Tank Reactor [35]. Under specific conditions, and notably where the interaction among cells is strong, the metabolism of all the population elements appear to oscillate synchronously, as measured by the average fluorescence of one intracellular chemical component. If the cells were perfectly identical, one could use macroscopic measurements to infer the features of the biochemical processes leading to intracellular oscillations. In this manner, the wealth of studies that have been performed on yeast extracts constitute a term of comparison and the parameters measured in these much more controlled systems could be used as a mean for gaining insight on the metabolic activity of eukariotic cells [68]. On the other side, the knowledge of the single-element behaviour is rather problematic due to the weak fluorescence of an isolated cell and is currently under study. It is therefore important to quantify the influence of microscopic disorder on the

macroscopic dynamics and evaluate when the variability among cells renders the observable dynamics different from the microscopic evolution.

In the second approach, all the details of the microscopic dynamics are neglected with the exception of the rules by which individuals belonging to different groups, whose weight within the population is measured by their frequency, interact with each other. The attention is then focused on how the microscopic units adapt to the composition of the population by dynamically changing group. Such a shift takes place when the individuals, analogously to physical particles, meet in pairs or in groups and is determined by some interaction, e.g. behavioural, rules.

For instance, if the individuals are assumed to play a one-shot game, whose payoff depends on the strategy each of the players adopts, the formalism of evolutionary game theory allows to determine what strategies will eventually be represented within the population and the dynamics of their frequencies [64]. When social interactions are taken into account, however, the evolutionary dynamics is determined by the statistics related to the group composition and no formal general method exists for deriving the equations at the population level.

In concordance with the above discussion, this thesis is divided into two parts. Analytical representations of the population dynamics is derived for classes of microscopic behaviours and is compared with the results of numerical simulations of the systems under study. Part I addresses how the synchronous dynamics of a population composed by generic dynamical systems is modified under the influence of microscopic disorder, in the form of either parameter mismatch or noise. There, we show that the collective dynamics for strong coupling can be described in terms of few effective macroscopic degrees of freedom, whose equations of motion can be systematically derived from the single-element evolution and are governed by population-level parameters.

Part II deals with a model for the evolution of altruistic behaviour in populations where the individuals interact in groups. In this case, the microscopic foundation of the model consists in the rules of the "public goods games", an extension of the "prisoner's dilemma" to a social context. The emergence of altruistic behaviour is explained within the framework of evolutionary game theory, where the paradoxical nature of cooperation first emerged, under the simple assumption that individuals can choose whether or not to take part in the game.

In both cases, we consider well-mixed populations, where we adopt a mean-field approximation approach and provide analytical expressions for the collective population dynamics.

The term "population" encompasses, in mathematics, physics, chemistry as well as in biology, a wealth of different meanings that cannot be reduced to a simple univocal definition. Common sense, however, assigns to this term two features: (i) the idea of an ensemble composed by more than one (and often many) individual components and (ii) the existence of some trait that is common to all such elements. It is this trait that allows us to identify the population as a unity at a higher description level. Rather than reflect the peculiar features of a system, the concept of population is thus related to the way in which we look at

it, and to the quantities we are able to measure and interpret.

In biology, the problem of describing and predicting the behaviour of a set of analogous elements has emerged in many different fields of investigation: at the cellular level, where a structured ensemble of molecules and proteins forms the basis of intracellular processes; at the physiological level, where groups of cells in a tissue coordinate to produce a coherent outcome, such as the contraction of a muscle or the production of insulin; at the level of one species, where natural selection acting on individual traits yields to the evolution of the population characteristics; at the ecological level, where analogous species competing for the same resources structure the ecosystem. In physics, the understanding of how macroscopically observable properties of a system are related to the characteristics of the particles of which it is composed has motivated the development of statistical mechanics. The formalism introduced for the study of physical phenomena however had to be widened for studying systems typically out of equilibrium, dissipative and composed of different species that can transform one into the other (e.g. through chemical reactions or predation). In general, moreover, biological populations intrinsically possess a further degree of complexity with respect to the physical ones, due on the one side to the absence of first principles that the system has to obey, on the other side to the co-existence of many description levels entangled into each other.

From a mathematical point of view, however, phenomena as different as chemical reactions and the evolution of animal behaviour are modelled by means of nonlinear differential equations or maps. The study of such models motivated the development of methods of mathematical techniques for addressing population dynamics within the framework of dynamical systems theory.

Part I

The first part of the thesis deals with ensembles of units, such as cells or organisms, that have a certain degree of homogeneity and can therefore be described by means of functionally identical dynamical systems. The collective properties of the population are addressed in the case when such units interact strongly, so that the emergent dynamics is sufficiently coherent to be plausibly related to the single-element behaviour.

In general, the formulation of any mathematically treatable, and therefore low-dimensional, model for a single population element disregards some other features that have only a minor impact on the dynamics and that may differ from one individual to the other. Models for biological populations are particularly prone to be affected by such oversimplifications, given their inherently structured and complex nature. A first attempt to take such neglected degrees of freedom into account is the introduction of some sort of microscopic disorder into the deterministic single-element equations. Typically, this is done either by distributing the microscopic parameters, so that a mismatch exists in the single-element behaviour, or

by adding independent stochastic terms (here called for simplicity noise), to each individual equation. In spite of their structural equivalence, hence, the dynamical components of the population will have a degree of diversity that can be measured by the statistical quantifiers of the distribution according to which disorder is assigned.

From the point of view of the mathematical description, each individual can be represented by an ordinary differential equation or by a map, accounting for the relevant degrees of freedom of the single-element dynamics. The way in which such dynamical systems interact then determines the coupling term that defines how many of the other components influence the considered element and how.

One of the simplest forms of interaction is the so-called *global*, *all-to-all* or *mean field coupling* , occurring when any individual dynamics is influenced by all the other elements through their average value. Here, we deal with populations of globally coupled dynamical systems. Due to their relatively simple structure, these populations have been used as prototypical models for the study of collective properties in systems with many degrees of freedom. On the other hand, they have been widely used as models of a range of physical, chemical and biological systems, some of which are reviewed in Chapter 2. All-to-all coupling is either implemented through an explicit choice of the connection topology, like in arrays of semiconducting elements (Josephson junctions) [169, 113, 170] and electrochemical oscillators [83], or due to the presence of a homogeneous common medium where all the elements are embedded, like in the case the yeast cells in a Continuous-flow Stirred Tank Reactor [35, 34]. Globally coupled oscillators moreover constitute a useful approximation for a larger class of spatially extended systems, provided that the range of the local interaction is sufficiently long [97]. This is the case in swarms of flashing fireflies [173, 175], networks of neurons [151, 156], cultured heart cells [150], mixed chemical reactions [112].

One of the properties of globally coupled nonlinear systems is that, if their interaction is strong, they tend to entrain their phases and to oscillate at the same frequency. This phenomenon of *synchronisation*, first described by Huygens in 1665, is still very actively discussed due to its generality and wide range of applications [175, 85, 127, 106, 154]. Synchronisation can occur between two or among many systems and for very different interaction schemes. Apart from the entrainment to an external forcing, of extreme practical relevance as far as technological development is concerned, a lot of attention has been given lately to the processes in which synchronisation occurs as a collective effect rather than being caused by an exogenous pace-maker. Here, we focus on the role that the individual-level features play on the properties that emerge in populations due to interaction rather than to an external driving.

The analysis of Chapters 3 and 5 starts out from the presence of a well characterised regime where all the elements have the same dynamics. Such *full synchronisation* occurs when all the components of the population are identical, given that the coupling is sufficiently strong. In this case, the average of the state variables behaves exactly like one single uncoupled oscillator, so that the macroscopic dynamics mirrors the microscopic one. This regime is now well understood and

methods are available for studying its stability [122, 127, 23].

Chapter 2 reviews the regimes that take place in populations of identical individuals when the coupling is too low for perfect synchronisation to occur. This regimes, including clustering and incoherence, have a inherently complex features with respect to the aforementioned case and do not provide an easy starting point for the analysis of how diversity affects the population dynamics. Hence, we assume that the coupling among the population elements is strong enough, so that the oscillators, if identical, get fully synchronised. We than perturb this regime by introducing different kinds of microscopic disorder, namely parameter mismatch and noise, and we study their effect on the collective behaviour.

In principle, one expects by continuity that the macroscopic behaviour of generic populations remains qualitatively identical to the synchronous one if only small microscopic perturbations are performed. This is however no longer true once disorder is increased: the collective dynamics becomes qualitatively different from the single-element uncoupled one, thus breaking the one-to-one correspondence that links the two observation levels when full synchronisation is attained.

This statement has important consequences for the interpretation and practical use of macroscopic measurements, hindering an immediate connection to the bottom level. The question then arises as to what kind of information one can extract from experimental observables when diversity is indeed present in the population. In particular, one would like to exploit the lack of correspondence between microscopic and macroscopic dynamics for evaluating population-level parameters, such as the amount of disorder or the strength of the interactions.

One commonly used approach consists in addressing the behaviour of the distribution of the population elements (snapshot probability distribution function). This distribution is in general different from that of the disorder and its time evolution is governed, in the limit of infinite population size (thermodynamic limit) , by continuity [138, 153], or Frobenius-Perron equations [124] or from the associated Fokker-Plank equations [41, 67, 128]. These equations can be solved, exactly or approximately, with different methods, among which self-consistent field [153, 124] and moment expansion techniques [41, 128] are the most commonly used. These approaches are especially well suited and provide exact results when one knows a priori some features of the population's probability distribution, as for the transition to synchronisation from incoherent motion.

Chapters 3 and 5 present a novel method for studying the collective dynamics of globally and strongly coupled systems. The observation that, even in the presence of microscopic disorder, a strong interaction among the microscopic units maintains a certain degree of coherence within the population, justifies the search for effective quantities able to capture the most important features of the macroscopic dynamics. Borrowing from synergetics [54], these macroscopic quantities will be called *order parameters*. They are meant to represent the relevant degrees of freedom of the emergent dynamics. The other, numerous and at times infinite, dimensions of the full population dynamics are interpreted as negligible perturbations of the collective behaviour.

Identification of the order parameters and formulation of their equations of

motion can be made systematic, under very general assumptions about the single-element dynamics and the kind of disorder introduced, through an *order parameter expansion*. The reduction to a low-dimensional dynamical system can be performed by introducing appropriate closure assumptions that exploit some population-level properties of the system, such as the coherency of the collective motion or the statistical features of the problem.

Although not exact, this method provides very useful insights into far-from-equilibrium regimes, such as the synchronisation of nonidentical units, where very few analytical results are available. Moreover, it allows us to point out how the collective dynamics is affected by various sources of microscopic diversity, and how the moments of the disorder distribution interact with the nonlinearities of the single-element dynamics.

In this way, disorder-induced qualitative changes in the collective behaviour can be interpreted as bifurcations of the macroscopic equations and shown to derive from the unfolding of the perfectly synchronous regime. Such equations moreover allow us to relate the phase transitions to specific values of the population-level parameters. The comparison of these parameters with the measured ones provides a scheme for testing the adherence of the model to the experimental population.

Chapters 3 and 4 address the case in which microscopic disorder takes the form of a parameter mismatch among the population elements. Section 3.1 presents several examples of the collective regimes of populations with parameter mismatch, focusing on those taking place for strong coupling. The derivation of the macroscopic equations of motion for such regimes is performed in Section 3.3 under general assumptions on the single-element dynamics and on the mismatch distribution. These results are applied to specific populations in Chapter 4. There, we show that the reduced system can reproduce the mean field behaviour in populations of Hopf normal forms with frequency mismatch, in globally coupled Ginzburg-Landau equations and in populations of chaotic systems with time-scale diversity.

Chapters 5 and 6 study the effect of additive noise on the collective dynamics of globally coupled maps. Section 5.2 is dedicated to introduce the phenomenon of noise-induced collective regimes. We show that, in the limit of infinite population size, the mean field displays a deterministic and apparently low-dimensional evolution. The macroscopic equations of motion for strong coupling are derived in Section 5.3 for generic microscopic feature. In the case of maximal coupling these equations are exact and allow us to conclude that the collective dynamics is strictly one-dimensional. The features and consequences of such an effective description of the macroscopic dynamics are discussed in Chapter 6, where the analytical results are applied to populations with different specific microscopic properties. Sections 6.1 and 6.2 consider populations of chaotic logistic maps, showing that truncations of the order parameter expansion to increasing orders account in more and more detail for the hierarchical structure of the mean field attractor and address the problem of the dimensionality of th4e macroscopic dynamics. In Section 6.4 the microscopic dynamics will be chosen to be excitable and the study of the macroscopic dynamics allows us to provide a different point of view on the mechanism of noise-induced coherence.

Chapter 7 compares the macroscopic effect of different sources of disorder in populations of globally coupled maps. The derivation of the corresponding order parameter expansions clarifies the role of the different microscopic statistical properties on the collective regimes. In Section 7.2 we draw general conclusions on the first part of the thesis and discuss in perspective the possible applications of the order parameter expansion approach to populations with other topologies and microscopic features.

Part II

The second part of this thesis addresses the dynamics of the frequency of characters in a large population, where individuals are subject to selective forces and to intraspecies competition. In the setting of evolutionary game theory, every population element is endowed with a *strategy*, that is a character that can be spread either by generating offsprings or by imitation, and according to which a score, the payoff, is assigned to the interaction with other individuals. Any other characteristic of the individual is disregarded as irrelevant with respect to the evolutionary dynamics. A strategy can, for instance, be a genetically determined property, like an instinct, or a culturally transmitted behaviour. Anyways, the meaning of the strategy is strictly related to the kind of interaction taking place among the individuals of the population, which is most easily formalized in terms of a *game*.

Once the relative frequencies of the different strategies are assigned, one wonders how the state of the population evolves when an external selective pressure gives the individuals a differential reproductive success.

Chapter 8 reviews the main motivation, problems and techniques of *evolutionary game theory*. In particular, we introduce one of the basic mathematical tools, the *replicator equation*, for studying how the frequency of any given strategy changes in time. Such equation states that, under the action of natural selection, the fitness value of the individuals adopting one strategy determine their differential reproductive success within the population. In the specific, fitness is identified with the score, or payoff, the player gets after having played the game with randomly chosen opponents. In spite of the fact that in the original formulation success has been initially thought of in terms of number of offsprings, equations with the same structure can be used in a social context, where imitation rather than actual genetic mediates the transmission of a strategy.

If the individuals play in pairs, formed by drawing at random two players from the population at each round, their fitness can be straightforwardly computed from the payoff matrix, that collects the outcomes of the interaction of any two strategies present in the population. The resulting replicator equations, although difficult to handle when the number of strategies grows, are quadratic and their study benefits of analytical results on parabolic differential equation [64]. Such two-players games represent the most simple and foundamental issues of game

theory, and it is in this context that the problem of the evolution of altruistic behaviour started to be addressed in game theory.

Following the aforementioned formalization scheme it became immediately evident that, while mutual cooperation would in principle be the best choice that two players could make, such an altruistic strategy would never take over a population under selective forces. This is the consequence of the fact that, no matter what the co-player will be doing, defecting always gives an individual a better payoff with respect to cooperating. Such paradoxical situation, tipically occurring in the paradigmatic game called "prisoner's dilemma" , has been faced in different ways, which will be briefly reviewed in Chapter 8.

Chapter 8 introduces a generalization of the prisoner's dilemma, the *"public goods game"*, that attracted a lot of attention recently as a prototype for studying cooperation in social settings, that is where players interact in groups rather than in pairs [59]. Analogously to the two-person game, the defecting strategy is always the most rational to adopt, while the best possible payoff is obtained when all the players cooperate. However, the actual outcome of the interaction depends on the composition of the group, that in general no longer reflects exactly to the composition of the population, as will be discussed in Chapter 9.

The theories accounting for the evolution of cooperation in two-persons games cannot be immediately extended to the case of n-persons games, or they would require unfeasible assumptions on the structure of the interactions. Therefore, no consensus theory still exists on how socially altruistic behaviour emerged and got established.

Chapter 9 presents a simple mechanism through which the population can not be entirely taken over by the egoistic strategy. The model is based on the idea that players may choose whether to take part in the game, and in this case to adopt either a cooperative or a defective strategy, or not to play at all, thus relying on an autharchic income. The individuals adopting this last strategy, named *loners*, choose to avoid both the risks and the advantages of the social interaction, in that their payoff is better than what one would get if all the coplayers were defecting, but still lower than what one would gain being in a group of cooperators.

In the presence of such a fallback solution, defectors cannot invade the whole population, since their abundance causes loners to spread. When the number of defectors reduces under a certain threshold, however, it becomes convenient again to enter the game as a cooperator, and cooperation thus increases in the population up to the following invasion of defection.

The cyclic behaviour of the relative abundance of the three strategies can be obtained by formally deriving the payoff of the three strategies, and consequently providing a microscopic foundation for the replicator dynamics. The equations thus obtained have a degree of nonlinearity equal to the size of the group of interacting individuals, nevertheless they can be analytically solved. In this way, one can demonstrate that the evolutionary dynamics of the three strategies has the well known form of a rock-scissor-paper cycle [64].

Such dynamics, characterized by the relation of dominance of each one of the three strategies on only one of the others, is reciving an increasing attention in

litterature, both from the theoretical and experimental community [155, 79]. In particular, Chapter 9 will discuss how the model relates to recent experiment performed on a bacterial population (*Pseudomonas fluerescens*) [130] and on humans [142].

Part I

Macroscopic effects of microscopic disorder

Chapter 2

Population dynamics in coupled dynamical systems

Self-sustained oscillations and other forms of complex behaviour are observed at all biological levels, ranging from intracellular biochemistry up to ecology and evolution of metapopulations. If oscillations are present on one scale of observation, one can ask the question of how they affect the dynamics at another scale, where the bottom-level (microscopic) features are summed into macroscopic information emerging at the top-level. If the elements of the population interact with each other, the answer is in general far from trivial, and a number of different phenomena arise reflecting, besides the characteristics of the microscopic dynamics, the structure of the interaction and its intensity.

As an example, consider a population of cells with oscillating biochemistry, such as those regulating the secretion of insulin, the contraction of muscles or the immune response. When cells of the same kind interact with each other, the measurable quantity of physiological interest is the resulting collective behaviour, that determines the functional role of the tissue. In spite of the fact that the recent advances in molecular biology provide a more and more detailed picture of the single cell, the problem of how such units coordinate their action is in many respects still an open question and is a very active field of study.

In general, the topology of the connection among cells, that is whether they communicate all-to-all, locally or according to some network, will influence the outcome of the emerging dynamics. However, if the interaction is sufficiently long-range, the assumption of global (all-to-all) coupling often furnishes a good approximation of the other interaction structures, and has the advantage of being the simplest in terms of mathematical formulation.

Populations of globally coupled oscillators are extremely useful models for the investigation of collective regimes of systems with many degrees of freedom. In particular, experiments on all-to-all coupled electrochemical [81] and 'biochemical' systems [34] provide controlled settings for the quantitative study of population

dynamics.

For instance, Hudson and coworkers have compared the single-element to the population dynamics in arrays of globally coupled chemical oscillators [166, 182, 82]. The possibility of measuring at the same time the microscopic behaviour of each unit and the collective average behaviour allowed them to reproduce a series of theoretical results on populations of oscillators in presence of parameter mismatch [83, 181] and of noise [80].

As far as biological populations are concerned, an example of a quantitatively studied collective phenomenon is the synchronous metabolic oscillations in yeast cells [35]. These cells are prepared in order to single out the first part only of the pathway that provides energy to all eukaryote cells, i.e. glycolysis. The addition of cyanide provides an effective decoupling of this pathway from the respiration taking place in mitochondria, so that the complexity of the cellular biochemical activity is greatly reduced. Then, the cells are coupled through a well-mixed, and thus homogeneous, suspension medium. In this experimental system, the problem of connecting the macroscopic description to the features of the intracellular biochemistry is more crucial than in the previous example, due to the fact that the only measures so far available consist in averages over many cells. On the other hand, the detailed knowledge of the chemistry involved in the glycolytic pathway allows us to write a model for the chemical kinetics. The parameters of the microscopic system, however, need to be determined on the basis of quantities measured at a higher level of observation. By exploiting the properties of the system close to the onset of macroscopic oscillations, Sørensen and coworkers have calibrated the parameters of the equations describing the biochemical dynamics in vivo under the approximation of identical cells [68]. Even if the diversity among cells does not seem to play a significant role in the regimes of very strong coupling, it is likely that it affects the macroscopic regimes in regions where the interaction among cells is weakened. The work presented in this thesis is intended on the one side to explore some general features of the influence of disorder on the collective regimes, on the other side to suggest experimental tools for quantifying the effect of such disorder.

The rest of this section presents general models for populations of globally coupled dynamical systems and briefly reviews the main existing results on the phenomena of synchronisation and of coherence resonance. The first part of this thesis will then present our results on the strong coupling regimes in populations of globally coupled dynamical system with microscopic disorder.

2.1 Global coupling

Globally coupled dynamical systems have long been studied as models for populations of interacting oscillators in several disciplines, reviewed for instance in [85, 175, 127, 51, 154]. Some examples are: semiconductors arrays (Josephson junctions) [53, 170] in physics; electrochemical oscillators [166, 83, 181] in che-

mistry; yeast cells [158, 35, 176, 34, 68] in cellular biology; pancreatic beta-cells [165], nephrons [65], cardiac cells [150] and neural cells [151, 156] in physiology; prey-predator systems in ecology [44, 14, 21]; clapping audiences [109, 110].

Typically, one makes some assumption about the *single-element* (or microscopic, or local) *dynamics* , in terms of a system of ordinary differential equations (ODEs, also referred to as flows or continuous-time dynamical systems):

$$\dot{\mathbf{x}} = \mathbf{f}(\mathbf{x}) \qquad \mathbf{x} \in \mathcal{R}^n$$

or in terms of a map (also referred to as discrete-time dynamical system):

$$\mathbf{x} \mapsto \mathbf{f}(\mathbf{x}) \qquad \mathbf{x} \in \mathcal{R}^n.$$

Since we are interested in studying populations of nonstationary elements, the dimensionality of the continuous-time system will be chosen to be larger than one, and larger than two in the cases in which the single element displays chaotic behaviour. As far as the maps are concerned, instead, this thesis addresses only populations of scalar maps, that can be thought as the Poicaré maps of chaotic attractors of highly dissipative continuous time systems.

Global coupling is in general expressed by the dependence of the equations for each element on the states of all the other elements, each of which gives an identical contribution. The interaction term is thus commonly written as a function of averages over the whole population. In the case of ODEs, the *global* or *mean-field coupling* is expressed in general in the form:

$$\dot{\mathbf{x}_j} = \mathbf{f}(\mathbf{x_j}) + \mathbf{K}\left(\langle \mathbf{x} \rangle\right) \qquad j = 1, 2, ...N$$

where $\mathbf{K} : \mathbb{R}^n \to \mathbb{R}^n$ is the global coupling function, N is the size of the population and $\langle y \rangle = 1/N \sum_{j=1}^{N} y_j$ is the operation of averaging over the population. These equations define the *individual* or *microscopic dynamics*.

Global coupling can be seen as a limit case of different interaction structures, as if the population elements are non-locally coupled, that is the strength of the interaction between two elements depends on their distance, or more generally if they are arranged in a network with long-distance correlations.

In many cases of practical relevance, the coupling among units is due to a diffusive process, as in the case of electrochemical oscillators or of cells in a suspension, so that the interaction term is commonly written in the form of a *linear coupling*, that approximates the diffusion operator if the time scale of diffusion is slower than that of the individual dynamics. In this case, the microscopic dynamics for the ODEs is recast in the form:

$$\dot{\mathbf{x}_j} = \mathbf{f}(\mathbf{x_j}) + \mathcal{K}\left(\langle \mathbf{x} \rangle - \mathbf{x}_j\right) \qquad j = 1, 2, ...N, \tag{2.1.1}$$

where the matrix $\mathcal{K}$ measures the intensity of the coupling among different components of the state vector of the individual elements. Here, we will consider for simplicity the case in which all the variables are coupled with the same intensity.

In this case, $\mathcal{K}$ is taken proportional to the identity matrix through a scalar coefficient K, that will be called the *coupling strength* and we will speak of *scalar coupling*. In most of this thesis, K is assumed to be a real non-negative number.

In the case of maps, the equations for the microscopic dynamics of linearly and globally coupled systems reads:

$$x_j \mapsto (1-K)f(x_j) + K\langle f(x)\rangle \qquad j = 1, 2, ...N. \tag{2.1.2}$$

While for ODEs it can take any positive value, in the corresponding discrete-time formulation the positive semiaxis is mapped into the interval $[0, 1]$, the maximum value 1 corresponding to infinite coupling among flows.

At the level of the collective behaviour, the quantities that can be measured are typically statistics over the population. In particular, the average value of some system variable (e.g. concentrations of molecules or biomasses of species), that will be referred to as *mean field*:

$$\mathbf{X} = \langle x\rangle = \frac{1}{N}\sum_{j=1}^{N}\mathbf{x}_j$$

is usually assumed to be the macroscopic observable.

Such statistics are macroscopic variables, that characterise the behaviour at the population level, indicating if the collective dynamics undergoes qualitative changes. Borrowing from the vocabulary of physics, where phase transitions are universally described in terms of averaged quantities, the macroscopic variables will be as well called *order parameters*.

A general question is thus how to characterise the behaviour of the mean field given the microscopic features (single-element dynamics and interaction strength) and, vice versa, how to extract information about the bottom level properties from purely macroscopic measurements.

The general solution to this question is not known, even if several results have been obtained for given subsets of microscopic conditions. These results rely mainly on the existence of limiting cases where the problem can be formulated in simpler terms, such as when the oscillators are uncoupled and when they all have the same trajectory.

The next section addresses the main results obtained for the cases of weak and strong coupling, and briefly overviews the phenomena observed for intermediate coupling. Next, the role of microscopic disorder, either in the form of parameter mismatch or of independent noise, in shaping the mean field dynamics will be addressed, focusing in particular on the phenomena of synchronisation and of coherence resonance. The last section resumes the existing results in the perspective of the approach proposed in the thesis.

2.2 Identical oscillators

Let us first assume that the population is composed by identical chaotic elements.

If these do not interact, that is $K = 0$, and the population size N is sufficiently large, one expects the contributions of different units, if initiated with random values, to average out. Due to the law of large numbers, indeed, the mean field of infinite populations is time-independent (zero if the time-average of the microscopic dynamics vanishes), while that of finite but large populations will show fluctuations whose amplitude decays as $1/\sqrt{N}$ when $N \to \infty$.

If the coupling strength is strictly positive, the mean field will remain zero up to a critical value of the coupling which is determined by the properties of the single-element dynamics. The knowledge of the features of such regime, called *incoherence*, where the oscillators are expected to maintain a uniform distribution over all the configurations they can take, allows us to address the question of its stability in the limit of infinite population size. Indeed, shifting to a description in terms of probability distributions, the evolution of the population as a whole can be described in terms of Liuville (continuity) equations in the case of ODEs and Perron-Frobenius equations in the case of maps [124, 123, 159]. The stability of the uniform distribution can then be addressed either using self-consistency for writing explicitly a nonlinear evolution operator [124] or through linear response theory [159].

This study however leads to different conclusions depending on the nature of the chaotic maps that have been considered and on the kind of coupling. Topaj, Kye and Pikovsky have derived the general condition for the incoherent solution to become unstable, and applied this result to show that the mean field of globally coupled identical Bernoulli maps undergoes a bifurcation to nonstationary behaviour for a nonvanishing value of the coupling [159]. Nakagawa and Komatzu [107, 108] and Chawanya and Morita [26, 104] have instead shown that tent maps display nontrivial collective behaviour for arbitrarily small coupling intensities, at least for a set of parameters of zero measure, and that the macroscopic bifurcation diagram has tongue-like structures for finite coupling strengths. These different results are however not in contradiction, the differences being due to the different properties of the logistic and of the tent maps. Logistic maps, that are topologically stable, indeed seem to display a transition out of incoherence for nonvanishing coupling strengths [75].

When incoherence becomes unstable, the mean field starts displaying fluctuations that do not vanish in the infinite size limit, and that in general appear more and more complex as the bifurcation boundary to incoherence is approached.

The second regime whose exact stability boundaries can be analytically computed is *perfect* (*complete* or *identical*) *synchronisation*. In this regime, all the population elements evolve exactly on the same trajectory, so that the mean field dynamics mirrors the individual behaviour. The linear stability analysis in this case proceeds from the study of the effect of small perturbations on the dynamics of each population element. A sufficient condition for this solution to become linearly unstable is that one Lyapunov exponent transverse to the synchronous

chaotic orbit becomes positive [129, 94].

Between the limit cases of incoherence and full synchronisation, a variety of more complex regimes can be observed. Typically, intermediate couplings lead to the appearance of multiple attractors, corresponding to different repartitions of the population into *clusters* [106, 126] Within one cluster, the oscillators follow the same trajectory, but those trajectories are different for each cluster. Figure 2.1 shows the first bifurcation diagram for a population of logistic maps as a function of the nonlinearity parameter a and of the coupling strength ϵ.

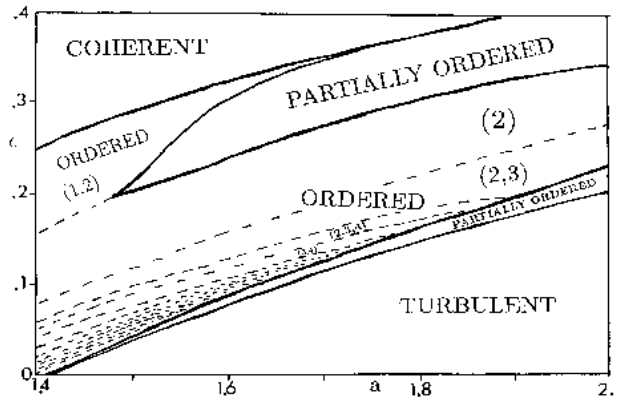

Figure 2.1: Bifurcation diagram for a population of globally coupled identical logistic maps ($f(x) = 1 - a\,x^2$), reproduced from [74]. The coherent phase corresponds to full synchronisation, the turbulent phase to incoherence, the ordered phases to the existence of different cluster (coded according to the number of coexisting subpopulations) and the partially ordered phase to the coexistence of a number of clusters that scale as the population size. This diagram is drawn by hand, so that some details are not correct. The partially ordered region for higher coupling has for instance been shown to be a numerical artifact due the presence of long transients [95]. The structure of this (hand-written) bifurcation diagram has been studied in much more detail by Mosekilde, Maistrenko and Postnov [106].

The loss of full synchrony can involve *riddling bifurcations* that occur when unstable periodic orbits embedded in the synchronous attractor lose their local stability, giving rise to intermittent bursts out of the synchronisation manifolds [93, 92, 94]. Now, the dynamics of the system takes place close to an invariant set, the so-called Milnor attractor [102], that contains a repelling set of zero measure, and such that the Lyapunov exponent computed on the chaotic orbits is nevertheless negative. A phenomenon associated with the presence of weak attraction is the existence of riddled basins of attraction, that is of fractal basins of attraction, as illustrated in Figure 2.2. If other attractors exist for the system, such as in the clustering regime, the phenomenon of chaotic itineracy can take place [72].

The Milnor attractor then disappears, when the coupling is further lowered, through *blowout bifurcations*, that consist in global bifurcations, or internal crises, through which the transversal Lyapunov exponent, averaged over the attractor, becomes positive. Shortly after the bifurcation has taken place, when the Lyapunov

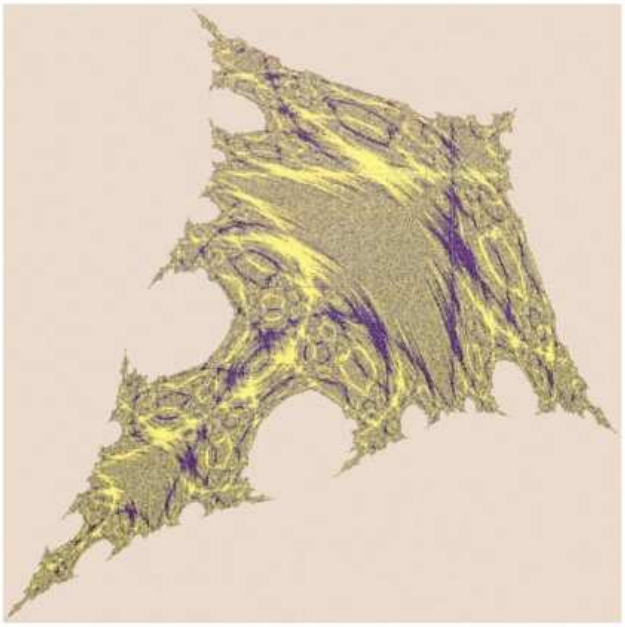

Figure 2.2: Intermingled basins for two Milnor attractors generated by two coupled logistic maps, reproduced from [93]

exponent is small but positive, the system displays on-off intermittent behaviour [92].

These regimes of intermediate coupling are characterised by multistability, long transients, critical dependence on the population size, complex structure of the phase space that allows for chaotic itineracy and attractor switching. Correspondingly, the mean field displays high-dimensional chaotic dynamics.

The first part of this thesis deals with coupling strengths belonging to the interval of "*strong coupling*", that is with K such that the completely synchronous regime, where the single-element and macroscopic dynamics coincide, is stable if the population is composed of identical units.

This simple scenario is significantly modified when disorder is introduced at the microscopic level, and the relation between bottom and top levels of description becomes dependent not only on the coupling strength, but also on the amount of diversity among different population elements. Relaxing the assumption of identity is a fundamental step towards the modelling of real systems, and is especially relevant when biological populations are studied. Even in the regimes of strong coupling microscopic disorder poses significant mathematical problems. The next two sections review the results established for two kinds of microscopic disorder, the first due to a mismatch in the parameters of the units composing the population, the second due to the addition of independent noise terms to each population element.

2.3 Populations with microscopic disorder: parameter mismatch

The study of the collective regimes of populations of nonlinear oscillators with parameter mismatch is presently very active, and a conclusive general approach has still not been formulated. Therefore, this section will present the prototypical case of limit cycle oscillators with natural frequencies mismatch, that has been widely studied as the simplest example of globally coupled nonstationary systems, and then address more specifically the topic of synchronisation for more general populations.

Let us first consider a population of globally coupled limit cycle oscillators (Andronov-Hopf normal forms) with frequency mismatch:

$$\dot{z_j} = (1 + i\omega_j - |z_j|^2)z_j + \frac{K}{N}\sum_{l=1}^{N}(z_l - z_j), \tag{2.3.1}$$

where $z_j = r_j\, e^{i\,\phi_j}$ represents the position of the jth oscillator in the complex plane and the natural frequencies ω_j are taken from a distribution of average ω_0 and standard deviation σ. These equations are chosen because they are the normal form for the generic *supercritical Andronov-Hopf bifurcation* , that occurs when a limit cycle is born by the loss of stability of a focus (i.e. when two complex conjugate eigenvalues of the dynamical system cross the imaginary axis). This bifurcation scenario is important because it is generic, that is, if it takes place in a system by varying one parameter, it will occur in almost all the one-parameter families close to it (according to an appropriate functional norm).

As we discussed in the previous section, if all the frequencies coincide, the perfectly synchronous solution exists. This is stable for any positive value of the coupling, due to the fact that any two oscillators in the population belong to the $1:1$ synchronisation Arnold tongue.

Since the first studies on populations of limit cycle oscillators with distributed natural frequencies by Wiener [168], Winfree [173] and Kuramoto [84], it became evident that the existence of some kind of disorder at the level of the individual dynamics would lead to significant changes in the aforementioned scenario. With frequency mismatch indeed perfect synchronisation is no longer a solution of the system, and the diversity gives instead rise to a phase-locked regime where oscillators of different natural frequency rotate at the same frequency, but have different phases and amplitudes. Moreover, the incoherent state becomes stable for strictly positive values of the coupling constant.

Figure 2.3 displays the bifurcation diagram of the mean field $Z = \langle z \rangle$ for Eq. (2.3.1) and uniform natural frequency distribution. Incoherence is possible in an interval of positive coupling strengths that becomes larger as the parameter γ, that is related to the width of the natural frequency distribution, increases.

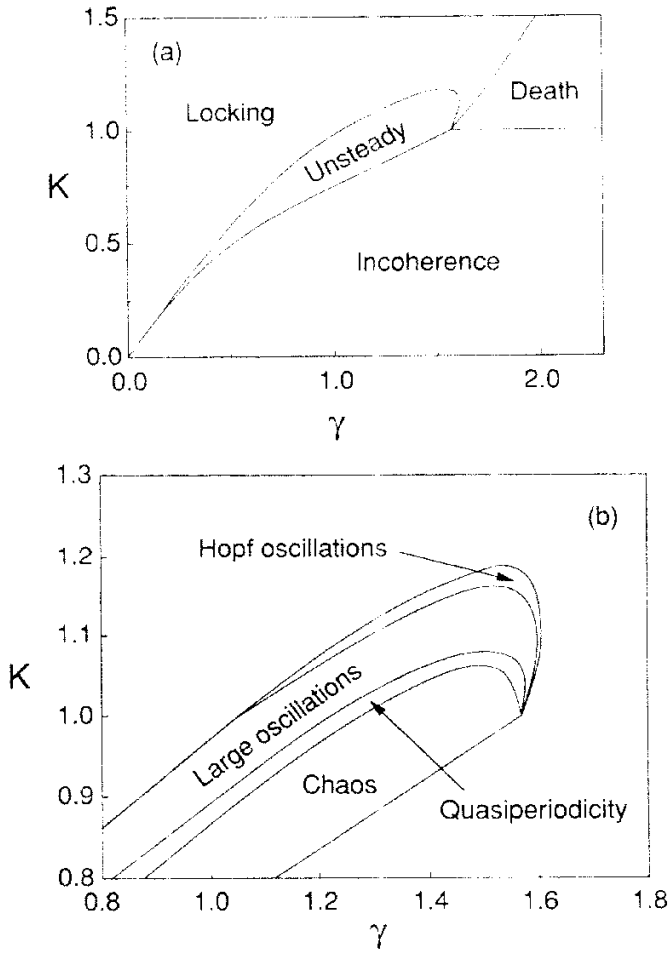

Figure 2.3: Bifurcation diagram for the mean field of the population defined by Eqs. (2.3.1), reproduced from Matthews et al. [98]. The bifurcation parameters are the coupling strength K and the parameter γ that is inversely proportional to the central value of the frequency distribution. Due to the fact that the distribution is normalised, this provides a measure of the parameter spread. Figure (b) is a magnification of the bifurcation diagram for intermediate coupling strengths and frequency variance, where the most complex collective behaviour appears. Hopf oscillations and large (amplitude) oscillations are periodic solutions in the rotating frame of reference (that is quasiperiodic regimes), the first originated by a Hopf bifurcation of the full locking equilibrium (represented by a point in the rotating frame of reference), the second by a saddle-node heteroclinic bifurcation, leading to the appearance of limit cycle of nonvanishing amplitude.

In the locking region, on the other hand, the oscillators evolve at the same frequency, equal to the average natural frequency in the population ω_0, but their phases differ from the mean field one proportionally to the mismatch with respect

to ω_0. By choosing a frame of reference rotating at the average frequency, the phase of the mean field can be arbitrarily assigned, so that the phase locked regime is conveniently studied as an equilibrium solution in a phase space of lower dimension. A number of other collective regimes are possible, among which amplitude death, when the oscillation amplitude vanishes due to the combination of strong coupling and of big heterogeneity in the natural frequencies, and quasiperiodic and chaotic behaviours, where the macroscopic dynamics is more complex than the single-element one. Some of these regimes will be discussed in Chapter 3.

Most of the studies on the emergence of collective behaviour in populations of globally coupled limit cycles have focused on the region of weak coupling, where Eq. (2.3.1) can be reduced to phase equations through a time scale separation. Indeed, Winfree pointed out that if the coupling is weak and the frequency mismatch small a fast relaxation of the oscillators on the limit cycle, associated with the generically nonvanishing Floquet multipliers of the single-element dynamics, is followed by a slow rearrangement of the phases, whose dynamics is described by the so-called Winfree model [174]:

$$\dot{\phi_j} = \omega_j + \frac{K}{N} \sum_{i=1}^{N} P(\phi_i)\, R(\phi_j). \tag{2.3.2}$$

In absence of coupling, thus, the phase of one oscillator evolves with velocity constantly equal to its natural frequency ω_j. In the presence of global coupling, instead, the j-th oscillator feels the presence of the others through the sensitivity function $R(\phi)$, whose contributions to the collective dynamics is weighted by $P(\phi)$.

The Winfree system Eq. (2.3.2), analysed in detail by Ariaratnam and Strogatz [5], can be further simplified through a center manifold reduction (in which only the slowest Fourier component of the coupling term is taken into account), which led Kuramoto to formulate the model that is now known under his name [84, 85]:

$$\dot{\phi_j} = \omega_j + \frac{K}{N} \sum_{i=1}^{N} sin(\phi_i - \phi_j). \tag{2.3.3}$$

Since its formulation, the Kuramoto model has been considered the prototype for studying the transition to coherence in nonequilibrium systems (also called "temporal phase transition" [174, 153]), characterised by the onset of a nonvanishing order parameter, defined as:

$$R = \sum_{j=1}^{N} e^{i\,\phi_j}.$$

Among the different approaches used for addressing the stability of the incoherent regime, the so-called thermodynamic limit of infinite population size allows us to describe the population in terms of a distribution of phases on the limit cycle and to exploit self-consistency for obtaining the bifurcation boundaries. This formulation led Matthews, Mirollo and Strogatz [103] to the conclusion that the uniform distribution corresponding to incoherence is always neutrally stable, and that the onset of coherence is due to the appearance of a discrete eigenvalue in the

spectrum of the evolution operator (obtained via the continuity equation) for the phase density.

However, this high degeneracy of the Kuramoto model was shown to be due to the fact that the center manifold reduction was accomplished by considering only the first harmonic of the coupling function. If the full Fourier expansion is included, so that the effects of weak nonlinearity are taken into account, the incoherent state displays a generic behaviour, and the transition to coherence has the form of a pitchfork bifurcation of the mean field. Daido, who first analysed the problem in this more general setting, determined the equilibrium solutions [30, 31, 32], while Crawford [28, 153] studied their stability.

The Kuramoto model has subsequently given rise to several other related problems. First of all, the singular properties of the incoherent state have led to the investigation of its sensitivity to noise, and to the study of the Fokker-Plank equation related to the Langevin formulation of the Kuramoto model [138]. Secondly, the original derivation of Kuramoto is valid not only for real coupling constants, as those considered so far, but also for the more general setting of the Stuart-Landau oscillators defined as:

$$\dot{z_j} = (\mu_j - |z_j|^2)z_j + K\frac{1}{N}\sum_{i=1}^{N}(z_i - z_j), \tag{2.3.4}$$

where μ_j and K are now complex variables. The bifurcation analysis of such populations is far from complete, the macroscopic behaviour being even more complex than in the aforementioned scenario [55, 23].

Apart from the limit of weak coupling, analytical results have been derived for the region of strong coupling. In this region, synchronisation phenomena typically take place.

2.4 Synchronisation

The phenomenon of synchronisation has been known since 1665, when Christian Huygens noticed that two pendulum clocks fixed to the same wall entrained their oscillations. The fact that oscillating units interacting with each other or with an external driving signal spontaneously modify their dynamics in order to adjust, when possible, their frequency, is now recognised as one of the most interesting phenomena in nonlinear dynamics. In particular, the possibility of mutual entrainment not only among limit cycle oscillators, but also among chaotic units, has widened the perspectives and the applied fall-out of these topic. Hence, a number of different definitions and points of view exist on how to handle the phenomena related to synchronisation [128].

As we mentioned before, the simplest possible state is *perfect synchronisation*, that occurs in a population when the composing units are identical and the coupling sufficiently strong (for lower couplings, clustering occurs, as discussed in

Section 2.2). In this case, every dynamical system composing the population follows exactly the same trajectory, whatever cyclic or chaotic, and so does the mean field.

When disorder is introduced in the form of parameter diversity (e.g. natural frequency mismatch, in the case of periodic attractors where the notion of frequency is well defined), the equations of motion for the population take in the case of ODEs the form:

$$\dot{\mathbf{x}_j} = \mathbf{f}\left(\mathbf{x}_j, p_j\right) + K(\mathbf{X} - \mathbf{x}_j), \tag{2.4.1}$$

where $\mathbf{x} \in \mathcal{R}^n$, $\mathbf{f} : \mathcal{R}^n \to \mathcal{R}^n$ defines the single-element dynamics, and in the case of maps:

$$\dot{\mathbf{x}_j} = (1 - K)\,\mathbf{f}\left(\mathbf{x}_j, p_j\right) + K\langle \mathbf{f}(\mathbf{x}, p)\rangle. \tag{2.4.2}$$

The parameters $p_i \in \mathcal{R}$, chosen to be scalar for simplicity, are assigned according to a given distribution.

A simple way of visualising what happens when such a distribution is not concentrated on a single value is to project the population on the phase space of one single oscillator, so that each population element will be represented by a point therein.

In the regime of perfect synchronisation, all the points will asymptotically move on the same orbit. When a small diversity in parameters is introduced, they spread around the mean field according to the value of their own parameter. In the case of limit cycle oscillators, shown in Figure 2.4, the representative points belong to a smooth manifold turning at the average natural frequency, whose equation can be determined self-consistently once the parameter distribution is assigned.

By reasons of continuity, we expect that this regime will keep the same character of perfect synchronisation when the parameter mismatch is small, and some degree of coherence among the population elements is maintained. In the literature this regime, in which the mean field maintains characteristics similar to the uncoupled element dynamics, has been named differently depending on which class of dynamical systems and which aspects of their dynamics the study has been concerned with.

For periodic dynamical systems, it corresponds to a configuration where all the oscillators have a fixed phase difference with respect to each other, therefore it is referred to as *phase* or *full locking* [98]. For chaotic systems the definition of a phase is instead not straightforward and the concept of perfect synchronisation had been weakened mainly in two ways[127, 106].

The notion of *generalised synchronisation* has been introduced in drive-response systems, that is systems with unidirectional coupling [137], as a time-independent functional relation between the states of the master (x_m) and of the slave (x_s) subsystems: $x_s = \mathcal{F}(x_m)$. The same concept can be used in the framework of globally coupled dynamical systems, where the mapping between one population element and the mean field would identify the synchronisation manifold in the phase space of one oscillator.

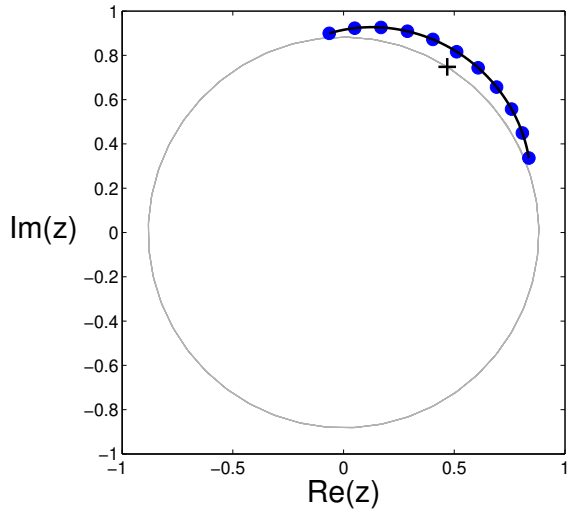

Figure 2.4: Projection of a population of limit cycle oscillators (Eq. (2.3.1) with $K = 0.9$ and uniform frequency distribution variance $\sigma = 0.3$) on the complex plane for the regime of full locking. The plus indicates the position of the mean field and the grey line the mean field attractor, that is a cycle of amplitude less then one. The arrangement of the oscillators (dots) along the synchronisation manifold (thick line) is parametrised by their natural frequency.

A second approach to the problem of defining synchronisation of chaotic systems relies on the definition of a generalised phase as basis for the comparison of the temporal patterns in the population. The notion of generalised phase is well defined when the chaotic attractor can be projected onto a plane so that a the trajectory turns around a "hole", as in the case of a Rössler system in the regime of spiral chaos. By means of the analytical extension of a signal $s(t)$ to the complex plane:

$$\psi(t) = s(t) + i\,\tilde{s}(t) = A(t)\,e^{i\,\phi(t)},$$

the instantaneous phase:

$$\phi(t) = \arctan\left(\frac{\tilde{s}(t)}{s(t)}\right) \tag{2.4.3}$$

can be obtained from the Hilbert transform of $s(t)$:

$$\tilde{s}(t) = \frac{1}{\pi}\int_{-\infty}^{\infty}\frac{s(\tau)}{t-\tau}d\tau.$$

The concept of phase locking has accordingly be extended to chaotic systems by Rosenblum, Pikovsky and Kurths [133], who proposed to compare oscillators with parameter mismatch on the basis of their instantaneous phase or of its long-time average. The same kind of analysis can be performed if other definitions of phase are considered, such as that proposed by Osipov et al. based on the curvature of an appropriate projection of the chaotic trajectories [118]. In general, one speaks

of *perfect phase synchronisation* or simply *phase synchronisation* [127, 3] if the relation among the phases:

$$|\phi_1 - \phi_2| < const, \tag{2.4.4}$$

is satisfied uniformly in time.

Other quantifiers of synchronisation are the *instantaneous frequency*:

$$\omega(t) = \frac{1}{\phi(t)},$$

the *mean frequency*:

$$\Omega = \langle \omega(t) \rangle_t = \lim_{\tau \to \infty} \frac{1}{\tau} \int_0^\tau \omega(t) dt,$$

the *mean frequency of returns*:

$$\Theta = 2\pi \lim_{tau \to \infty} \frac{R(\tau)}{\tau},$$

where $R(\tau)$ is the number of return times within the time τ [179] or the *winding number*:

$$\theta = 2\pi \lim_{\tau \to \infty} \frac{r(\tau)}{\tau},$$

where $r(\tau)$ is the number of revolutions about the origin [3].

The condition of perfect phase synchronisation implies perfect frequency locking, that is:

$$\Omega_1 = \Omega_2 \tag{2.4.5}$$

and therefore phase synchronisation is also called *full locking* or *phase-frequency synchronisation* or *synchronisation in the sense of Huygens* [3]. However, there are regimes where phase slips occur at a rate that does not alter significantly the mean frequency, and synchronisation can be detected by the presence of the same peaks in the frequency spectrum of different oscillators. In this case, one speaks of *weak* or *imperfect phase synchronisation* [179], the degree of imperfection being quantified by the ratio of nonsynchronous over synchronised turns:

$$\epsilon = \frac{|\Theta_1 - \Theta 2|}{\Theta_1}.$$

In order to take into account also the degrees of freedom other than the phase, Rosenblum, Pikovsky and Kurths introduced a second quantity for measuring the degree of synchronisation among oscillators. This is the minimum value of a similarity function [134], defined for two oscillating variables $x_1(t)$ and $x_2(t)$ as:

$$S(\tau) = \frac{\langle [x_2(\tau) - x_1(\tau)]^2 \rangle_t}{\sqrt{\langle x_1^2 \rangle_t \langle x_2^2 \rangle_t}}.$$

The time lag τ_0 where the minimum is attained corresponds to a phase difference and thus to an angular distance of the two oscillators in the projection on the single-element phase space. The minimum of the similarity function $S(\tau_0)$ measures

instead the difference in amplitude of the oscillations, and becomes zero in the limit of identical systems. Other indicators of the degree of synchronisation among chaotic units, such as the mutual normalised autocorrelation function and the coherence function, are illustrated in the recent book by Anishchenko et al. [3] and can be used alternatively to the similarity function.

The term *lag synchronisation* [134] defines a regime where the minimum of the similarity function becomes zero (in which case $S(\tau_0)$ identifies the functional required for generalised synchronisation, see Figure 2.5) and the generalised phases of two oscillators (or of every population element and the mean field, in the case of a population) satisfy the condition for phase synchronisation Eq. (2.4.4).

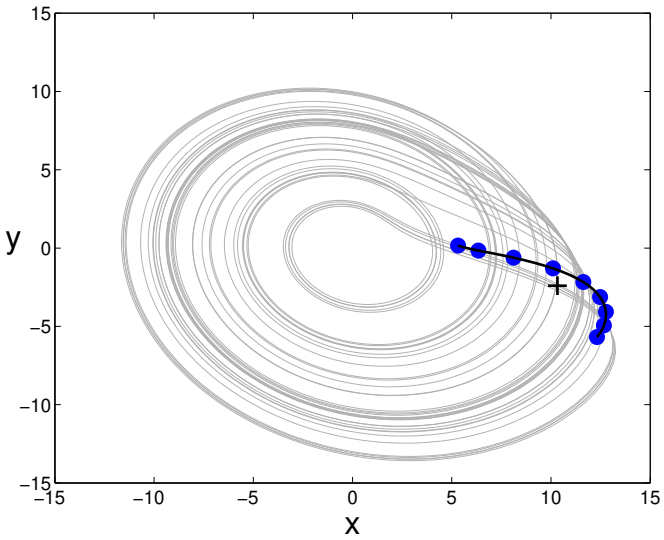

Figure 2.5: Macroscopic attractor of a population of 32 Rössler oscillators with time scale mismatch (for details about the population, see Chapter 3) in a regime of lag (generalised) synchronisation. The mean field (plus) has a chaotic attractor (continuous line) resembling the uncoupled element funnel attractor, but the elements of the population (dots, only 9 shown) are arranged around it on a manifold (thick line).

When the coupling becomes too weak to preserve an ordered disposition of the chaotic oscillators around the mean field, that is observed in the case of lag synchronisation, other forms of synchronisation have been found for two interacting Rössler attractors, depending on which of the conditions for lag synchronisation is lost first and how [118].

In order to discuss these different scenarios, it is convenient to consider not only the phases, but also the Lyapunov exponents of the full system. The lag-synchronous regime is characterised by the existence of one positive exponent, related to the fact that the dynamics is chaotic, one zero exponent, corresponding to the motion along the trajectory, while the other exponents are negative and the synchronisation manifold is attracting both for the phase and for the amplitude.

The transition to *phase synchronisation* [133, 134, 118] occurs when the stability of the synchronisation manifold is first lost for the amplitudes. Correspondingly, one of the negative Lyapunov exponents becomes positive. In the phase synchronous regime, the phases remain entrained, that is they satisfy Eq. (2.4.4) (and Eq. (2.4.5)), while the amplitudes vary chaotically, so that the system can be modelled as coupled noisy phase oscillators . This reduction effectively decouples the phases, whose dynamics is deterministic, from the amplitudes, that are supposed to behave as stochastic variables. The transition between lag and phase synchronous regimes is associated with phenomena of intermittency and riddling analogous of those mentioned above for the loss of complete synchronisation.

If the perfect phase synchronisation is lost first, the system enters a regime of weak phase synchronisation where the amplitudes remain correlated but the phases remain similar only on a short timescale, while on a longer one phase slips occur. This happens for instance when the chaotic oscillators present a broad distribution of frequencies of the embedded unstable periodic orbits, as in the case of Rössler oscillators with funnel attractors [118].

In this thesis, we will study synchronous regimes of populations of chaotic oscillators. Rather than examining the relative phases and frequencies, however, we will focus on the existence of a low-dimensional effective dynamics of the mean field. Therefore, we will focus on regimes where conditions of *coherence* hold. In general, we will speak of a coherent regime when the distance of each oscillator

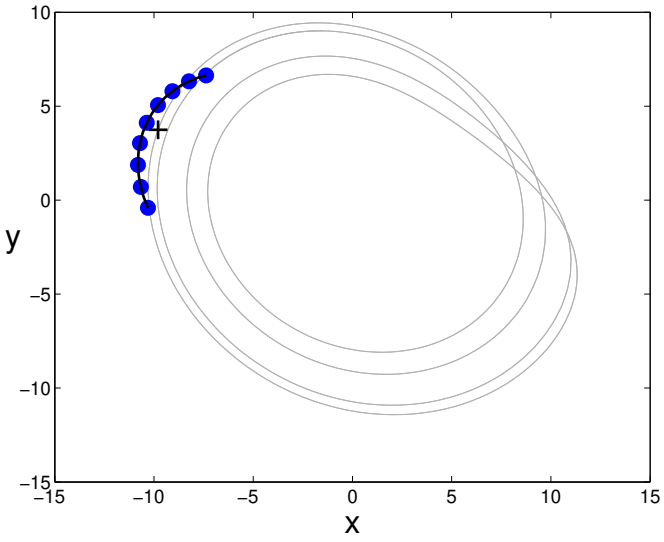

Figure 2.6: Macroscopic attractor of a population of 32 Rössler oscillators with time scale mismatch (for details about the population, see Chapter 3) in a regime of generalised synchronisation with periodic macroscopic dynamics. The mean field (plus) evolves on a period four cycle (continuous line), in spite of the fact that each element, if uncoupled, is chaotic. The thick line indicates the synchronisation manifold on which the elements of the population (dots) are arranged.

from the mean field, computed in the single-element phase space on which the population is projected, remains limited in time:

$$||\mathbf{x}_j(t) - \mathbf{X}(t)|| < c, \tag{2.4.6}$$

where the norm is chosen Euclidean and the constant $c \ll 1$ must be sufficiently small with respect to the linear dimension of the attractor. This definition, discussed in more detail in Chapter 3, is less precise than the aforementioned definitions, but is still enough for the kind of phenomena that will be addressed here.

It is moreover important to notice that if in the coherent regimes the cloud of points representing the population in the single-element phase space moves solidly, this motion can be qualitatively different from the single-element dynamics, as shown for example in Figure 2.6. Rössler chaotic oscillators with funnel attractor, for which the phase is ill-defined also in a general sense, can for instance display a collective regime of macroscopic spiral chaos, where the generalised phase exists, or even lock to a common frequency and display synchronous cyclic behaviour, in which case one can use the concept of synchronisation introduced for periodic oscillators. This point and the transition among different coherent regimes will be addressed in Chapter 3.

2.5 Populations with microscopic noise

Besides imposing a spread in the parameters across the population, microscopic disorder can also be modelled by adding a stochastic term, called noise, to each population element. Indeed, in describing the single-element behaviour by means of a low-dimensional dynamical system, one neglects other degrees of freedom that can be collectively summarised in a stochastic process acting independently on each population unit.

The effect of noise on the geometrical properties of a low-dimensional chaotic attractor and on its bifurcations have been addressed in the case of maps by Crutchfield and coworkers [29] and Ott and coworkers [121, 147]. This studies focused in particular on the scalings when the geometry of the attractor was smeared by relatively weak noise.

A series of other studies have successively focused on cases were the noise was arbitrarily strong and looked at the statistical properties of the time series of noisy systems. For a review on the topic of noise-induced behaviour, see the recent book by Anishchenko et al. [3].

A vast literature exists in particular on the role of noise in excitable systems, which are extremely relevant for biological, and in particular physiological, applications. A detailed review on this topic is provided by Lindner et al. [90].

In the following sections, we will review the phenomena of stochastic and coherence resonance for low-dimensional systems and then provide a brief description of the noise-related phenomena in systems with many degrees of freedom.

2.5.1 Stochastic and coherence resonance

The term *stochastic resonance* indicates the phenomenon by which a dynamical system subjected to an appropriate amount of noise responds more efficiently to an external forcing. Typically, this happens for systems of the form:

$$\dot{\mathbf{x}} = \mathbf{s}(\mathbf{x}) + \mathbf{F}(t) + \xi(t), \tag{2.5.1}$$

where $\mathbf{s}$ defines the autonomous system dynamics, $\mathbf{F}$ is the forcing term and ξ is an additive noise term, defined as the realisation of a stochastic process. A variety of systems have been addressed in this framework, with different uncoupled dynamics (e.g. bistable, cyclic or chaotic ODEs and maps), forcing function (e.g. periodic or quasiperiodic signals) and noise terms (e.g. white or coloured noise, Gaussian or Poissonian or uniform distribution) [48].

The power spectrum of the $\mathbf{x}$ variables contains the eigenfrequencies of the forcing, but their importance relative to the rest of the spectral components is negligible in the absence of noise. The characterising feature of stochastic resonance is that, even if the forcing signal is weak, its frequency can becomes important in the spectrum of the noisy system and reach its maximal relevance with respect to the background at an "optimal", or resonant, noise intensity. Such an optimum is commonly defined, in the theoretical as well an the experimental field, as the intensity that maximises the signal-to-noise ratio, computed from the time series power spectrum.

For instance, if the autonomous dynamics is bistable, one can think about the forced system in terms of a particle inside a stochastically moving double-well potential. The phenomenon of stochastic resonance tells that there exists an optimal noise intensity for which the particle crosses the potential barrier separating the two wells in phase with the forcing, thus providing an amplification of even weak input signals. When the noise intensity is too high, it is the noise term that dominates and blurs out the outcome, so that the spectral lines relative to the forcing term fade.

The effect of noise on a dynamical system is most pronounced in the vicinity of bifurcation points, where a fluctuation can lead the system to explore the neighbourhood of the attractor, causing thus an effective displacement of the bifurcation value. An example of this phenomenon are the so-called noise-induced self-sustained oscillations [3, 80].

When no forcing signal is present, noise still modifies the power spectrum of a system with respect to the case where no fluctuation are present. This phenomenon of stochastic resonance without forcing has been called *coherence resonance* [125], *internal stochastic resonance* or *autonomous stochastic resonance* and is defined by the existence of an optimal noise intensity by which the dynamics of the noisy system is maximally regular [90].

The degree of coherence in the dynamics is typically measured by a quantifier of the normalised dispersion $\Delta\omega$ of the spectrum $S(\omega)$ around its peak frequency

ω_{max}:

$$\beta = \frac{S(\omega_{max})}{\Delta\omega/\omega_{max}}.$$

Note that in the the case of stochastic resonance the frequency of the peak remained fixed, being determined by the forcing signal. If such forcing does not exists, instead, the dominant frequency can change with the noise intensity and its peak is usually broader with respect to that obtained for stochastic resonance.

Theoretical explanations have been given for the phenomena of stochastic and coherence resonance, linking the response of the system to its dynamical properties and to the features of the noise term. This has mainly been done by the analysis (mostly qualitative) of the Fokker-Plank equation corresponding to the Langevin dynamics, by means of linear response theory or by modelling the system as a multistate process with stochastic hopping [125, 3, 90].

2.5.2 Effect of noise on populations

When systems with many degrees of freedom are considered, the analysis of the noise-induced phenomena becomes more complicated.

The fact that noise induces qualitative changes in the population dynamics has been shown and experimentally demonstrated in spatially extended systems, where the spatial organisation or coherence is maximised for optimal values of the intensity [63].

A problem related to the fact that noise acts (independently or not) on more than one copy of the same dynamical system is whether those different units attain some kind of coherence or of synchronisation. A long-standing debate took place for instance about whether the realisation of the stochastic process that acts on a dynamical system univocally identifies its asymptotic noisy trajectory. Rephrased alternatively, the question was whether non-interacting dynamical systems get fully synchronised under the action of a common noise term (for a review of this topic, see Toral and coworkers [161]).

The effect of noise has been moreover investigated in couples or populations of interacting dynamical systems. Several works on this topic have dealt with ODEs subjected to additive independent noise, focusing for instance on the amplification properties of noise when the system is close to bifurcations [169], on "stochastic resonance" [49], on noise-induced coherence [131], on the attractor selection [23], on the modification by noise of the synchronisation frequency [105], on the enhancement of phase synchronisation [66, 2, 182], on the effect of noise on clustering [152, 180], on the noise-induced regularisation of bursts in excitable systems [136] and , on the noise-induced phase transitions to bistable [78] or oscillatory regimes [178].

The role of noise in populations of coupled maps has been relatively little investigated with respect to the wealth of literature dedicated to continuous-time systems. Chapters 5, 6 and 7 are dedicated to this subject. Specifically, we will deal with the noise-induced macroscopic bifurcations in the regimes of strong coupling.

That is, we will study how a synchronous regime is affected by microscopic-level independent stochastic terms. Therefore, the last part of this section is dedicated to a review of the existing work on globally coupled discrete-time systems.

One of the first studies on the effect of noise on globally coupled maps is related to experimental that fluctuations get amplified if the noiseless dynamical system is close to bifurcation. This research, conducted by Wiesenfeld initially on ODEs models [169], led to the use of maps as a simpler system where to study the phenomenon [113]. By a linear stability analysis of the periodic regimes, Nichols and Wiesenfeld were able to reproduce the divergence of noise-induced fluctuations of one individual map in the population, associated with nearly constant fluctuations of the average value. In Chapter 5 we show that in the limit of infinite population size the mean field of globally coupled noisy maps evolves deterministically. Its fluctuations are hence only determined by finite-size effects, even if the trajectory of every unit of the population is strongly affected by noise.

Several works have then addressed the robustness of collective regimes, usually studied in the absence of noise, after fluctuations were added at the microscopic level. Shibata et al., in particular, examined how the weak coupling regimes for populations of chaotic (logistic) maps were affected by noise. They showed that even extremely weak noise let the population leave the incoherent state, where the mean field dynamics is infinite-dimensional, and show instead a structured, apparently low-dimensional dynamics [144, 143]. The analysis of the dimensionality of the macroscopic attractor, measured as the number of positive Lyapunov exponents, revealed that indeed the effective dimension of the collective motion scales as $-\log \sigma^2$. They also conclude that when noise is added, the macroscopic dynamics is actually deterministic. A qualitative analysis of the Lyapunov spectrum for the evolution operator of the probability distribution function provide a theoretical explanation of this fact.

Teramae and Kuramoto addressed the effect of weak noise in regimes of strong coupling, where the the noiseless population is perfectly synchronous [157]. They study how the linear dimension of the cloud of points representing each individual within the population scales with the noise intensity. In this work, they consider both populations of chaotic ODEs and of maps. They show that as the system got close to the boundary where perfect synchronisation is lost, that is lowering the coupling, anomalous scalings appear on the moments of the probability distribution of the population. Indeed, the q-th moment increases with the noise intensity f as $f^{\alpha(q)}$, where α is not, as one would expect for uncorrelated variables, linear in q. They derive the form of the anomalous scaling by perturbing the fully synchronous regime and conclude that this effect is mostly visible when the coupling is close to that where this regime looses stability. Moreover, they predict that "the anomalous fluctuations could be visible through the higher moments in the range of stronger coupling where no anomaly is visible through lower moments". In Chapters 5 and 6 we will get to the same conclusions and we will show how the moments of the population distribution can be assigned a dynamics, that accounts for the anomalous behaviour observed by Teramae and Kuramoto.

The same authors moreover state that the effect of weak noise should be identical to that of weak parameter mismatch. In Chapter 7 we will show that this is not true in general: the macroscopic effects of noise reflect the different statistical properties of the way in which microscopic disorder is modelled.

2.6 Effective dynamics

In this elaborate, we will deal with globally coupled dynamical systems in regimes where there exist observables whose dynamics is measurable at a macroscopic level. For this reason, we will focus on the regimes of strong coupling and describe the population behaviour mainly looking at the average variable, the mean field, rather than at the individual trajectories. Indeed, our ultimate aim is to study how microscopic disorder, whose features can be in principle unknown, affect the collective evolution and interacts with the features of the single-element, uncoupled, dynamics. In doing this, we dedicate a stronger attention to the qualitative, or effective, dynamics, in the same search for generality that animates bifurcation theory. Accordingly, we consider the bifurcation diagrams of the mean field as reflecting the most important features of the disorder-induced regimes.

This choice is reflected in the analytical approach that we propose, the order parameter expansion . Formally, such an expansion is a sort of moment expansion around the mean field dynamics in the perfectly synchronous regime, where the mean field equation of motion results coupled with other macroscopic variables, the order parameters . Instead of providing an approximation of the order parameters on the basis of some properties of the population, we consider their evolution in time as if they were macroscopic degrees of freedom. Altogether, this give rise to an infinite hierarchy of equations, that are closed making use of different assumptions depending on the microscopic features of the population. In this manner, we are able to derive a low-dimensional dynamical system that not only approximates very well (as long as the closure assumptions are satisfied) the effective macroscopic dynamics of the population, but that as well reflects a hierarchical structure that seems to be present in the collective degrees of freedom.

Although this program is developed in detail only in the cases of globally coupled dynamical systems with parameter mismatch and additive independent noise, the ideas that motivate it seem to be applicable also to systems with different microscopic structures. Among these, it is worth mentioning spatially extended systems. An extended medium can indeed be thought as a divided into a “local” environment, where the microscopic oscillators sitting on each of its points are globally coupled (this is an approximation of long-range, relative to the local scale, coupling), and by the rest of the system, loosely correlated to the local population. The interaction between such two mesoscopic components can be given again an effective description, as done by Lemaitre, Chaté and Manneville [87, 88, 86].

Other systems where the application of a similar approach is promising is that of stirred oscillatory media. These display a series of qualitative changes in the

mean oscillation amplitude while going from a completely mixed state, where the oscillations are homogeneous, to a state where the oscillators are only locally coupled. The reaction-advection-diffusion equations describing such a system can be developed in a series of eigenfunctions around the main oscillating mode. Finding an opportune closure assumption for this system could allow to justify the close correspondence of their behaviour with the bifurcations observed in globally coupled systems, observed by Neufeld et al. [112].

Finally, systems that seem prone to a macroscopic analysis are populations of stochastically updated chaotic maps. Morita and Chawanya have shown that a change in the probability of updating can cause qualitative modifications of the mean field dynamics [104], in something that resembles closely what one observes for globally coupled noisy systems.

Chapter 3

Parameter mismatch

Although populations of identical dynamical systems have revealed extremely useful in the study of the collective properties of systems with many degrees of freedom, real populations, and notably biological ones, inevitably possess some degree of microscopic diversity. The differences among the units that compose the population can reveal themselves at the level of the emergent dynamics, thus giving rise to regimes that cannot be observed when the components are strictly identical.

Since Winfree [174] stressed the importance of relaxing that assumption, including diversity in the form of paramter mismatch, a wealth of theoretical investigation, briefly reviewed in Chapter 2, has addressed the collective regimes of populations with microscopic disorder.

One way of modelling such disorder is to assume that all the individual units are described by the same functional form, but that they possess intrinsically different parameter values. Such a generalisation is important in comparing mathematical models with the experimental results on the population they are meant to describe.

This chapter presents in greater detail the properties of the strong coupling regimes in populations with parameter mismatch, addressing the influence that this kind of microscopic disorder has on the collective dynamics. In particular, we will show that the spread in the mismatch distribution acts as a control parameter, inducing qualitative changes of the macroscopic attractor.

Such mismatch-induced bifurcations are demonstrated in Sec. 3.1 for populations of globally coupled chaotic oscillators with time-scale mismatch. This populations, that will be used as a prototype in this chapter, and others with different microscopic features, such as size, nature of the single-element dynamics and parameter distribution are addressed in more detail in Chapter 4.

Section 3.3 introduces the analytical approach that will be used throughout the first part of this thesis, the order parameter expansion. By means of such approximation technique, we derive the equations of motion for two macroscopic variables, the order parameters, that account for the effective dynamics of the population's coherent regimes. The asymptotic and transient behaviour of these macroscopic degrees of freedom will be compared in Chapter 4 to the collective be-

haviour of several populations with parameter mismatch. The agreement between the numerical simulations of the high-dimensional full system and the effective description derived in Section 3.3 testifies the generality of the proposed method.

Chapters 5 and 6 deal with a second modelling approach to microscopic disorder. According to this, diversity is introduced by adding an independent stochastic term (called "noise") to each individual equation. The consequences of different choices in the nature, parametric or stochastic, of microscopic disorder will eventually be addressed in Chapter 7, where we also discuss in general the results of the first part of the thesis and their perspectives of future developments.

3.1 Populations with parameter mismatch

As specified in Chapter 1, the present dissertation deals with populations of dynamical systems coupled *all-to-all*, described by the set of equations:

$$\dot{\mathbf{x}}_j = \mathbf{f}\left(\mathbf{x}_j, p_j\right) + \frac{\mathcal{K}}{N}\sum_{i=1}^{N}\left(\mathbf{x}_i - \mathbf{x}_j\right) \qquad j = 1, 2, \ldots, N. \tag{3.1.1}$$

Here, the single-element (or microscopic) dynamics $\mathbf{f}_j(\mathbf{x}_j) = \mathbf{f}\left(\mathbf{x}_j, p_j\right)$, defined by the smooth function $\mathbf{f}_j : \mathbb{R}^n \to \mathbb{R}^n$, describes the evolution of n state variables, that are the entries of the state vector $\mathbf{x}_j \in \mathbb{R}^n$.

We speak of *linear coupling* because the equation of motion of one element is altered by a term that is a linear combination of the difference between the the state vector of the considered elements and the state vectors of the other elements. This form of coupling approximates a *diffusive coupling* (used for chemical systems, where $\mathbf{x}$ is a set of concentrations) for the cases in which the diffusion is sufficiently slow with respect to the time-scale of the phenomena described by the single-element dynamics. The linear form of the coupling term is a consequence of a linearisation of the diffusion operator around a fixed point [33] and holds strictly close to a stationary uniform state. When the systems are further out of equilibrium, the approximation of diffusive coupling can be insufficient. Here, we mainly consider populations with linear coupling, even if in the derivation of the macroscopic equations, presented in Section 3.3, is susceptible of an extension to a case where nonlinearities enter into play.

In Equation (3.1.1), the influences of the state vector components of one population element on the others are quantified by the entries of the *coupling matrix* $\mathcal{K}$. When this matrix is proportional to the identity matrix, that is $\mathcal{K} = K\mathbb{I}$, we will speak of *isotropic vectorial coupling*, and call $K \in \mathbb{R}$ the *coupling strength*. Instead, when only one of the components is coupled (the coupling matrix has just one non-vanishing term, on the diagonal), we will speak of *scalar coupling*. Since the fully synchronous solution is unstable even for identical units if it is repelling in any direction, we require the eigenvalues of the coupling matrix to be have a positive real part, and correspondingly $K > 0$ when the coupling is isotropic.

When each population element is equally influenced by all other units, the all-to-all coupling term can be recast into the form of a *global coupling*:

$$\frac{1}{N}\sum_{i=1}^{N}(\mathbf{x}_i - \mathbf{x}_j) = (\mathbf{X} - \mathbf{x}_j)\,,$$

where the individual element is influenced by the average state vector, that is by the *mean field*:

$$\mathbf{X} = \langle \mathbf{x} \rangle = \frac{1}{N}\sum_{i=1}^{N}\mathbf{x}_i.$$

In the following we will consider a more general formulation of Eq. (3.1.1):

$$\dot{\mathbf{x}_j} = \mathbf{f}\,(\mathbf{x}_j, p_j) + \mathbf{K}\,(\mathbf{X}, \mathbf{x_j}) \qquad j = 1, 2, \ldots, N, \tag{3.1.2}$$

where the form of the feedback of the collective onto the individual dynamics, is defined by the global coupling function $\mathbf{K} : \mathbb{R}^n \to \mathbb{R}^n$. In order it to be consistent with the scenario of perfect synchronisation of identical systems, the coupling function has to satisfy the relation $\mathbf{K}\,(\mathbf{X}, \mathbf{X}) = 0$ and the eigenvalues of its Jacobian matrix $D_{\mathbf{x}}\mathbf{K}\,(\mathbf{X}, \mathbf{X})$ must have positive real part. In the applications, however, we will go back to the case of linear vectorial coupling, and use the relation $\mathbf{K}\,(\mathbf{X}, \mathbf{x_j}) = \mathcal{K}(\mathbf{X} - \mathbf{x}_j)$.

The parameter N defines the size of the population. We speak of *thermodynamic limit* when the population size is let go to infinity.

For simplicity, we assume that the diversity within the population can be accounted for by a scalar parameter $p_j \in \mathbb{R}$, from which the single-element dynamics depends linearly (in the sense that the partial derivatives of $\mathbf{f}\,(\mathbf{x}_j, p_j)$ of order bigger than one in p_j are all zero).

The mismatch of the parameters, an example of which is displayed in Figure 3.1, does not change in time and is assumed to consist in a distribution $G : \mathbb{R} \to \mathbb{R}$. In principle, we do not require any regularity property of this distribution, except that it has finite moments $m_q = \langle [G(p) - G(p_0)]^q \rangle$. This allows us to consider finite as well as infinite population sizes.

In the context of the present study, we will distinguish between individual-level parameters, i.e. the parameters p_j governing the evolution of the single elements, and population-level parameters. These latter will be for us the coupling constant and the parameter distribution moments, that are related either to the interaction between individuals or to the coarse-grained description of the diversity within the population. In particular, in order to address the effect on the collective dynamics of a change in the microscopic disorder, the variance σ^2 of the parameter distribution will be chosen as a control parameter. This choice, that might at first seem arbitrary, will later be justified on the basis of theoretical arguments.

The change of the focus from the detailed description of the dynamics of each population element to that of macroscopic, averaged quantities reflects on the observation of the population dynamics. Rather than following the behaviour of

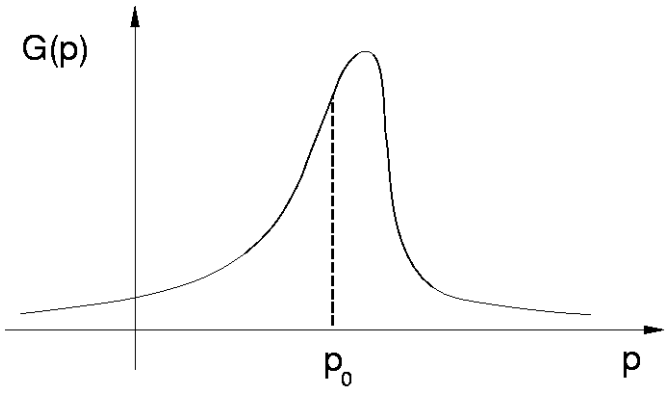

Figure 3.1: Example of an assigned distribution for the parameters of Eq. (3.1.1). The distribution is univocally identified by its moments, the first of which is the mean p_0.

one individual within the population, we will concentrate on the mean field and on other quantities averaged over the whole population, that will be called *order parameters*. This term is used in synergetics [54], to indicate the slow degrees of freedom of a system, to which fast variables are slaved. In cases where a center manifold reduction can be explicitly performed, the slow variables are those that identify the manifold. The values of these variables, then, play the role of parameters in the equations for the fast modes. In the following, we propose a method for identifying systematically such order parameters (also called *macroscopic variables*) in populations of globally coupled dynamical systems with disorder. These quantities will be shown to provide an effective description of the collective dynamics, that is of the behaviour of the mean field for populations with parameter mismatch.

3.2 Collective dynamics

Let us now examine what kind of regimes one can observe in a population defined by Eq. (3.1.1). Chapter 2 reviews the main results for populations of limit cycle oscillators with natural frequency mismatch. Here, we will present an overview of the collective regimes of populations with time-scale mismatch, that can be viewed as a generalisation of the aforementioned case to populations of dynamical systems whose frequency is not univocally defined, such as chaotic attractors.

The j-th element of the population is ruled by the equation:

$$\dot{\mathbf{x}}_j = \tau_j \mathbf{f}\left(\mathbf{x}_j\right) + k\left(\mathbf{X} - \mathbf{x}_j\right), \tag{3.2.1}$$

which is a special case of Eq. (3.1.1) with parameter τ_j defining the time-scale of the single-element dynamics and with isotropic vectorial coupling.

The case in which the single-element dynamics is defined by a map rather than by an ODE will be discussed in Section 3.3 and again in Chapter 7.

The uncoupled element equation of motion $\mathbf{f}(\mathbf{x})$ will be chosen to be chaotic, so that the population elements differ from each other with respect to the speed at which they move along the trajectory, but not for the shape of their attractor. The parameters that define the dynamics of one uncoupled individual are kept constant, and thus not explicitly included in the formulation of the single-element dynamics. The only changes we will perform are on the distribution of the time-scale τ.

The state vector $\mathbf{x} = (x, y, z)$ of the uncoupled element will be chosen to evolve (modulus a time rescaling) according to the equations of motion $\mathbf{f} = (\dot{x}, \dot{y}, \dot{z})$ of two systems, those of Rössler and of Lorenz, that are prototypes of chaotic attractors in $\mathbb{R}^3$.

The *Rössler system* is the defined by the following ODEs:

$$\begin{cases} \dot{x} = & -(y+z) \\ \dot{y} = & x + a\,y \\ \dot{z} = & b + x\,z - c\,z. \end{cases} \tag{3.2.2}$$

The parameters of all the population elements take the values $a = 0.1$, $b = 0.4$ and $c = 8$. Accordingly, every individual evolves asymptotically on the so-called funnel attractor. By looking at the projection of this attractor onto the plane (x, y), displayed in Figure 3.2, it is evident that in the lack of a "hole" in the trajectory around the origin hampers the definition of a generalised phase for the chaotic motion.

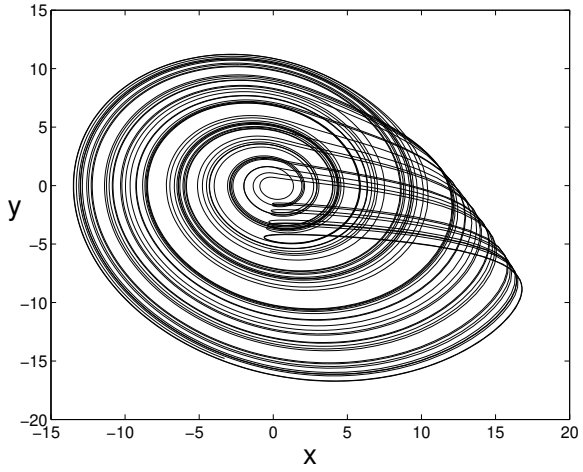

Figure 3.2: Projection onto the plane (x, y) of the chaotic attractor for the Rössler system Eq. (3.2.2), with parameters indicated in the text.

The *Lorenz system* is defined as:

$$\begin{cases} \dot{x} = & p\,(y - x) \\ \dot{y} = & -x\,z + r\,x - y \\ \dot{z} = & x\,y - b\,z. \end{cases} \tag{3.2.3}$$

Here, we will use the parameters $p = 10$, $b = 8/3$ and $c = 28$ introduced by Lorenz. All the population elements evolve, when uncoupled, onto the attractor displayed in Figure 3.3.

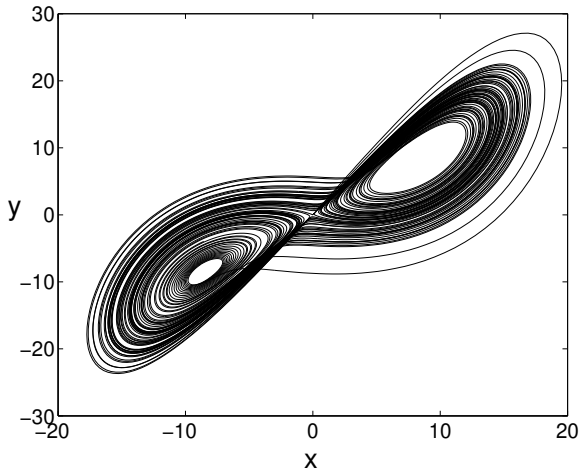

Figure 3.3: Projection onto the plane (x, y) of the attractor for the Lorenz system Eq. (3.2.3) and parameters indicated in the text.

In the examples presented in this section, the time-scales are distributed uniformly around the average value $\tau_0 = 1$ and the population size is $N = 32$. Other sets of parameters, distribution shapes and population sizes will be considered in Chapter 4.

We will mainly focus on the regimes of strong coupling, where the dynamics of the population is sufficiently coherent (in a sense that will be more precisely specified in the next section). In order to visualise the state of the population, this will be projected onto the phase space of one single oscillator (or onto a subspace therein), as illustrated for the case of limit cycles in Chapter 2.

Let us start by considering the case in which the parameters are all identical, and thus their distribution is a Dirac's delta cantered on τ_0. The regime where all the population elements evolve on the single-element attractor $\mathbf{x}_j = \mathbf{x}_i = \mathbf{X} \quad \forall j, i$ is a solution of Eq. (3.1.2) that exists independently of the linear properties of the coupling function around 0 (i.e., in the case of linear coupling, independently of the coupling strength). For isotropic couplings, this solution is linearly stable

when the coupling strength exceeds a threshold K^*, above which the population is in a regime of perfect synchronisation. The way in which such stability and the property of global stability are lost for couplings below K^* depends on the features of the single-element dynamics. Two typical scenarios are the appearance of phase-locked solutions, where the oscillators entrain their average frequency (for more details, see Section 2.3), shown in Figure 3.4, and clustered solutions, where the population splits into subpopulations, or clusters, while the mean field maintains a chaotic dynamics similar to the single-element attractor (Figure 3.5).

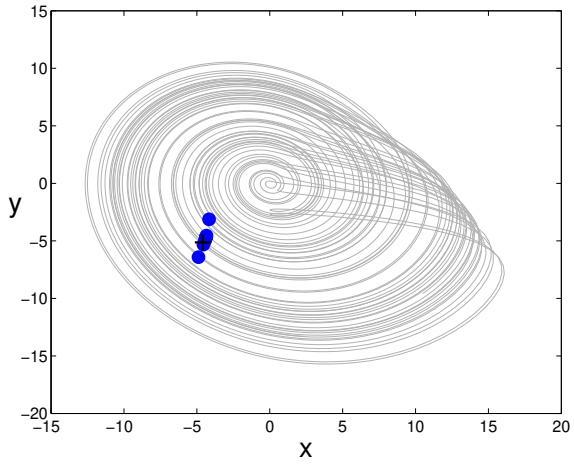

Figure 3.4: Phase-locked solution for a population of $N = 32$ Rössler attractors (single-element parameters specified in the text, $\sigma = 0$, $K = 12$).

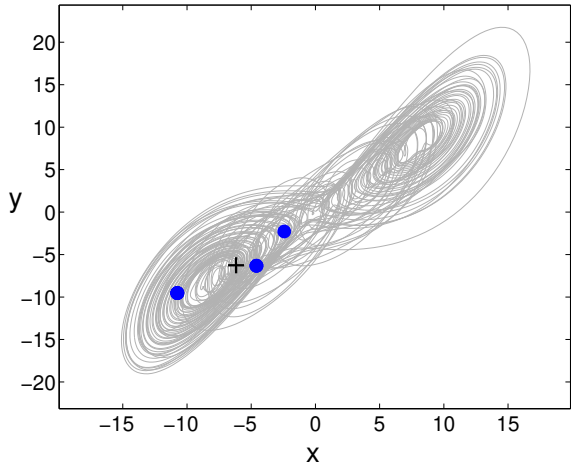

Figure 3.5: Three-cluster solution for a population of $N = 32$ Lorenz attractors (single-element parameters specified in the text, $\sigma = 0$, $K = 0.5$).

In the region of strong coupling, where the perfectly synchronous solution is stable, one expects the introduction of a small mismatch in the time scales not to alter the mean field dynamics qualitatively. If this was not true, the fully synchronous regime would appear as a non-generic case, and its relevance for the modelling of real systems would be greatly reduced.

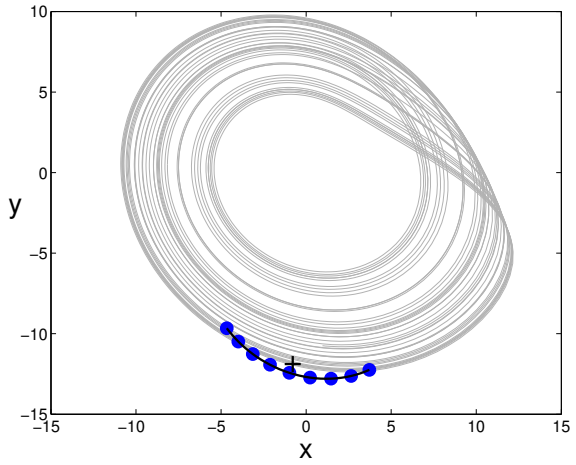

Figure 3.6: Regime of general (lag) synchronisation in a population of $N = 32$ Rössler attractors (single-element parameters specified in the text, $\sigma = 0.24$, $k = 1.1$). The dots indicate population elements, disposed on the synchronisation manifold (black line). The grey line is the attractor of the mean field (cross).

When the parameters are distributed, the population elements dispose themselves, in the projection onto the phase space of one individual, along a manifold that moves solidly with the mean field. This is shown for a population of Rössler systems in Figures 2.5 and 3.6. In spite of the fact that the shape of this manifold changes in time, the arrangement of the oscillators on it does not vary, so that the position of one population element is parametrised by the value of its time-scale. This regime corresponds to the concept of generalised synchronisation [137] applied to populations, where the mean field plays the role of the forcing signal on the individual dynamics. This regime also corresponds to the so-called lag synchronisation [134], since the arrangement along the synchronisation manifolds maintains an effective phase shift among the microscopic oscillators.

Similar synchronous regimes of macroscopic chaos are found for the Lorenz system, as shown in Figure 3.7.

As long as the mismatch in the parameters remains small, the mean field dynamics is chaotic and the attractor is at first sight indistinguishable from the single-element one. When the mismatch becomes larger, however, the mean field displays a dynamics qualitatively different from that of the single element.

At first, an increase in the parameter mismatch induces a change in the geometry of the chaotic attractor: from a “funnel attractor” similar to the single-element

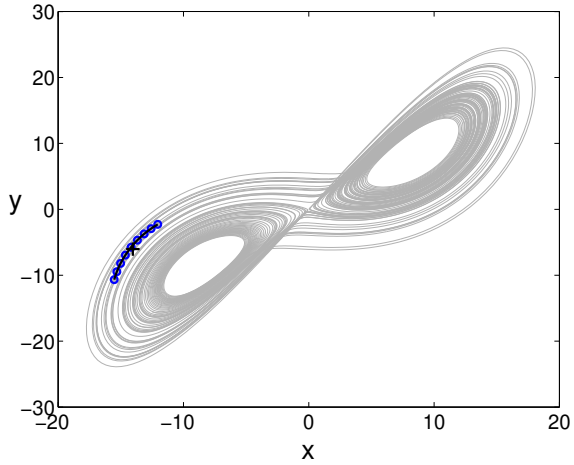

Figure 3.7: Regime of general synchronisation for a population of $N = 32$ Lorenz attractors (single-element parameters specified in the text, $\sigma = 0.8$, $K = 6$).

one Figure 3.2 the mean field bifurcates into a regime of "spiral chaos", as shown in Figures 2.5 and 3.6. This attractor is characterised by the fact that the orbit never lies in a neighbourhood of the origin, so that a generalised phase can be properly defined according to Eq. (2.4.3).

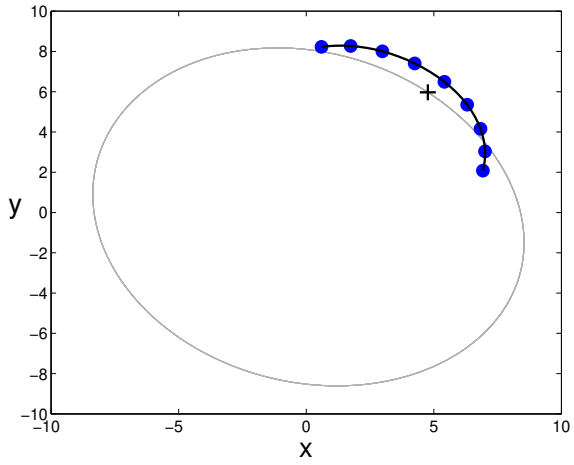

Figure 3.8: Regime of general (lag) synchronisation in a population of $N = 32$ Rössler attractors (single-element parameters specified in the text, $\sigma = 0.23$, $K = 1.1$). The dots indicate population elements, disposed on the synchronisation manifold (black line). The grey line is the attractor of the mean field (cross).

The collective regimes of populations of oscillator with parameter mismatch

can however be completely different in nature from the single-element behaviour. For instance, fig. 2.6, 3.8 and 3.9 show three different cyclic regimes of the collective dynamics for a population of Rössler oscillators. The first two cases, where the mean field dynamics has periods four and one, respectively, take place for large mismatch. In this cases there is no neighbouring chaotic regime that can be reached by changing continuously the parameter mismatch. The third case, on the other hand, corresponds to a period six window that appears in a region of otherwise chaotic dynamics.

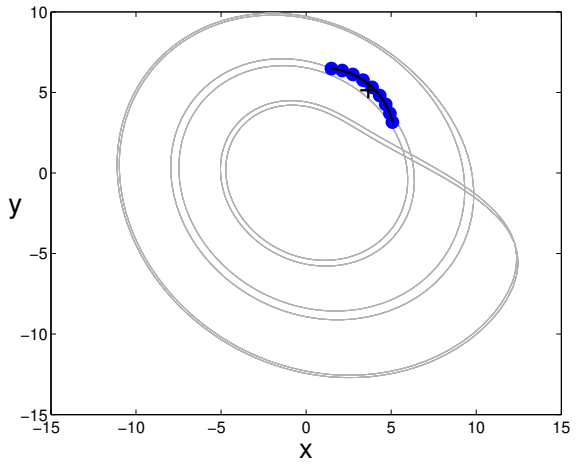

Figure 3.9: Regime of general (lag) synchronisation in a population of $N = 32$ Rössler attractors (single-element parameters specified in the text, $\sigma = 0.35$, $K = 1.1$). The dots indicate population elements, disposed on the synchronisation manifold (black line). The grey line is the attractor of the mean field (cross).

For still greater parameter mismatch, the limit cycle shown in Figure 3.8 shrinks and eventually the mean field stops oscillating. This regime of *amplitude* or *oscillator death* has been discovered in populations of limit cycle oscillators by Yamaguchi and Shimitzu [177] and then extensively studied by Shiino and Frankovicz [145], Ermentrout and coworkers [46, 6, 45] and Strogatz and coworkers [99, 153]. The existence of the same phenomenon in populations with non-cyclic microscopic dynamics has been shown for coupled Rössler systems [119], Brusselator systems [10], bursters [165]. Moreover, a number of studies have been conducted on the role of oscillator death in populations with delayed coupling [132, 8, 7], in spatially extended systems [135] and in reaction-advection-diffusion equations for stirred stirred oscillatory media [112].

In Section 4.3 we will show that this is indeed a general phenomenon occurring in a large class of dynamical systems and that the mechanism at the basis of oscillator death is the stabilisation of a focus solution for the single-element dynamics.

In the case of the population of Rössler oscillators considered above, the regime

of amplitude death consists in all the population elements, and consequently the mean field itself, lying stationary on the origin, that is the only equilibrium point.

If the single-element dynamics possesses two ore more saddle-focus equilibria, these become macroscopically linearly stable for sufficiently large parameter mismatch, therefore causing the collective dynamics to be bistable. In the case of the Lorenz system, for instance, the two non-vanishing symmetric solutions are susceptible of becoming macroscopic attractors, but not the origin, that is an unstable node.

Hence, parameter mismatch leads the mean field to have a completely different behaviour as compared with an uncoupled individual of the population. The strong interaction among heterogeneous population components leads not only to the loss of the chaotic nature of the dynamics, but also to the disappearance of the emergent oscillations and of the mixing properties of the system.

Macroscopic multistability in the Lorenz system is not only present in the case of very large diversity, when two equilibria become stable for the mean field dynamics, but also for intermediate mismatch. For instance, the macroscopic chaotic attractor shown in Figure 3.7 coexists with the cycle shown in Figure 3.10 and with its symmetric with respect to the origin.

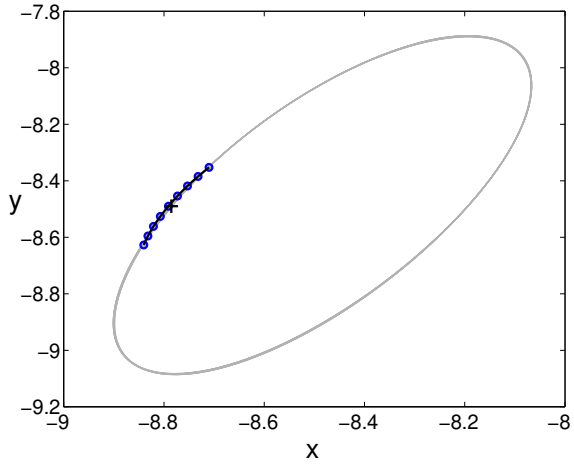

Figure 3.10: Regime of general synchronisation for a population of $N = 32$ Lorenz attractors (single-element parameters specified in the text, $\sigma = 0.8$, $K = 6$). This cyclic attractor coexists with the chaotic attractor displayed in Figure 3.7.

It is important to notice that such strong-coupling synchronous regimes are characterised by the presence of a defined synchronisation manifold along which the oscillators are arranged. In this respect, they differ from the partially (imperfectly) synchronous regimes that take place for weaker couplings, where the oscillators with the most extreme parameter values detach from the synchronisation manifold and evolve independently, analogously to what happens to limit cycle oscillators, shown in Figure 3.11, where the synchronisation manifold folds onto itself and

looses its smoothness when the loops of the manifold close on themselves.

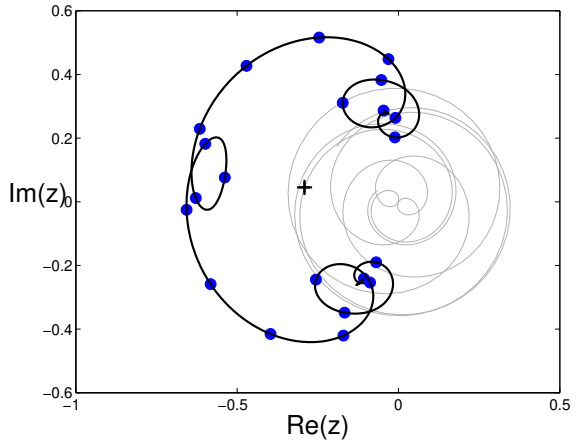

Figure 3.11: Partially locked regime for the population of limit cycles Eq. (2.3.1) ($\sigma =$). The mean field (cross) evolves along the trajectory indicated by the Gray line. The oscillators of a population of size $N = 1000$ are disposed along the black line, the big dots indicating a sample of equally spaced (in terms of natural frequency) elements of the population.

The regimes of generalised synchronisation that we observe for high coupling are also distinguished from the clustering regimes, where the synchronisation manifold, if it exists, is not continuously parametrised by the times scale values.

In the synchronous regimes we are interested in, there exists a *synchronisation manifold* $M(X, p)$ in the phase space $\mathbb{R}^n$ of the single-element dynamics. If the population depends smoothly on the parameter, the oscillators are orderly arranged along a curve embedded in the synchronisation manifold:

$$\mathbf{x}_j(t) = \mathbf{M}(\mathbf{X}(t), p_j).$$

The parameter p here plays the role of a coordinate along this curve, defining the position of the j-th population element on the synchronisation manifold. In the cases in which the relaxation over the synchronisation manifold is much faster than the collective dynamics this manifold can be approximately defined by the implicit function:

$$\mathbf{F}(\mathbf{M}, p) + \mathbf{K}(\mathbf{X}, \mathbf{M}) = 0.$$

In the cases of generalised synchronisation considered above, the oscillators tend to spread in the direction of the orbit. This way of loosing the perfect synchrony is generic for strong couplings, where the perfectly synchronous solution is stable for identical oscillators. Indeed, it is the vanishing Floquet multiplier parallel to the orbit that identifies the first direction that will become unstable. When the coupling is weak, instead, the transverse instability can take place even for identical individuals, and thus be attained before than that along the orbit.

Given a sufficiently strong coupling one can thus study how the collective dynamics changes when the parameter mismatch is gradually increased. Taking the

standard deviation σ of the parameter distribution, that measures the mismatch, as the control parameter, the bifurcation diagram for the mean field can be numerically obtained (Figure 3.12).

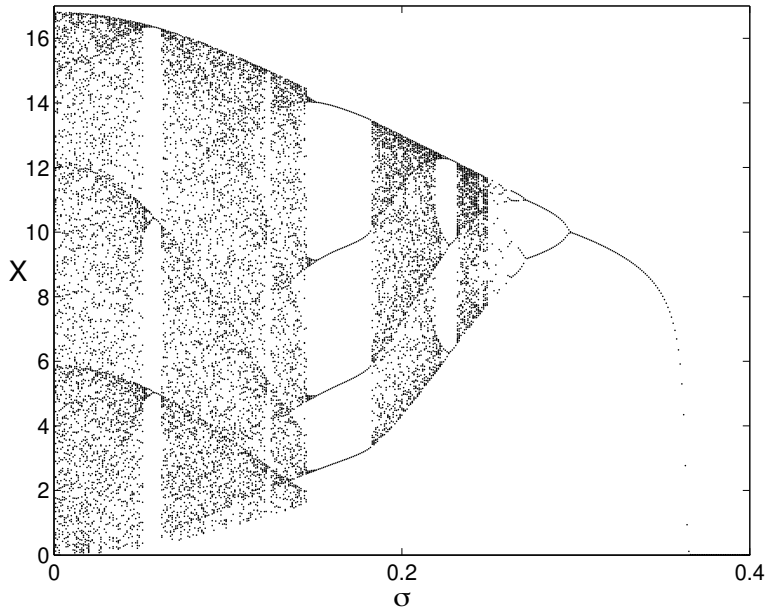

Figure 3.12: Bifurcation diagram of the mean field of a population of Rössler oscillators (Eq. (3.2.2) with parameters in the text, $k = 1$) with respect to the standard deviation σ of the time-scale distribution. The figure displays the Poincaré map obtained by considering the successive maxima in the time series of the coordinate $X = \langle x \rangle$.

This bifurcation diagram summarises the different regimes mentioned above, displaying periodic windows within the chaotic region (Figure 3.9), a backward period-doubling bifurcation cascade, to which the cycles of period equal to a power of two (Figures 3.8 and 2.6) belong, and eventually, for large parameter mismatch, oscillator death.

One last thing to be noticed is that, contrary to the cases of clustering and partial synchronisation, the strong-coupling regimes are very robust with respect to a change in the population size: changing the number of interacting oscillator in general only weakly affects the mean field dynamics. This point will be discussed in more detail in the next Chapter.

In the next section, we will propose a method, the order parameter expansion, and an approximation scheme that will allow us to describe in a parsimonious way all the regimes illustrated here. Chapter 4 is then dedicated to the application of such method to populations of dynamical systems with different microscopic structures.

3.3 Order parameter expansion

As we have just seen in Section 3.2, the fact that a mismatch in parameters causes the loss of perfect synchrony hinders the possibility of describing the mean field dynamics as a "magnification" of the single-element behaviour. The coherence in the motion of the population, due to the existence of a synchronisation manifold, however seems to constrain the macroscopic attractor to remain low-dimensional, independently of the actual size of the population. This section develops a method for deriving systematically an effective low-dimensional system of ODEs, that account for the observed collective dynamics, starting from the microscopic features of the population, that are the single-element dynamics and the distribution of parameters.

Since we are interested in considering both the cases of continuous and discrete time dynamical systems, the equations for the j-th population element are here recast into the form:

$$\mathcal{T}\mathbf{x}_j = \mathbf{F}(\mathbf{x}_j, p_j) + \mathbf{K}(\mathbf{X}, \mathbf{x}_j), \tag{3.3.1}$$

where the evolution operator $\mathcal{T}$ stands for the time derivative $\mathcal{T}\mathbf{x} = \dot{\mathbf{x}}$ in the case of ODEs, and for the time iterate $\mathcal{T}\mathbf{x}(t) = \mathbf{x}(t+1)$ in the case of maps. The global coupling term $\mathbf{K} : \mathcal{R}^n \to \mathcal{R}^n$ makes the evolution of each population element depend on the mean field $\mathbf{X}$. The parameters $p_j \in \mathbb{R}$ are taken from a distribution of average $p_0 = \langle p \rangle$ and variance $\sigma^2 = \langle (p - p_0)^2 \rangle$.

We will moreover assume for simplicity that the single-element dynamics $\mathbf{F}$ depends linearly on the parameter p. Even if this is not strictly true, it is a good approximation as long as the parameter mismatch is sufficiently small.

We now perform the change of variables:

$$x_j = X + \epsilon_j, \tag{3.3.2}$$

that is we express the position of every element of the population in terms of the mean field. This transformation is helpful because of the time-scale separation between the fast relaxation on the synchronisation manifold, on which the mean field acts as a forcing term, and the comparatively slower collective dynamics.

The next step consists in feeding back the evolution of the oscillators, embedded in the time-dependent synchronisation manifold, onto the mean field dynamics. In performing this last step, we will make some approximations that allow us to disregard the details of the manifold geometry.

Let us start by deriving the mean field equation of motion in a way that decouples the mean field dynamics from that of the displacements of the oscillators from it. In order to do this, we expand Eq. (3.3.1) in series both with respect to ϵ_j and with respect to the parameter mismatch $\delta_j = p_j - p_0$:

$$\begin{aligned} \mathcal{T}\mathbf{x}_j = \quad & \mathbf{F}(\mathbf{X}, p_0) + D_{\mathbf{x}}\mathbf{F}(\mathbf{X}, p_0)\,\epsilon_j + D_p\mathbf{F}(\mathbf{X}, p_0)\,\delta_j + \\ & D_{\mathbf{x},p}\mathbf{F}(\mathbf{X}, p_0)\,\epsilon_j\,\delta_j + \mathbf{R}(X, p_0, \epsilon_j) + \mathcal{K}(\mathbf{X})\,\epsilon_j, \end{aligned} \tag{3.3.3}$$

where the coupling matrix is the Jacobian of the coupling function evaluated in the perfectly synchronous regime: $\mathcal{K}(\mathbf{X}) = D_{\mathbf{x}}\,[\mathbf{K}(\mathbf{X}, \mathbf{X})]$.

Averaging these equations over the population provides a description of the mean field dynamics in terms of the mean field itself and of other *order parameters*. These are macroscopic variables, consisting in averages over the population of terms of different degree in ϵ and δ. Their equations of motion can be derived from the single-element dynamics analogously to what done for the mean field. In this way, the population dynamics is described by an infinite hierarchy of equations for macroscopic degrees of freedom, that we will call *order parameter expansion*. The actual definition of the relevant order parameters reflects the specificity of the population and is different in the case in which disorder is due to parameter mismatch or noise. In this section we build the order parameter expansion for the population with parameter mismatch defined by Eq. (3.3.1) and in Chapter 5 we will write another one for populations with microscopic noise.

Due to the linear dependence of the single-element dynamics on the parameter, the term $\mathbf{R}(X, p_0, \epsilon_j)$ is independent of δ_j and it contains terms of order greater than one in ϵ_j.

We will now make the assumption that:

$$||\epsilon_j|| = ||\mathbf{x}_j - \mathbf{X}|| \ll 1, \tag{3.3.4}$$

where the norm is the Euclidean distance in $\mathbb{R}^n$. This condition reflects the idea that, contrary to the case of incoherence where the oscillators evolve "far away" form the mean field, in the synchronous cases we address the points representative of the population follow solidly the motion of the mean field. We will refer to Eq. (3.3.4) as the assumption of *coherence*.

Under this assumption, we can neglect the term $\mathbf{R}$ in Eq. (3.3.3) and hence get, by averaging, the equation of motion for the mean field:

$$\mathcal{T}\mathbf{X} = \mathbf{F}(\mathbf{X}, p_0) + \mathcal{D}_{\mathbf{x},p}\mathbf{F}(\mathbf{X}, p_0)\langle\delta\,\epsilon\rangle. \tag{3.3.5}$$

Now we can see that the mean field is coupled to a second order parameter, that is a macroscopic variable obtained by averaging over the population. We will call this the *shape parameter* and define it as:

$$\mathbf{W} = \langle\delta\,\epsilon\rangle. \tag{3.3.6}$$

The reason for such a name is that this quantity is related to the way in which the oscillators are arranged around the mean field. Indeed, large values of the norm of the shape parameter indicate the population elements are dispersed in the phase space around their average, while the fact that W is oriented perpendicular to X corresponds to situations where the synchronisation manifold lies along the orbit.

We now want to determine the dynamics of the shape parameter in order to obtain, eventually, a closed system for two macroscopic variables. By differentiating Eq. (3.3.6) and by substituting Eq. (3.3.3), we obtain:

$$\mathcal{T}\mathbf{W} = [D_{\mathbf{x}}\mathbf{F}(\mathbf{X}, p_0) - \mathcal{K}(\mathbf{X})]\ \langle\delta\,\epsilon\rangle + D_p\mathbf{F}(\mathbf{X}, p_0)\,\langle\delta^2\rangle + D_{\mathbf{x},p}\mathbf{F}(\mathbf{X}, p_0)\,\langle\epsilon\,\delta^2\rangle, \tag{3.3.7}$$

where we have again neglected terms of order higher than one in ϵ.

To close the system, let us notice that the term $D_{\mathbf{x},p}\mathbf{F}(\mathbf{X}, p_0)\,\langle \epsilon\,\delta^2\rangle$ is negligible in two cases. With respect to $D_{\mathbf{x}}\mathbf{F}(\mathbf{X}, p_0)\,\langle \delta\,\epsilon\rangle$, if the parameter mismatch, and thus the δ_j, are small. With respect to $D_p\mathbf{F}(\mathbf{X}, p_0)\,\langle \delta^2\rangle$ if the ϵ_j are small, that is for sufficiently strong coupling. The approximation that it is strictly zero is accurate enough for the study of the regimes of strong coupling, and we will therefore discard the last term of Eq. (3.3.7). The accuracy of the macroscopic description can however be improved by estimating such term on the basis of the geometry of the synchronisation manifold, that leads to an additional term proportional to the shape parameter.

Equations (3.3.5) and (3.3.7) hence provide a macroscopic dynamical system, or *reduced system*, that reads:

$$\begin{cases} \mathcal{T}\mathbf{X} = \mathbf{F}(\mathbf{X}, p_0) + \mathcal{D}_{\mathbf{x},p}\mathbf{F}(\mathbf{X}, p_0)\,\mathbf{W} \\ \\ \mathcal{T}\mathbf{W} = \sigma^2\,\mathcal{D}_p\,\mathbf{F}(\mathbf{X}, p_0) + \left[\mathcal{D}_{\mathbf{x}}\,\mathbf{F}(\mathbf{X}, p_0) - \mathcal{K}(\mathbf{X})\right]\,\mathbf{W}. \end{cases} \tag{3.3.8}$$

This set of equations provides a description of the collective dynamics in terms of population-level parameters, that are those related to the features of the coupling function in the completely synchronous regime $\mathcal{K}$ and the first moments (average value p_0 and variance σ^2) of the parameter distribution.

In the limit of identical oscillators, when $p_j = p_0 \quad \forall j$, the shape parameter vanishes and we retrieve the case of perfect synchronisation, where the macroscopic evolution is ruled by the same equations as the single-element dynamics $\mathcal{T}\mathbf{X} = \mathbf{F}(\mathbf{X}, p_0)$. With increasing parameter mismatch, the shape parameter becomes nonzero and the mean field dynamics results to be effectively coupled to the geometry of the synchronisation manifold.

Equation (3.3.8) thus consist of an unfolding of the single-element dynamics. This means that the macroscopic behaviour that is attained by changing the parameter distribution, even if it is qualitatively different from the fully synchronous regime, nevertheless belongs to a family of dynamical systems containing the single-element dynamics.

It is important to notice that the reduced system has been derived without making any assumption on the size of the population and is itself independent of N. This property reflects the fact that a change in the population size only weakly affects the qualitative features of the synchronous regimes that one observes for strong coupling. Moreover, this explains why the results obtained for the thermodynamic limit, where the population can be described in terms of a probability distribution function [153], can be applied also to finite, and even small, populations.

Similarly, the fact that we have made no explicit assumption about the parameter distribution, except that it possesses finite moments, establishes a relation of equivalence on the space of the distributions, one class of equivalence being identified by the values of its first moments. From Eq. (3.3.8) follows that different parameter distributions having the same mean value and variance will cause

an analogous change in the macroscopic dynamics, and this independent of their symmetry, modality and kurtosis.

The choice of truncating the infinite-dimensional order parameter expansion to the first order in ϵ is due to the fact that an increase in the approximation level leads to extremely complicated equations (Eq. (3.3.8) is already six-dimensional for the examples of chaotic ODEs presented in Section 3.2). Furthermore, already this crude approximation provides an accurate description of the collective regimes if the coupling is sufficiently strong. The next chapter will present a case, that of identical Ginzburg-Landau oscillators, in which the expansion is carried on up to the second order.

When maps are considered, instead of ODEs, the mathematics associated with the order parameter expansion becomes more treatable. In Chapter 5 we will address thus cases in which more and more details on the collective dynamics are obtained by increasing the degree of the neglected terms.

The next chapter is dedicated to the application of Eq. (3.3.8) to populations with different microscopic features (single-element dynamics, size and parameter distributions). With the support of numerical simulations, we will show that the reduced system is actually able to capture the essential features of the collective dynamics of strongly and globally coupled dynamical systems.

Chapter 4

Order parameters in populations with parameter mismatch

In the previous chapter we have derived in a general form equations for the macroscopic dynamics of populations of globally coupled dynamical systems with parameter mismatch. These are equations for two order parameters, the mean field and the shape parameter, that consist in averages over the population. We have shown that when the coupling is strong, so that the collective regime is coherent, the equations of motion of these two macroscopic degrees of freedom can be systematically derived from the single-element dynamical system. The changes in the macroscopic dynamics due to parameter mismatch are thus interpreted as an unfolding of the perfectly synchronous regime. This unfolding contains as population-level parameters the coupling constant and the variance of the parameter distribution, but are independent of the size of the population.

In this chapter, we will compare the equations formulated in Section 3.3 with the direct numerical simulation of populations. The agreement between theoretical predictions and the observed collective behaviour is tested for populations with different single-element dynamics. When possible, Eq. (3.3.8) will be addressed analytically.

As a first example, in Section 4.1 we investigate Andronov-Hopf normal forms with natural frequency mismatch. As reported in Chapter 2, this system has been the subject of extensive studies, especially centred on the features of weak-coupling regimes, where the individual dynamics can be reduced to a scalar phase model. Here, we will instead focus on the strong coupling regimes, where Eq. (3.3.8) can be recast into a planar system for the amplitudes of the order parameters. An analytical study of the amplitude equations allows us to describe not only the asymptotic, but also the transient properties of the population. In particular, the response to macroscopic perturbations suggests that measurements of average

quantities could be used as a tool for gathering information about the microscopic structure of the population.

The reduction of the macroscopic equations to a two-dimensional system can not be achieved in general if the parameters of the single-element limit cycle and the coupling term are complex (rather than real) variables. This occurs when the population dynamics is defined by the so-called globally coupled complex Ginzburg-Landau oscillators. In Section 4.2 we first address the case of identical oscillators and study the stability properties of the perfectly synchronous regime. Since the shape parameter vanishes when there is no parameter mismatch, we will close the order parameter expansion to the second order. A linear analysis of the macroscopic equilibrium provides an alternative derivation of the exact stability condition obtained by Hakim and Rappel [55]. Then, we derive the macroscopic equations for the globally coupled complex Ginzburg-Landau oscillators with parameter mismatch. A complete analysis of such equations and the identification of its limits of validity is a far too difficult task to be possibly achieved here. We limit ourselves to present an example of nontrivial collective perturbation response that can be reproduced by the equations for the mean field and the shape parameter.

Finally, in Section 4.3 we consider the population of chaotic oscillators time-scale mismatch. Examples of their collective regimes have been used as explanatory examples in Chapter 3. In this case, the numerical study of the reduced system reveals that Eq. (3.3.8) capture the essential features of the mean field effective dynamics. The descriptive approach developed in the previous chapter let us interpret the qualitative changes in the collective regimes (sometimes called phase transitions [99]), taking place when the parameter diversity is enhanced, as bifurcations of a macroscopic dynamical system. In particular, we perform a detailed study of the regime of oscillator death, where one equilibrium unstable for the single-element dynamics, becomes stable for the population as a whole. The linear stability analysis of the macroscopic equations allow us to find when this regime occurs and identify the class of single-element dynamics that give rise to it.

A general discussion about the advantages and limits of the order parameter expansion method and on its possible future developments is delayed until Chapter 7. Indeed, there we will treat together populations with different sources of microscopic disorder, including also the results of Chapters 5 and 6 on globally coupled noisy maps.

4.1 Andronov-Hopf normal forms

Units with regular oscillatory dynamics, and among those the physical, chemical and biological systems listed in Section 2.1, are commonly modelled by means of the supercritical Andonov-Hopf normal form. This equation indeed accounts for the generic behaviour of a dynamical system close to a supercritical Hopf bifurcation, through which an equilibrium becomes unstable and gives birth to a limit cycle. Although in principle valid only close to the bifurcation point,

this equation has been widely used as a prototypical single-element dynamics for populations of limit cycle oscillators [175, 85]. The evolution equations for the globally coupled Andronov-Hopf normal forms are often written in the rescaled form:

$$\dot{z_j} = \left(1 + i\omega_j - |z_j|^2\right) z_j + K\left(Z - z_j\right). \tag{4.1.1}$$

Here, $z_j \in \mathbb{C}$ represents the position of the jth oscillator in the complex plane. All the oscillators, when decoupled, have the same unitary oscillation amplitude, but different natural frequencies $\omega_j \in \mathbb{R}$. Such frequencies are chosen according to a distribution with average ω_0 and standard deviation σ.

The mean field (also called *centroid* of the population [98, 37]) is in this case the complex variable:

$$Z = \langle z \rangle = \frac{1}{N} \sum_{1}^{N} z_j \tag{4.1.2}$$

and the shape parameter is the other complex macroscopic variable:

$$W = \langle (\omega - \omega_0)\ (z - Z) \rangle.$$

The reduced system Eq. (3.3.8) is now four-dimensional (for a detailed derivation, see De Monte and d'Ovidio [37] and d'Ovidio [42]) and reads:

$$\begin{cases} \dot{Z} = \left(1 - |Z|^2 + i\omega_0\right) Z + i\, W \\ \\ \dot{W} = i\, \sigma^2 Z + \left(1 - K - 2\,|Z|^2 + i\omega_0\right) W - Z^2 W^*. \end{cases} \tag{4.1.3}$$

It is easy to see that if all the frequencies are equal, the macroscopic dynamics corresponds to the case of perfect synchronisation, with all the population elements coinciding with the centroid. When the frequencies are dispersed, the mean field is effectively coupled with the shape parameter, whose evolution depends on the population-level parameters K and σ.

In spite of their formal simplicity, Eq. (4.1.3) are still difficult to handle analytically. However, they can be reconduced to two coupled amplitude equations by noticing that the reduced system admits a two-dimensional invariant manifold, stable for sufficiently strong couplings, on which Eq. (4.1.3) can be projected [42]. This manifold is identified by the relation of orthogonality between the two order parameters and by the choice, arbitrary, of a phase ϕ for a frame of reference rotating at the average natural frequency ω_0, that is at the frequency of the mean field oscillations.

The components of the two macroscopic variables in such a plane are expressed by the relations:

$$Z = R\, e^{i(\phi + \omega_0 t)}$$

and

$$W = w\, e^{i(\phi + \frac{\pi}{2} + \omega_0 t)}.$$

By substituting these expressions into Eq. (4.1.3) we obtain the following equations for the amplitudes R and w of the mean field and of the shape parameter respectively:

$$\begin{cases} \dot{R} = (1 - R^2)\, R - w \\ \\ \dot{w} = \sigma^2\, R + (1 - K - R^2)\, w. \end{cases} \tag{4.1.4}$$

Equations (4.1.4) define a planar dynamical system that can be fully studied by analytical means. Its bifurcation diagram as a function of the coupling strength k and the standard deviation σ of the frequency distribution is reported in Figure 4.1.

Let us now see what the regions of this bifurcation diagram correspond to in the phase space of the reduced system Eq. (4.1.3), taking into account that a point (R^*, w^*) in the phase space of the amplitudes is a periodic solution for the mean field of frequency ω_0 and amplitude R. Correspondingly, the shape parameter undergoes oscillations with the same frequency, but $\pi/2$ out-of-phase, and with amplitude w.

Region (1) of Figure 4.1 corresponds to the regime of amplitude or oscillator death [45, 98], where all the population elements lie in the origin. Oscillator death is a particular case of phase-frequency locking, occurring when the coupling is strong enough to maintain coherence within the population, but the mismatch in the frequencies is too large to be compatible with a non-vanishing solution. In Section 4.3 we will show that the stabilisation of an unstable focus (or saddle-focus) equilibrium through an increase in time scale-related parameters is a universal property of a class of populations including, among others, ensembles of chaotic systems.

When the mismatch in the natural frequencies is reduced, the origin undergoes a pitchfork bifurcation, that corresponds to an Andronov-Hopf bifurcation in Eq. 4.1.4. In region (2), thus, the mean field and the shape parameter have oscillations of amplitudes:

$$\begin{aligned} R^* &= \sqrt{1 - \alpha} \\ \\ w^* &= \alpha \sqrt{1 - \alpha} \\ \\ \text{with} \quad \alpha &= \frac{K}{2} + \sqrt{\left(\frac{K}{2}\right)^2 - \sigma^2}. \end{aligned} \tag{4.1.5}$$

These oscillations correspond to the regime of full (phase) locking, for which the microscopic configuration of the population is displayed in Figure 2.4.In this regime, the diversity in the natural frequency manifests itself as a phase difference of the single oscillator relative to the mean field and in a decrease of the its oscillation amplitude.

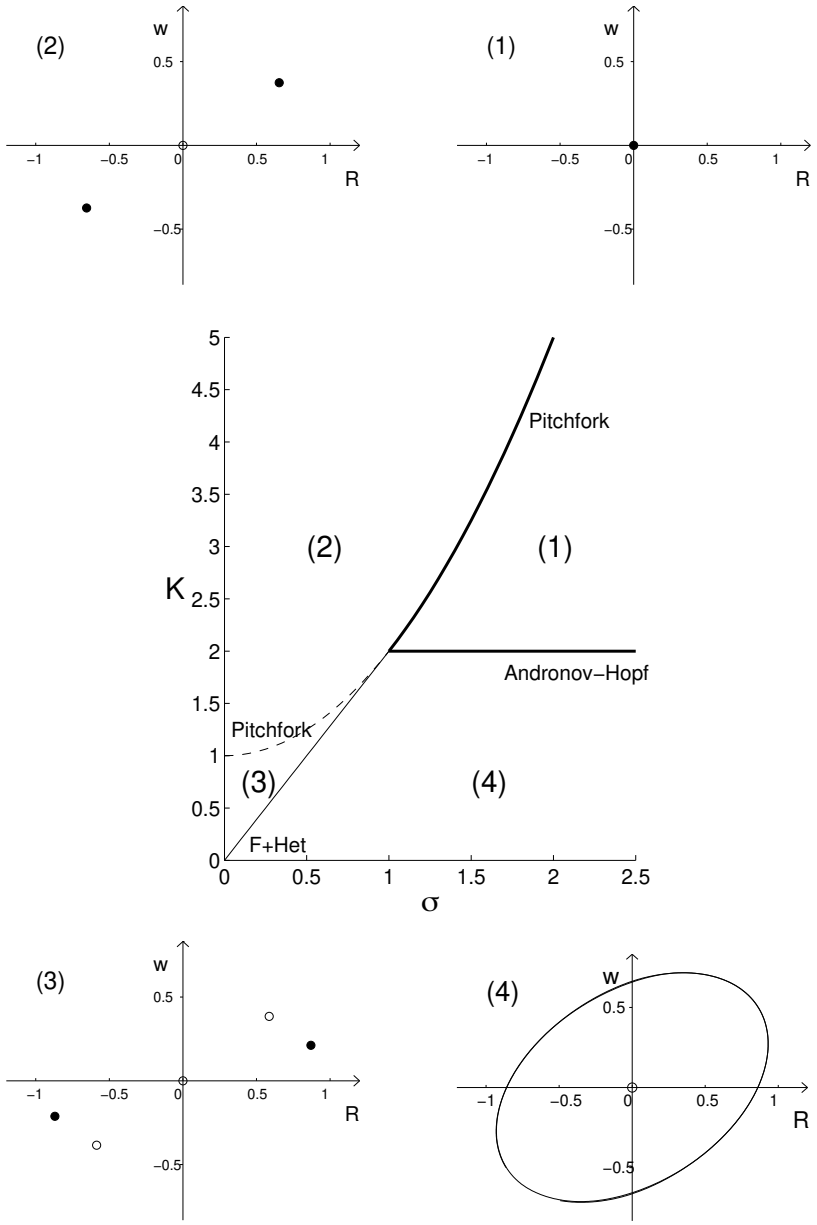

Figure 4.1: Bifurcation diagram for the order parameter expansion, after the reduction to the amplitude equations Eq. (4.1.4). The inserts show the asymptotic regimes in each of the four regions of the plane (σ, K). Stable and unstable equilibria are plotted with a black and white dot respectively, while in region (4) a stable limit cycle is present. The central panel indicates the bifurcations that take place between two of these regions (F+Het. in the lower left corner denotes a heteroclinic+fold bifurcation).

The effect of mismatch on the dynamics of one individual within the population is stronger the further away from the average its frequency is.

The bifurcation boundary separating regions (1) and (2) is the line:

$$K = \sigma^2 + 1 \qquad \text{for } K > 2.$$

When $K \to \infty$, this parabola is asymptotic to the boundary obtained by Matthews, Mirollo and Strogatz [99]. Their derivation, based on self-consistency arguments, assumes infinite population size and symmetrical distribution of natural frequencies. Based on the numerical analysis of the eigenvalues spectrum of the population, these authors also concluded that the "phase transition" to non-vanishing oscillations takes place through a Andronov-Hopf bifurcation. Such a transition has been experimentally demonstrated by Hudson and coworkers for the case of two coupled electrochemical oscillators [181]. In our case, we interpret this qualitative change in the mean field dynamics as a bifurcation occurring on a system of effective macroscopic variables, the order parameters and give a description of it that is independent on the system size.

Which of the two non-vanishing symmetric stable equilibria of the amplitude equations will be the asymptotic solution depends of the initial relation between the phase of the mean field oscillations with respect to that of the rotating frame of reference.

It is known that an increase in the frequency mismatch leads the oscillators to spread along the synchronisation manifold producing a progressive reduction of the mean field oscillation amplitude, up to the point where it vanishes. Equations (4.1.5) give us an estimation of the amplitude of the collective oscillations as a function of the standard deviation of the parameter distribution, as shown in Figure 4.2.

Numerical simulations of the full population shows that the stronger the coupling strength is, the better the assumption of coherence holds and, accordingly, the more precise the estimate of the mean field oscillation amplitude. The right panel of Figure 4.2 displays the amplitude of the shape parameter's oscillations. As a general trend, an increase in the mismatch first leads the oscillators to enhance their distance from the mean field, and then to a steep decrease in the volume of the cloud as the mean field approaches the oscillator death regime.

While the strength of the coupling is a determining factor of the esteem accuracy, we can see that this is only weakly affected by the population size and by the actual shape of the parameter distribution. In this sense, the order parameter reduction can be seen as a universal two-body approximation of the population of limit cycles. The bifurcation diagram of the amplitude equations indeed resembles that obtained by Aronson et al. for a system of two coupled limit cycle oscillators [6].

An important feature of the order parameter expansion is that it is based on the perturbation of a dynamical system, the perfectly synchronous solution, and not of an equilibrium. Therefore, as long as the assumption of coherence holds,

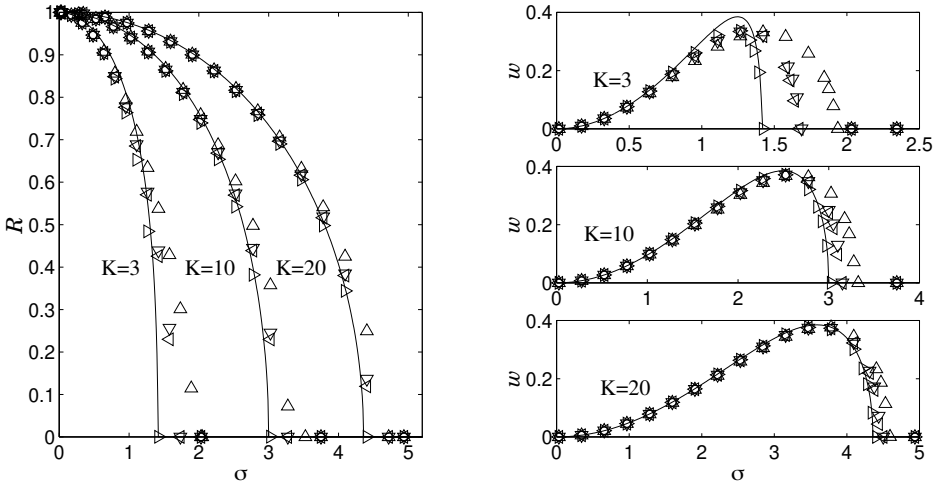

Figure 4.2: The estimated values for the amplitude of the oscillations of the centroid Z and of the shape parameter W (Eq. (4.1.5)) versus the standard deviation σ (solid lines) are compared to those numerically computed according to Eq. (4.1.1). Populations with different size and frequency distribution are considered: $N = 800$, Gaussian distribution ($\triangle$); $N = 800$ uniform distribution ($\triangledown$); $N = 5$, uniform distribution ($\triangleleft$); $N = 2$ ($\triangleright$).

the reduced system should be able to describe not only the asymptotic regimes, but also their *transient dynamics* after macroscopic perturbations.

The possibility of linking the response to external perturbations to the microscopic structure of the population is of extreme experimental relevance, since a number of protocols are commonly used to "test" ensembles of units by means of global changes. For instance, one can apply to populations the technique of *quenching* [69], consisting in displacing a dynamical system onto the stable manifold of one of its saddle equilibria, with a consequent temporary disappearance of the oscillations. This procedure has been used by Danø, Sørensen and Hynne as a mean for determining the geometry of the concentration space close to a limit cycle in yeast cell metabolism [35, 68].

Hence, let us now address the structure of the phase space in region (2) (for a more detailed analysis, see d'Ovidio [42]). The important features determining the transient behaviour of the amplitude equations are the stable and unstable manifolds of the origin. The stable one, coinciding with the origin's eigenspaces, is spanned by the eigenvector:

$$e^0 = \{1, \alpha\}$$

and is shown in Figure 4.3 together with the nullcline for the mean field amplitude R. The first of these curves determines the basins of attraction of the full locking solution (positive equilibrium) and of its symmetric (anti-phase) solution. The nullcline instead affects the properties of the transient mean field trajectory.

According to what part of the amplitudes plane (R, w) the system is initiated in, we can observe three qualitatively different transient evolutions of the mean field amplitude.

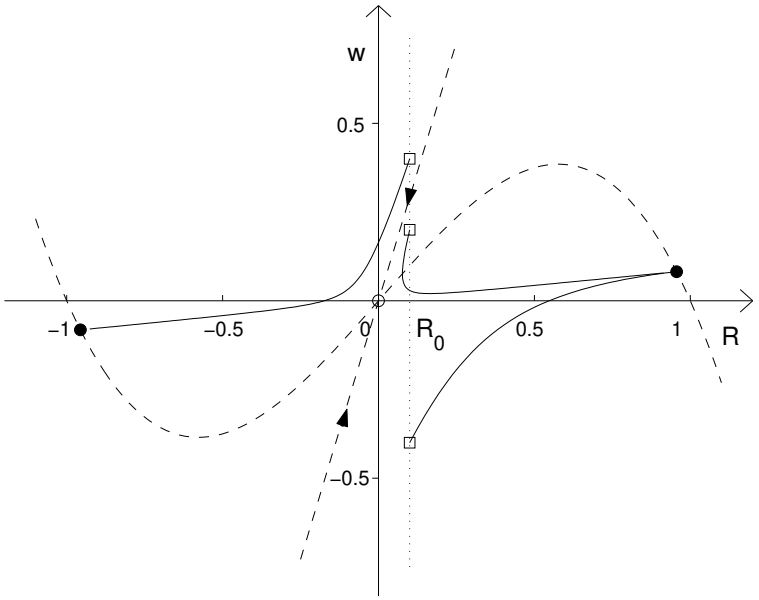

Figure 4.3: Phase space of the amplitude equations Eq. (4.1.4). The dashed lines indicate the stable manifold of the origin and the R nullcline. The black dots are the stable full-locking equilibria, and the solid lines are the trajectories after the system has been initiated in three configurations (squares) with the same amplitude R_0, but different shape parameter.

For instance, one can choose three initial microscopic configuration that share the same macroscopic amplitude, but have different arrangements of the oscillators around the mean field, and thus different shape parameters (three squares in Figure 4.3.

These three types of transient dynamics, shown in Figure 4.4 consist in: I) a monotonous increase of the mean field oscillation amplitude (trajectory relative to the lower w initial value); II) an initial decrease in the amplitude of the macroscopic oscillations, followed by an increase (middle case) that eventually leads to the same in-phase solution as in the previous case; III) a decrease of the amplitude to zero, followed by a monotonous approach of the solution in anti-phase with respect to the initial one.

The same transient modes are also present in the response to a *macroscopic perturbation*, that consists in a rigid shift of all the population elements. In this case, the shape parameter remains the same before and after the perturbation, while the amplitude of the macroscopic oscillations is changed by a given amount, as is the amplitude of each microscopic oscillator. Correspondingly, the representative point in the amplitude plane displaces along a line parallel to the R axis

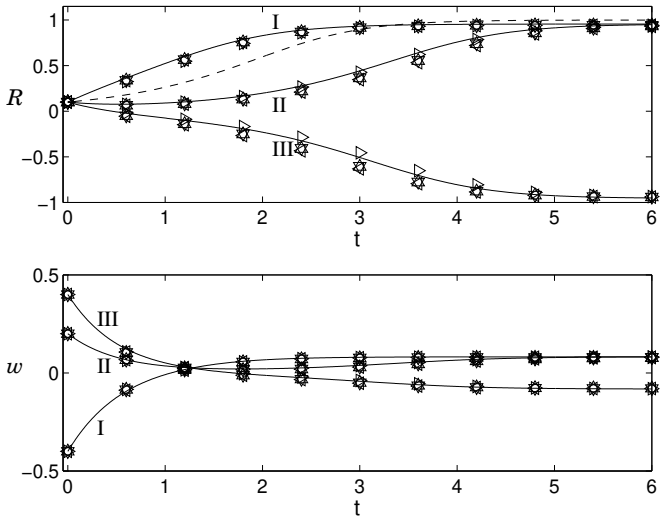

Figure 4.4: The transient behaviour predicted by Eq. (4.1.4) (solid line) is compared to that of the full system Eq. (4.1.1) (triangles) and of the single-element (dashed line) for $\sigma = 0.5$ and $K = 3$. The initial states have the same mean field value $|Z| = R_0$, but different $|W|$. The simulations have been performed for different population sizes and parameter distributions (symbols as in Figure 4.2).

and passing through the full locking equilibrium. The point in which such a line crosses the origin's stable manifold defines a critical radius. We will refer to this radius as the *quenching radius*. If the system is started from this radius, the mean field oscillations are completely suppressed.

The value of the quenching radius can be analytically obtained and reads:

$$R_q = \frac{\alpha^2\sqrt{1-\alpha}}{\sigma^2}, \tag{4.1.6}$$

where α is defined according to Eq. (4.1.5).

Figure 4.5 shows the quenching radius versus the coupling strength according to Eq. (4.1.6) and for the direct simulation of the previously considered populations (in this last case, the value of the quenching radius is determined by the divergence of the return time to the full locking equilibrium). Again, the accuracy in the estimate improves with an increase of the coupling strength and a decrease of the frequency mismatch, both conditions that render the collective motion more coherent.

Let us now address the phase portrait of the system for weak couplings. Since the hypothesis of coherence is in general no longer satisfied in this region, we do not expect Eq. (4.1.4) to be able to describe the mean field behaviour. However, we will see that even if not quantitatively accurate, the amplitude equations can still

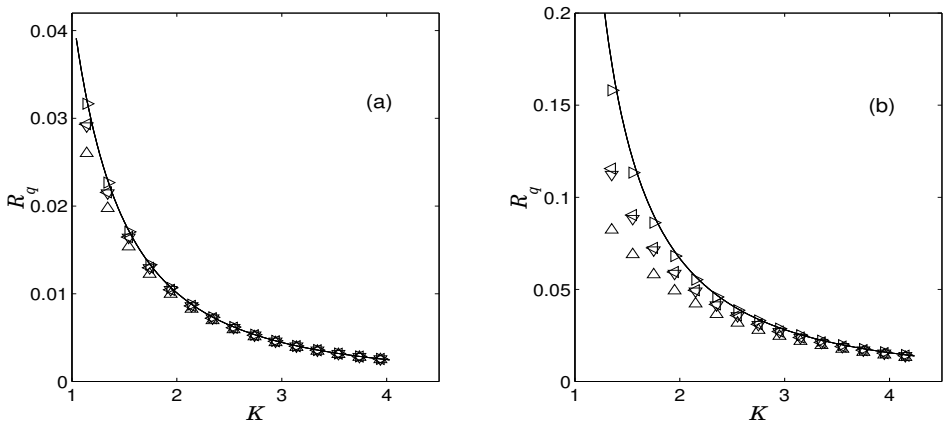

Figure 4.5: The estimated values for the quenching radius Eq. (4.1.6) versus the coupling constant K (solid lines) are compared to the numerically computed ones (triangles), for (a) $\sigma = 0.2$ and (b) $\sigma = 0.5$ (symbols as in Figure 4.2).

give some insight into the emergence of complex collective dynamics for sufficiently small mismatch.

In region (4) of the bifurcation diagram Figure 4.1 the system has acquired two symmetric saddle equilibria in addition to the already existing stable nodes. These unstable points are generated through a pitchfork bifurcation on the line $K = \sigma^2 + 1$. Each of the four non-vanishing equilibria is heteroclinically connected to those of the others with different stability character. The presence of this structure accounts for the "excitable" nature of the collective dynamics for intermediate couplings and parameter mismatch, since a small perturbation off the stable equilibrium can lead to a large excursion up to the anti-phase solution.

The two pairs of non-vanishing equilibria merge on the line $K = 2\sigma$ through a heteroclinic+fold bifurcation, thus giving rise to a limit cycle in the amplitude phase space. In the phase space of the order parameters, this cycle corresponds to a quasiperiodic solution, with this new frequency superimposed to the mean natural frequency ω_0.

A distinguishing characteristic between the Andronov-Hopf bifurcation scenario and the heteroclinic+fold onset of oscillations is the behaviour of the oscillation amplitude close to the bifurcation. In the first case, the mean field amplitude grows as the square root of the distance of the parameter from the value at which the transition takes place. In the heteroclinic+fold bifurcation scenario, on the other hand, the limit cycle is born with finite amplitude and the period of the oscillations diverges as the bifurcation point is approached by decreasing the value of the parameter mismatch. Figure 4.6 shows that this second type of bifurcation scenario is indeed present in the collective dynamics, in spite of the fact that the actual values for which it takes place are larger for the population than for the reduced system.

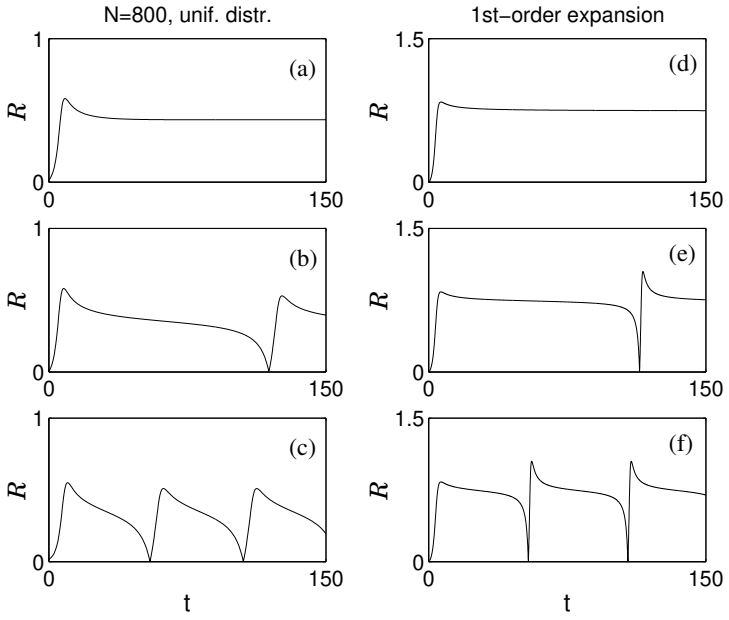

Figure 4.6: Time evolution of the mean field close to (and to the right of) the stability boundary of the fully locked state for $K = 0.9$. Cases (a)-(c): population of 800 oscillators, uniform distribution, $\sigma = 0.5, 0.505, 0.51$. Cases (d)-(f): amplitude equations Eq. 4.1.4, $\sigma = 0.45, 0.451, 0.454$.

In the projection onto the phase space of one single oscillator, the quasiperiodic oscillations thus generated (called large-amplitude oscillations [99]) correspond to a periodic quasi-static rearrangement of the synchronisation manifold. Its shape at a given time is close to the geometry it would attain if the mean field was constant and had the value it takes at the considered time instant.

Close to the regime of quasiperiodic large-amplitude oscillations, the population displays so-called Hopf oscillations and apparently low-dimensional chaotic behaviour, as shown in Figure 2.3. The Hopf bifurcations are characterised by the mean field amplitude having a limit cycle born by a Hopf bifurcation of the positive equilibrium. This corresponds to asymmetric oscillations of the mean field, whose average in time is not vanishing.

It is conceivable that closing the order parameter expansion through a truncation to a higher degree in ϵ would allow us to reproduce also these other regimes. In particular, the case of quasiperiodic macroscopic dynamics defines a motion on a two-dimensional torus in the space (Z, W). This attractor is structurally unstable and can be destroyed by the addition of any generic term to the amplitude equations. According to KAM theory for dissipative systems [27], thus, we expect to observe a tongue-like structure at the boundary with the chaotic regime, with some parameter values, those for which the frequency of the amplitude oscillations is commensurable to the average natural frequency ω_0, that will have

in their vicinity a quasiperiodic solution, and other parameter values where the torus will break giving rise to a chaotic attractor. The fact that the regions in which the quasiperiodic solution survives are closely intermingled to those where it breaks apart let this boundary depend essentially on the microscopic structure of the population. A large effect of small modifications of the microscopic structure, such as the extreme values of the parameters represented in the population, can also be expected for the bifurcation boundary between the regimes of full and partial locking.

These predictions have been numerically confirmed by a preliminary numerical study of the boundary of the fully locked regime. Moreover, the simulation of the second-order order truncation of the order parameter expansion has revealed the existence of asymmetric Hopf oscillations in regions of the parameter space with weaker coupling compared to those where large-amplitude oscillations are observed.

Finally, the transition between large-amplitude oscillations and amplitude death in the amplitude equations takes place through a Hopf bifurcation. However, we do not expect this transition to have any relevance with respect to the collective regimes of the population, since the region of the parameter space where it occurs has both weak coupling and broad frequency distribution. There, indeed, the population exhibits a transition from amplitude death to incoherence that is undetectable at a macroscopic level, since in both cases the mean field vanishes. In the incoherent regime the microscopic configuration consists in oscillators distributed on a circle, rather than being concentrated on the origin. The difference with respect to the oscillator death regime can hence be detected by observing the fluctuations induced by finite-size effects or by inhomogeneities in the initial state, both of which are factors that are not taken into account in the description through the order parameters.

The existence of the codimension-two point of Bogdanov-Takens $\sigma = 1$, $K = 2$, though, suggests that also the population could have an "organising center" of higher codimension. The presence of such a center would structure the macroscopic bifurcation diagram for the regimes, like quasiperiodicity and chaos, where the collective dynamics is more complex than that of the single-element.

4.2 Ginzburg-Landau oscillators

The choice of describing the single-element dynamics by means of a Hopf normal form is the most natural for the study of the collective regimes in populations of oscillators. In order to translate the results of this analysis into quantities that can be experimentally measured, it is often convenient to consider another form for the equations of the limit cycle oscillator. This other formulation, anterior to the rescaling that leads to obtaining the frequency as the only parameter, is given

by the *Stuart-Landau equation* for the complex variable c:

$$\dot{c} = (i\omega_j + \chi)\, c + g\, |c|^2\, c, \tag{4.2.1}$$

where $\chi \in \mathbb{C}$ and $\omega \in \mathbb{R}$.

Close to a Hopf bifurcation point, the equations for a chemical reaction are often formulated in the form Eq. (4.2.1), and the parameters of this expression can be linked, thanks to a center manifold reduction, to the kinetic constants of the chemical system [85].

This type of reduction has been used by Sørensen et al. for instance for describing the chemical kinetics of glycolysis. In this case, the original chemical system involving 35 chemical species has been reduced to the two-dimensional Eq. (4.2.1) and its parameters experimentally determined [114]. These results have then been used for addressing the collective metabolic oscillations in yeast, that are the effect of the synchronised chemical activity of living cells in a Continuous-flow Stirred Tank Reactor (CSTR) [35, 68]. In modelling such a population, Eq. (4.2.1) plays the role of the single-element dynamics, while the diffusion of the chemicals between the cells and the medium they are embedded in introduces a complex coupling constant [34]. The problem of connecting the macroscopic observable, i.e. the average fluorescence of one chemical species in the whole population, to the chemical kinetics of metabolism, taking place within each cell of the suspension, is one of the starting points of the work presented in this elaborate. Indeed, one would like to quantify the parameters in Eq. (4.2.1) by means of purely macroscopical measurements and to exclude or quantify the role that microscopic disorder has on the population dynamics.

Coming back to Eq. (4.2.1), we can rewrite it by choosing a rotating frame of reference and by rescaling parameters and variables, obtaining the equations:

$$\dot{z_j} = h\left(\mu - |z_j|^2\right) z_j + \mathcal{K}\,(Z - z_j) \qquad J = 1, \ldots, N, \tag{4.2.2}$$

where $h, \mathcal{K} \in \mathbb{C}$ $\mu \in \mathbb{R}$ and the mean field is defined according to Eq. (4.1.2).

This equations can be seen as the mean-field version of a discretisation on a lattice of the *complex Ginzburg-Landau equations* , that is commonly used for modelling reaction-diffusion systems [55].

Due to the presence of complex parameters, the dynamics of the mean field of Eq. (4.2.2) is richer than the case examined in the previous section [24, 23]. Again, one of the possible regimes is perfect synchronisation, where all the population elements oscillate on a limit cycle of amplitude $|Z| = \sqrt{\mu}$. One question that one can ask is thus when such a regime is locally stable.

The answer to this question has been given by Hakim and Rappel, who performed a linear stability analysis of the system of N differential equations for $\mathcal{R}(\mathcal{K}) > 0$, providing the following condition for the perfectly synchronous regime to be stable [55]:

$$1 + \beta^2 + 2\,\mu(1 + \alpha\,\beta) < 0, \tag{4.2.3}$$

where $\alpha = \mathcal{R}e(h)$ and $\beta = \mathcal{I}m(\mathcal{K})$.

Here, we show another way of retrieving the same result by means of the order parameter expansion truncated to second order in the displacements from the mean field. Since the oscillators of Eq. (4.2.2) are identical, the shape parameter is zero by definition, so that the order parameters that influence the mean field are the averages of second degree in the displacements:

$$S_1 = \langle |\epsilon|^2 \rangle$$

and

$$S_1 = \langle \epsilon^2 \rangle.$$

The reduced system for the order parameters , computed analogously to the approach we used in Section 3.3, is the five-dimensional (S_1 is a scalar) set of equations:

$$\begin{cases} \dot{Z} &= h\left(\mu - |Z|^2\right) Z - 2h\, Z\, S_1 - h\, Z^*\, S_2 \\ \dot{S}_1 &= 2\left[(\mu - 2\,|Z|^2) - 1\right]\, S_1 - h^*\, Z^{*2}\, S_2 - h\, Z^2\, S_2^* \\ \dot{S}_2 &= 2\left[h\,(\mu - 2\,|Z|^2) - \mathcal{K}\right]\, S_2 - 2\,h\, Z^2\, S_1 \end{cases}$$

The stability analysis of the equilibrium:

$$|Z| = \sqrt{\mu} \qquad S_1 = 0 \qquad S_2 = 0$$

leads to the previously stated condition Eq. (4.2.3).

The role of parameter mismatch in populations of globally and strongly coupled Stuart-Landau oscillators can also be addressed by means of an order parameter expansion, that leads to four-dimensional system of equations for the mean field and the shape parameter W:

$$\begin{cases} \dot{Z} &= (i\,\omega_0 + \chi)\; Z + g\,|Z|^2\, Z + i\, W \\ \dot{W} &= i\left(\langle \omega^2 \rangle - \omega_0^2\right) + \left(i\,\omega_0 + \chi\; - \mathcal{K}\; + 2\,g\,|Z|^2\, Z\right)\; W + g\, Z^2 W^* \end{cases} \tag{4.2.4}$$

This reduced system reproduces for instance the qualitative properties of the transient after a macroscopic perturbation, as shown in Figure 4.7.

4.3 Oscillators with time-scale mismatch.

This section will address a class of dynamical systems with parameter mismatch, those where the individual elements differ for the time-scale of their evolution. As we pointed out in Chapter 3, populations of oscillators with time-scale mismatch

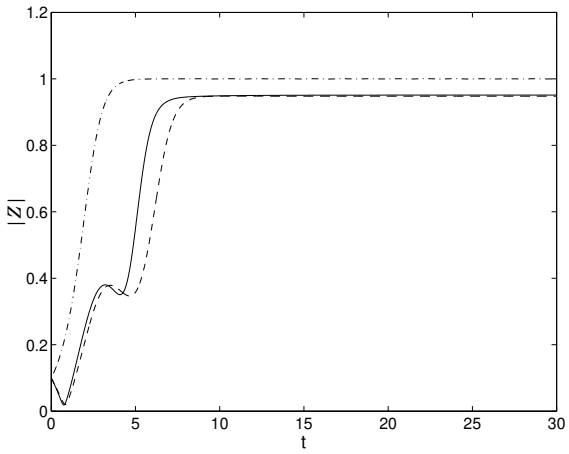

Figure 4.7: Transient collective dynamics of a population of globally coupled Stuart-Landau oscillators with parameter mismatch after a macroscopic perturbation of the phase synchronous state (solid line). The reduced system Eq. (4.2.4) (dashed line) reproduces the qualitative difference with respect to the case of identical oscillators (dash-dotted line). .

can be viewed as a generalisation of the Winfree model to situations in which there exist no univocally defined phase for the single-element dynamics, as for the Rössler systems with funnel attractor illustrated in Section 3.2. This formulation allows us to address the effect of parameter diversity upon the collective dynamics of populations of chaotic units. Analogously to what we have done in the previous sections, we will consider an isotropic vectorial coupling, so that the full system obeys the equations [40]:

$$\dot{\mathbf{x}_j} = \tau_j \, \mathbf{f}(\mathbf{x}_j) + K \, (\mathbf{X} - \mathbf{x}_j) \qquad j = 1, \ldots, N, \tag{4.3.1}$$

where $\mathbf{x_j} \in \mathbb{R}^n$ is the individual state variables. The time-scales $\tau_j > 0$ are assigned according to a given distribution that, without loss of generality, can be chosen with average $\tau_0 = 1$ (this can always be achieved via a time rescaling) and variance σ^2. The mean field X is defined according to Eq. (3.3.5).

The choice of such a class of populations has two main motivations. On the one side, the perfectly synchronous solution is most easily destabilised in a direction parallel to the single-element trajectory, so that a difference in time-scale seems to provide the most natural way to produce a generic regime of general synchronisation. By analogy, in the case of limit cycle oscillators, the most natural parameter to spread is the natural frequency. On the other side, Eq. (4.3.1) are sufficiently simple for the order parameter reduction to produce intuitively meaningful results.

By substituting Eq. (4.3.1) into Eq. (3.3.8), we easily obtain the general formulation of the reduced system for the population with time-scale mismatch. This

consists in the equations for the mean field X and the shape parameter W:

$$\begin{cases} \dot{\mathbf{X}} = \mathbf{f}(\mathbf{X}) + \mathcal{D}_{\mathbf{x}}\mathbf{f}(\mathbf{X})\,\mathbf{W} \\ \\ \dot{\mathbf{W}} = \sigma^2\,\mathbf{f}(\mathbf{X}) + \left[\mathcal{D}_{\mathbf{x}}\,\mathbf{f}(\mathbf{X}) - K\right]\,\mathbf{W}. \end{cases} \tag{4.3.2}$$

Note that the reduced system has $2\,n$ variables, while the full system Eq. (4.3.1) is a set of $N\,n$ differential equations. For this reason, Eq. 4.3.2 are an extremely parsimonious description of the collective population dynamics.

When the single-element dynamics is described by chaotic ODEs, as in the examples presented in Section 3.2, anyway, Eq. (4.3.2) is at least six-dimensional, which renders their analytical study difficult except than in particularly simple regimes. The comparison between the collective dynamics of the population to that predicted by Eq. (4.3.2) will be thus performed mainly by means of numerical simulations both for the full and the reduced system. The case in which an equilibrium, that of oscillator death, exists for the macroscopic dynamics will be analytically studied in the last part of this section.

In order to compare the collective dynamics of the population with the behaviour of the reduced system, we will consider as a prototypical single-element dynamics the Rössler system Eq. (3.2.2) with parameters $a = 0.1$, $b = 0.4$ and $c = 8$. We recall here that the asymptotic evolution of any individual of the population takes place on the funnel attractor displayed in Figure 3.2, but its motion along the orbit has a speed different with respect to the other population elements. Equations (4.3.2) for the mean field and the shape parameter $\mathbf{W} = (W_x, W_y, W_z)$ read in this case:

$$\begin{cases} \dot{X} = & -(Y+Z) - W_y - W_z \\ \dot{Y} = & X + a\,Y + W_x + a\,W_y \\ \dot{Z} = & b + X\,Z - c\,z + z\,W_x + (X-c)\,W_z \\ \dot{W}_x = & -\sigma^2\,(Y+Z) - K\,W_x - (1+K)\,W_y - (1+K)\,W_z \\ \dot{W}_y = & \sigma^2\,(X + a\,Y) + (1-K)\,W_x + (a-K)\,W_y - K\,W_z \\ \dot{W}_z = & \sigma^2\,(b + X\,Z - c\,Z) + (Z-K)\,W_x - K\,W_y + (X - c - K)\,W_z. \end{cases} \tag{4.3.3}$$

We can now consider the peak-to-peak map of the macroscopic attractor, that is defined as the Poincaré map on the manifold containing the maxima of one variable. Figure 4.8 shows the peak-to-peak map of the first variable X of the mean field, as a function of the standard deviation of the parameter distribution. The population (top left) and the reduced system Eq. (4.3.2) (bottom left) has very similar bifurcation diagrams even if the coupling is in this case very low (close to the boundary where general synchronisation is lost). For higher couplings, the diagrams are almost indistinguishable.

The fact that the reduced system actually captures some essential feature of the population dynamics is confirmed if we compare the peak-to-peak maps of the

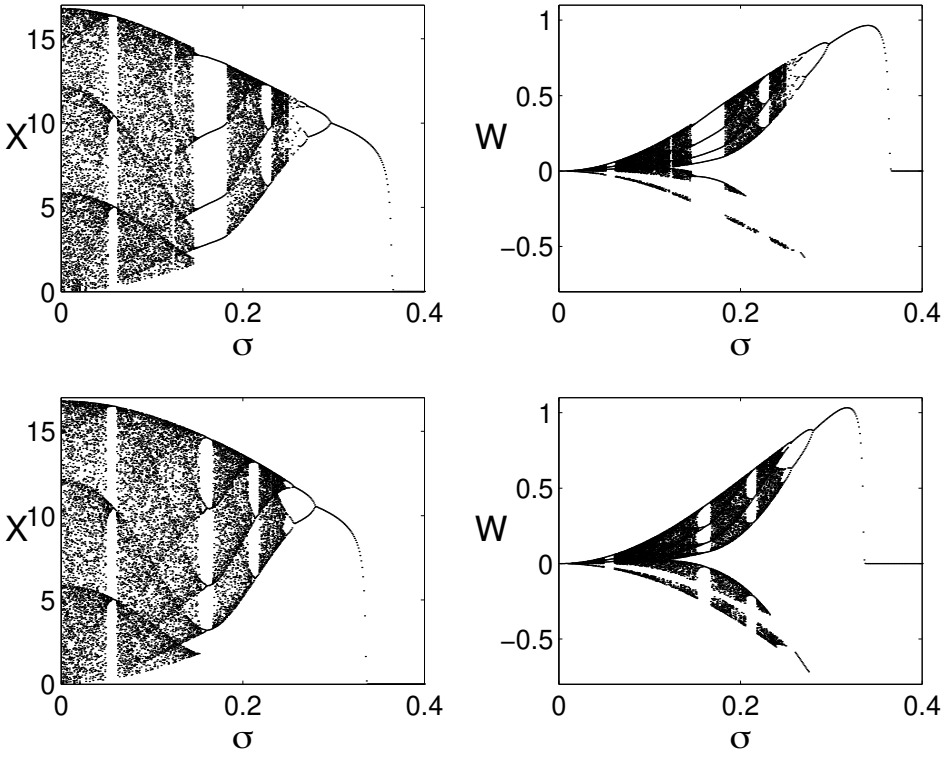

Figure 4.8: Poincaré section of the mean field and of the shape parameter for a population of 32 coupled Rössler oscillators ($a = 0.25$, $b = 1$, $c = 8.5$) with time-scale mismatch (top) and for its order parameter reduction (bottom). The coupling is $k = 1$. The systems go from chaos to oscillator death when the standard deviation σ of the parameter distribution increases. The reduced system reproduces the bifurcation cascade of the population with remarkable quantitative agreement.

shape parameter (Figure 4.8 top right for the population, bottom right for the reduced system). As in the case of the coupled Hopf normal forms, discussed in Section 4.1, the shape parameter first increases its maximal amplitude when the mismatch is enhanced, then drops suddenly to zero when all the individual units stop oscillating and the population enters a regime of oscillator death.

The qualitative changes of the mean field dynamics induced by an increase of the time-scale mismatch – transition from funnel attractor to spiral chaos, to periodic regimes and eventually to oscillator death – can be interpreted as bifurcations of the macroscopic dynamical system defined by Eq. (4.3.2). This possibility of reducing the effective dimensionality of the population dynamics to only twice the dimension of the single-element dynamical system is due to the fact that the coupling is sufficiently strong to guarantee that the motion is coherent. For weaker couplings, indeed, the interaction among element is not constraining enough to

induce a solid motion of the individuals together with the mean field. There, Eq. (4.3.2) no longer provides a valid approximation for the order parameters of the population.

Let us now focus on the regime of *amplitude* or *oscillator death*. As discussed in Section 3.2, this is the regime where all the population elements lie in a point that is an unstable equilibrium for the single-element evolution. Due to the combined effect of strong coupling and parameter mismatch, this becomes a stable equilibrium for the macroscopic dynamics, whose oscillations are thus completely suppressed. Several authors have speculated about the generality of the phenomenon, that appears in the context of strongly interacting units endowed of different individual dynamics [10, 45, 165].

Here, we address the regime of oscillator death in generic populations of globally coupled oscillators by means of the reduced system Eq. (3.3.8) [42]. In order to compare this with the simulations of the population dynamics, we consider again the case of time-scale mismatch.

Let us start by noticing that if $\mathbf{X}^*$ is an equilibrium for the single-element dynamics, that is $\mathbf{f}(\mathbf{X}^*) = 0$, than this is also an equilibrium for the mean field dynamics. In order to determine whether it is attractive, we must perform a linear stability analysis of the solution:

$$\begin{cases} \mathbf{X} = \mathbf{X}^* \\ \mathbf{W} = 0 \end{cases} \tag{4.3.4}$$

of Eq. (4.3.2). In this way, we find universal conditions, related to the character of the equilibria of the single-element dynamics, for the regime of oscillator death to occur when the coupling strength and time-scale diversity are both sufficiently large.

Let us start by writing the Jacobian matrix of the macroscopic equations (4.3.2):

$$\mathcal{J}(\mathbf{X}, \mathbf{W}) = \begin{bmatrix} \mathcal{D}_{\mathbf{x}}\mathbf{f}(\mathbf{X}) + \mathcal{D}_{\mathbf{xx}}\mathbf{f}(\mathbf{X})\,\mathbf{W} & \mathcal{D}_{\mathbf{x}}\mathbf{f}(\mathbf{X}) \\ \sigma^2\,\mathcal{D}_{\mathbf{x}}\mathbf{f}(\mathbf{X}) + \mathcal{D}_{\mathbf{xx}}\mathbf{f}(\mathbf{X})\,\mathbf{W} & \mathcal{D}_{\mathbf{x}}\mathbf{f}(\mathbf{X}) - K \end{bmatrix}.$$

On the equilibrium Eq. 4.3.4, this takes the form:

$$\mathcal{J}(X^*, 0) = \begin{bmatrix} \mathcal{D}^* & \mathcal{D}^* \\ \sigma^2\,\mathcal{D}^* & \mathcal{D}^* - K \end{bmatrix}, \tag{4.3.5}$$

where $\mathcal{D}^* = \mathcal{D}_{\mathbf{x}}\mathbf{f}(\mathbf{X}^*)$. Already at this point it is evident that the main determinant of the oscillator death regime is the linearisation of the single-element dynamics close to the equilibrium that is stabilised. Hence, the other features of the individual decoupled behaviour, such as the fact of possessing a chaotic attractor, or even of possessing one attractor at all, will be of little importance as far as the suppression of the oscillations is concerned.

The stability conditions for the equilibrium Eq. (4.3.4) can be now expressed in terms of the eigenvalues of the Jacobian matrix for the single-element dynamics:

$$\lambda^l = a_l + i\, b_l \qquad l = 1, \ldots, n. \tag{4.3.6}$$

The eigenvalues of the matrix Eq. (4.3.5) can be explicitly obtained as functions of Eq. (4.3.6) thanks to the structure of the Jacobian, that can be block-diagonalised through the transformation:

$$\begin{bmatrix} \mathcal{Q} & 0 \\ 0 & \mathcal{Q} \end{bmatrix}$$

such that $\mathcal{Q}$ diagonalises $\mathcal{D}^*$.

In this way, we get the eigenvalues for the macroscopic dynamics (two for every eigenvalue of the single-element dynamics):

$$\Lambda^l_{1,2} = \lambda_l - \frac{K}{2} \pm \sqrt{\left(\frac{K}{2}\right)^2 + \lambda_l^2\, \sigma^2}. \tag{4.3.7}$$

In order the equilibrium Eq. (4.3.4) to be stable, these eigenvalues must all have negative real part. Since the square root is always larger that $K/2$ for real eigenvalues, it is evident that a necessary condition for oscillator death to take place is that the single-element dynamics equilibrium has no real positive eigenvalues. Hence, the equilibrium that is stabilised must be a saddle-focus. This is actually observed for all the populations, listed in Section 3.2, where the phenomenon of amplitude death has been observed. In order this saddle-focus to be stable, the real and imaginary parts of the eigenvalues of $\mathcal{J}(\mathbf{X}, 0)$ must satisfy the condition:

$$\max_l \left\{ \mathrm{Re}(\Lambda^l_1), \mathrm{Re}(\Lambda^l_2) \right\} < 0. \tag{4.3.8}$$

For every couple of complex conjugate eigenvalues of the single-element dynamics $\lambda = a \pm i\, b$, the real part of Eq. (4.3.7) can assume two values. By imposing that those values vanish, we obtain a bifurcation condition:

$$\left| \mathrm{Re}\left(\sqrt{1 + 4\,(1 + i\gamma)^2 \left(\frac{\sigma}{k^*}\right)^2} \right) \right| = 1 - \frac{2}{k^*} \tag{4.3.9}$$

in the form of a relation between the rescaled parameters $\gamma = b/a$ and $k^* = K/a$, corresponding to a normalisation to 1 of the real part of the microscopic dynamics. Equation (4.3.9) must be generalised to a set of conditions if the equilibrium for the single-element dynamics has more than one couple of complex conjugate eigenvalues. In this case, Eq. (4.3.8) defines piece-wise the boundary of the region where the oscillator death regime is stable.

The stability of the oscillator death regime is thus reconduced to a relation among only three parameters: the ratio γ between imaginary and real part of

the microscopic eigenvectors, the effective coupling constant k^* and the standard deviation σ of the parameter mismatch. Equation (4.3.9) thus provides a universal condition for the linear stability of oscillator death in any population of globally coupled dynamical systems with time-scale mismatch. It identifies a surface in the parameter space (γ, σ, k^*) that delimits the region where the macroscopic dynamics is suppressed.

If the single-element dynamics possesses more than one equilibrium, the possibility of having macroscopic multistability depends on how many of those equilibria simultaneously satisfy Eq. (4.3.8). In the case of the Lorenz system, for instance, the amplitude death regime is always bistable, since the two symmetric saddle-foci have the same eigenvalues and hence get simultaneously stabilised.

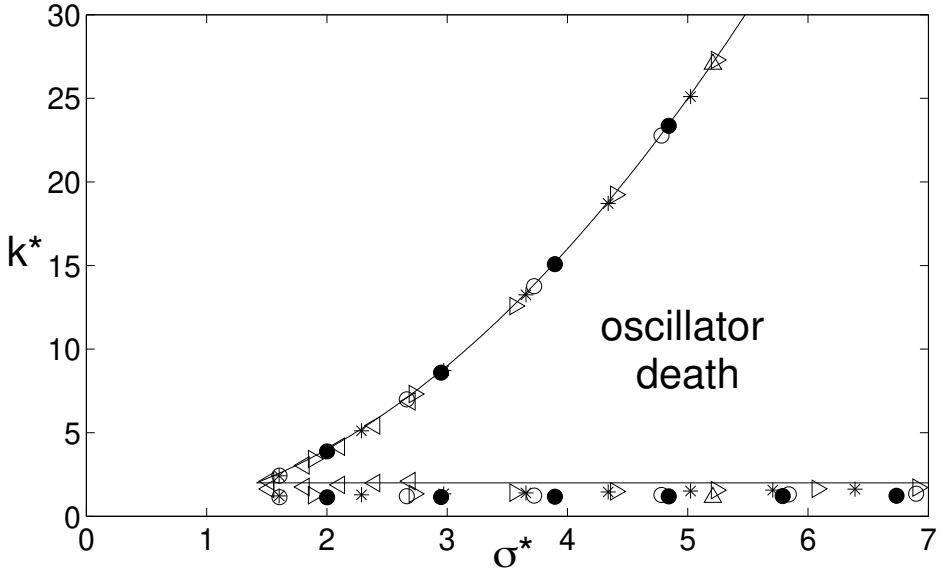

Figure 4.9: Data collapse of the numerically computed boundary to oscillator death for populations with time-scale mismatch (Gaussian distribution) and different single-element dynamics: Lorenz system Eq. (3.2.3) with parameters $p = 10$, $b = 8/3$ $r = 28$ and (•), $r = 32$ (○), $r = 50$ (∗); Rössler system Eq. (3.2.3) with parameters $b = 0.4$, $c = 8$ and $a = 0.01$ (△), $a = 0.1$ (▷), $a = 0.4$ (◁). The solid lines are the two analytic boundaries Eq. (4.3.10).

Let us now compare the results obtained for the reduced system to the oscillator death boundaries in populations of $N = 100$ dynamical systems ruled by different single-element equations. In order to simplify this comparison, we consider situations in which the imaginary part b of the single-element eigenvalues is much larger than the real part a. In this case, the asymptotic solutions of Eq. (4.3.9) can be computed for the remaining two parameters σ and k^* and yield the

two curves:

$$\begin{cases} k_1^* = \gamma^2\sigma^2 \\ k_2^* = 2 + 2\sigma. \end{cases}$$

Performing the further rescaling $\sigma^* = \gamma\sigma$ and taking the limit $\gamma \to \infty$, we are left with the boundaries:

$$\begin{cases} k_1^* = {\sigma^*}^2 \\ k_2^* = 2 \end{cases} \tag{4.3.10}$$

that can now be compared with the numerical results on the populations.

Figure 4.9 shows that Eq. (4.3.10) capture the essential properties of the oscillator death regime in populations of globally coupled dynamical systems.

The reduced system moreover predicts that on the upper boundary the transition to a synchronous regime takes place through a Hopf bifurcation, that is confirmed but the numerical simulations we have performed for Rössler and Lorenz systems.

On the lower boundary, the estimate of the bifurcation condition appears to have a systematic error. This is not surprising because we do not expect the hypothesis of coherence to hold any longer in this region of the parameter space, as already pointed out for limit cycles in Section 4.1.

Chapter 5

Populations with additive noise: phenomenology and order parameter expansion.

5.1 Introduction

A great number of natural phenomena can be described accurately by means of deterministic equations that reproduce the most relevant features of their behaviour in time. In many cases, however, the deterministic structure of the dynamics is altered by the presence of degrees of freedom others than those included in the equations. Such degrees of freedom cannot be explicit formulated in the model because their features and actual influence on the observable time evolution are not known. It is commonly assumed that their effect on the deterministic dynamics can be accounted for by stochastic terms – generally designated by the name 'noise' – that are added to, or multiplied onto, the deterministic equations (for a wider discussion on noise, see San Miguel and Toral [139]).

As discussed more extensively in Chapter 2, two main effects of fluctuations on low-dimensional systems have been identified: stochastic resonance, by which an optimal amount of noise generates the maximal response to an external forcing, and coherence resonance, where noise regularises the system behaviour.

The dynamics of the stochastic equations describing such situations must be studied by statistical means, since any specific realisation of the noise term leads to a different temporal behaviour of the system. Several approximation methods have been developed, which account for the changes in the probability density functions (pdfs) of the state variables and of their cumulants [48, 3, 90]. In this way, the system observables can be assigned expectation values. Such results can be extended to populations of uncoupled dynamical systems subjected to the same kind of noise, where each system represents a replica of the uncoupled case for

different initial conditions and for different realisations of the stochastic process.

Besides studies of the effect of noise on a single low-dimensional dynamical system, a lot of attention has recently been devoted to the investigations of stochastic perturbations in sets of interacting elements. The nature of such populations ranges from two coupled dynamical systems to large ensembles of elements connected according to an assigned topology (globally coupled, arranged in a lattice or in a network). The features of the noise term also vary widely: identical on each element or independent, additive or multiplicative, white or coloured.

In this chapter, we will focus on the macroscopic dynamics, rather than on the single-element behaviour, of large populations of globally coupled identical maps, by examining the evolution of the average state variable, the mean field. This represents another point of view on the phenomenon of coherence resonance. In the following we will also briefly address the behaviour of a single population element within the population.

If the population elements do not interact, one can invoke the central limit theorem and the law of large numbers [124]: in the limit of infinite population size, the mean field is stationary and takes the average value of the individual pdf (that is in general different from the noise distribution), while for large but finite populations its fluctuations around this value obey a Gaussian distribution.

However, when the populations elements are interacting, even weakly, the collective dynamics displays Non Trivial Collective Behaviour [25]. The nature of the collective motion of weakly coupled identical maps has been actively discussed during the past decade [73, 74, 96, 124, 123, 107, 26, 95, 146]. Some of this works have also addressed the role of small noise or parameter mismatch on such regimes [74, 76, 124, 144, 159].

This chapter deals instead with the effect of noise on strongly coupled maps. Nichols and Wiesenfeld [113] already pointed out that the collective dynamics is interestingly affected by noise when the individual map is close to a bifurcation point, where differences between individual and collective fluctuations emerge. Teramae and Kuramoto [157] later studied the effect of weak noise in the proximity of the loss of synchronous behaviour, where anomalous scalings occur in the moments of the population distribution.

Here we present an analytical method for deriving the mean field behaviour from the single element dynamics and from the features of an additive noise term [39, 38]. The results are general with respect to the specific form of the map and of the noise distribution. In particular, the stochastic term does not need to be chosen neither weak nor Gaussian. This method thus provides an answer to the problem of building macroscopic equations of motion starting from the microscopic structure of the population, as discussed in [22] and justifies the use of specific system choices as representatives of a class of noise-induced phenomena.

The first phenomenological observation is that, in spite of the fact that all the individual population elements may be chaotic and even though their trajectories are blurred by noise, the collective motion is deterministic up to finite-size effects. This can be explained by the fact that the population is infinite and that the noise is added independently to each element, so that every realisation of the

stochastic term is represented in the population. The question is then, whether this deterministic collective dynamics can be described, at least effectively, by a finite number of degrees of freedom.

We will answer this question in the regimes of strong coupling when, in the absence of noise, perfect synchronisation occurs, so that the mean field dynamics exactly mirrors the single-element (the noiseless instantaneous pdf is a Dirac's delta and coincides with the noise distribution).

Our analytical method is based on the direct computation of the dynamics of convenient macroscopic variables, or order parameters, representing the effective degrees of freedom of the collective dynamics. In the derivation of the closed system of macroscopic equations we will justify why the Gaussian closure is often sufficient for describing macroscopic bifurcations [78, 90] and discuss the possibility of retrieving the hierarchical structure of the macroscopic attractor. This approach is complementary to the moment expansion method [41, 124, 159, 128, 90], where the macroscopic equations are derived from the cumulant expansion of the Fokker-Planck or Perron-Frobenius equation for the Langevin dynamics.

When the coupling is maximal, we can derive analytically the exact equation for the mean field evolution. In this case, the reduced system is scalar and it accounts for the interaction between the nonlinearities of the single-element dynamics and the moments of the noise distribution.

For weaker couplings, the main features of the mean field dynamics are still described by a low-dimensional macroscopic map. The study of different approximation levels allows us to address the structure of the macroscopic attractor and its dimensionality.

The comparison between the analytically derived equations and the population collective behaviour will be performed for some prototypical cases: chaotic logistic maps, chaotic quartic maps and excitable maps. It will be shown that, in spite of the fact that in some cases noise simplifies the collective behaviour, in general it produces an unfolding of the synchronous regime. Such unfolding of the macroscopic dynamics is determined by changes in some population-level parameters such as the coupling strength or the moments of the noise distribution.

Section 5.2 of this chapter presents numerical simulations of populations of globally coupled logistic maps with additive independent noise. The mean field dynamics will be compared to the microscopic evolution for different values of the coupling strength.

Section 5.3 introduces the order parameter expansion in its general form.

In Section 5.4 the formulae for the zeroth and second order reduced system are computed, and the significance of the various approximation levels discussed.

The results of Section 5.3 are applied in Chapter 6 to populations with different microscopic features (single-element dynamics, noise distribution).

5.2 Noise-induced collective regimes

Globally coupled dynamical systems have been widely used to model a range of physical, chemical and biological systems. All-to-all coupling is either implemented through an explicit choice of the connection topology, like in arrays of semiconducting elements (Josephson junctions) [169, 113, 170] and electrochemical oscillators [166, 83], or due to the presence of a homogeneous common medium where all the elements are embedded, like in the case of yeast cells in a continuous-flow stirred tank reactor [35, 34]. Globally coupled oscillators moreover constitute a useful approximation for a larger class of spatially extended systems, provided that the range of the interaction is sufficiently large [4]. This is the case in swarms of flashing fireflies [173, 174], networks of neurons [151], cultured heart cells [150], mixed chemical reactions [112].

In particular, a lot of attention has recently been dedicated to the macroscopic effect of noise on ordinary differential equations, as reviewed in Chapter 2.

Globally coupled scalar maps constitute a prototype of such class of systems, due to the simplicity of their formulation that allows the simulation of large populations. Each map of the population is ruled by the equation:

$$x_j \mapsto (1-K)\, f(x_j) + K\, \langle f(x) \rangle + \xi_j(t) \quad j = 1, \dots N, \tag{5.2.1}$$

where $f : \mathbb{R} \to \mathbb{R}$ defines the single-element dynamics, that is the behaviour of one population element when it is decoupled from the rest of the population. The analytical method that will be proposed in sec. 5.3 requires f to be smooth.

The form of the global coupling corresponds to a diffusive coupling if the map is interpreted as the Poincaré map of an ordinary differential equation. The parameter K ranges from zero, when the population elements are decoupled, to one, when every element is mapped, in the absence of noise, into the same average value. With this scope, we address the evolution in time of the average state variable, the *mean field*:

$$X = \langle x \rangle = \frac{1}{N} \sum_{j=1}^{N}$$

and take the variance σ^2 of the noise distribution as the control parameter.

Let us start with the case of maximal coupling $K = 1$, corresponding to the limit of infinite coupling if the map is the Poincaré map of an ODE. As one would expect by continuity, if only a small amount of noise is added, the population's configuration is a perturbation of the fully synchronous regime: the time series of one single element remains close to that of the mean field, that in turn displays chaotic behaviour. This is illustrated in Figure 5.1(a) for a population of 2^{22} logistic maps of the form:

$$f(x) = 1 - a\, x^2, \tag{5.2.2}$$

with the nonlinearity parameter $a = 1.57$ inside the chaotic region. The noise term is chosen to be uniformly distributed around zero. All the examples presented in this section will refer to such a population.

Figure 5.1: Time series for the mean field X (black dots) and for one element of the population (grey circles) for $K = 1$. Population of $N = 2^{22}$ logistic maps in the chaotic region ($a = 1.57$) with uniformly distributed noise.(a) In the case of weak noise ($\sigma^2 = 0.05$), the dynamics is a small perturbation of the synchronous, chaotic, noiseless one; (b) In the case of stronger noise intensity ($\sigma^2 = 0.4$), the mean field has a regular, periodic behaviour while the time series of one population element of is scattered by noise.

The solidity of the motion within the population is lost when the noise is large, since the evolution of any element is now blurred by the stochastic term, thus

making it impossible to recognise any underlying deterministic behaviour from the sole detection of one individual time series. The mean field, however, evolves deterministically up to finite-size effects. Such a lack of concordance between the fluctuations of a single population element, that increase the closer it is to a bifurcation point, and those of the mean field, essentially governed by the population size, has been pointed out by Nichols and Wiesenfeld [113].

The regimes of macroscopic dynamics induced by noise are not coherent in the sense discussed in Chapter 3. There, a synchronisation manifold existed, along which the oscillators were locked to the average dynamics, so that if the mean field displayed a cycling behaviour, then all the population elements possessed periodic trajectories too. On the other hand, in the case of noise, the individual trajectory does not reproduce the mean field one, as it is evident from Figure 5.1.

It is remarkable that, when the noise is sufficiently intense, not only does the mean field evolution appear to remain low-dimensional, but it can be qualitatively different from the single-element uncoupled dynamics. Figure 5.1(b) shows for instance that, in the presence of microscopic noise, the mean field can display regular cyclic behaviour in spite of the fact that every element of the population is in itself chaotic.

Figure 5.2: Mean field bifurcation diagram obtained by changing the noise intensity σ^2 for maximal coupling $K = 1$. Population as in Figure 5.1.

This phenomenon is related to the fact that noise leads the trajectory of any individual element to away from the chaotic attractor, so that its dynamics is mainly influenced by the structure (attractive and repulsive manifolds, basins of attraction) of the single-element phase space in the proximity of the asymptotic

solution. The coupling among the elements then lets this different processes 'synchronise', in the sense that the probability for one individual system to be in one region of its own phase space is larger if many other individuals are also there. Hence, by averaging over the whole population the emergent collective dynamics will be mainly determined by how is the phase space structured.

Between the two cases shown in Figure 5.1, a series of other macroscopic regimes occurs, ranging from (one or two-band) chaos to cycles of different periods, that can be summarised in the bifurcation diagram shown in Figure 5.2. For noise intensities still higher, the system diverges if the single-element map is defined in an interval, as in the case of the logistic map considered here.

In spite of its resemblance with the bifurcation scenario obtained for one single-element when changing the nonlinearity parameter a, it is important to remember that such macroscopic transitions are purely due to the effect of the noise, while the population parameters are left unchanged. Nonetheless, Figure 5.2 induces the idea that a low-dimensional map could exist, whose bifurcations reproduce the qualitative changes in the mean field dynamics. Section 5.3 will be dedicated to the derivation of such an effective dynamical system.

It is worth noticing that the aforementioned macroscopic bifurcations resemble those observed for globally coupled maps with stochastic updating [104], where the uncertainty on the mean field that every element feels is given by the nature of the updating rather than by an explicit noise term, and for coupled map lattices [87, 88, 86], where the fluctuation of the local field are due to the existence of a finite correlation length.

In order to examine the microscopic features of the population in a noise-induced regime, we will consider three kinds of probability distribution functions (pdfs): the *population* (or *instantaneous*, or *snapshot*) *pdf*, relative to the values assumed by the individual maps at any fixed time, the *individual pdf* and the *mean field pdf*, computed over a given time interval for one map of the population and for the mean field respectively.

In the regime of perfect synchronisation, the first is a Dirac's delta centred on the value of the mean field, while the last two coincide and give the probability measure of the single-element chaotic attractor. When noise is increased, the pdfs are in general non trivially modified by the interplay of noise, that tends to blur the individual dynamics and broaden both the population and the individual pdfs, and coupling, that maintains a degree of coherency within the population.

As a first example, we will consider the case in which the coupling is maximal and the mean field displays a period-two cycle. It is easily seen from Eq. (5.2.1) that in this limit case the population is distributed exactly like the stochastic term. Accordingly, Figure 5.3(b) shows that the instantaneous pdf of the population of logistic maps previously considered is uniformly distributed around the mean field (not shown). This is also reflected in the individual pdf if this is computed at even and odd times separately (Figure 5.3(a)). The fact that the individual pdf is slightly broader with respect to the instantaneous one and that the mean field pdf is not exactly concentrated on the values taken during the deterministic motion is a consequence of finite size effects. These effects introduce fluctuations that will

vanish for $N \to \infty$.

Figure 5.3: Pdfs for the population of Figure 5.1, maximal coupling $K = 1$ and noise variance $\sigma^2 = 0.016$. (a) Instantaneous pdf for two successive time steps. (b) Mean field and individual pdfs.

Let us now consider the case in which the coupling is intermediate, but still strong enough to ensure full synchronisation in the absence of noise. For the population considered so far, $K = 0.4$ is right above the region where clustering occurs.

As Figure 5.4 illustrates, an increase in the noise intensity still leads to a seemingly low-dimensional bifurcation diagram. However, when comparing it to that of Figure 5.2, it is noticed that all the bifurcations are displaced towards smaller values of σ^2, so that for weaker coupling a smaller amount of noise is necessary to let the system move out of the chaotic region. Moreover, by looking carefully at the chaotic region, one can notice that the diagram appears to be

"doubled" and cannot thus be trivially rescaled to that of a scalar map.

Figure 5.4: Mean field bifurcation diagram changing the noise intensity σ^2 for intermediate coupling $K = 0.4$. Same population as Figure 5.2.

The fact that the macroscopic dynamics is no longer strictly one-dimensional is evident if the first return map of the mean field is plotted (Figure 5.5).

Figure 5.5: Folded structure of the first return map for the mean field for $K = 0.6$ and $\sigma^2 = 0.03$ (black dots). The single-element dynamics takes place in the parabola indicated by the dashed line.

In the case of a scalar map (and of maximal coupling, as we will discuss in Chapter 6), the chaotic attractor is embedded in a one-dimensional manifold, that in the case of the logistic maps is a parabola. In the chaotic region for intermediate coupling, instead, the first return map is folded, so that the macroscopic dynamics can no longer be described by means of a purely scalar equation, and the effective degrees of freedom must thus at least be two.

Figure 5.6: Pdfs for the population of Figure 5.1, intermediate coupling $K = 0.4$ and noise intensity $\sigma^2 = 0.015$. The mean field displays a period-two cycle, as in Figure 5.3. (a) Instantaneous pdf for two successive time steps. (b) Mean field and individual pdfs.

The microscopic picture of the system is also significantly changed for intermediate coupling strengths. If we consider $K = 0.4$ and $\sigma^2 = 0.015$, where the mean field displays a period-2 cycle, like in the case of maximal coupling we discussed before, we notice immediately that the correspondence between the instantaneous pdf and the noise distribution is lost (Figure 5.6). The individual pdfs for odd/even

times still reflect the instantaneous pdf and the mean field pdf is peaked around the values taken during the cycle.

If the noise intensity is also reduced, so that both the coupling and the noise intensity are sufficiently weak, the possibility of inferring the individual pdf from the instantaneous distribution is lost. For $\sigma^2 = 0.003$, indeed, the mean field displays two-band chaos. Figure 5.7 shows that the population distribution changes in time depending on the actual position of the mean field on the macroscopic attractor. The individual pdfs for odd/even times still allow us to recognise a periodicity in the motion, while the mean field pdf corresponds to the probability measure of the macroscopic attractor.

Figure 5.7: Pdfs for the population of Figure 5.1, intermediate coupling $K = 0.4$ and noise intensity $\sigma^2 = 0.003$. The macroscopic dynamics takes place on a a two-banded chaotic attractor. (a) Instantaneous pdf for two successive time steps. (b) Mean field and individual pdfs.

Even if in our further analysis we will focus on the region of strong coupling, it is interesting to look at the bifurcation diagram for fixed noise intensity, and observe how the mean field dynamics changes when the coupling strength is decreased (Figure 5.8).

Figure 5.8: Bifurcation diagram for fixed noise intensity ($\sigma^2 = 0.005$), changing the coupling strength K. Same population as Figure 5.1.

The mean field exits again the region of chaoticity, even if the period doubling bifurcation cascade appears in this case strongly distorted with respect to that of the single uncoupled map. For low coupling, the mean field is stationary, corresponding to a region of incoherent motion. In the limit of zero coupling, the maps are decoupled and their average is given by the average of the probability measure of the single-element chaotic attractor.

It is beyond the scope of this paper to discuss the weak coupling regimes, where the collective motion is expected to display bi/multistability. We just want to mention that Figure 5.8 is in agreement with Shibata, Chawanya and Kaneko [144] who found that even weak noise is sufficient for destroying the structure of the noiseless macroscopic attractor, drastically reducing its dimensionality.

Moreover, we can notice that the bifurcation to the stationary solution takes place through a subcritical bifurcation, and thus an interval in coupling strength exist where the system is bistable (or multistable), which corresponds to the existence of clusters for the noiseless case [106].

Figures 5.2, 5.4 and 5.8 can be summarised in the bifurcation diagram with respect to the two population-level parameters K, measuring the coupling strength, and σ^2, measuring the noise intensity. Figure 5.9 shows the lines where the first three period doubling bifurcations of the mean field occur, that encompass the region of collective chaotic behaviour.

Figure 5.9: Bifurcation diagram for the population of Figure 5.1 with respect to K and σ^2, showing the lines where period-doubling bifurcations occur. The dots are the period-doubling bifurcation points numerically detected in the population of Figure 5.7. The bifurcation lines are obtained by connecting such points.

For sufficiently high noise intensities and strong coupling, the macroscopic dynamics is periodic of period two. By decreasing the noise intensity or increasing the coupling (for sufficiently low noise) the macroscopic dynamics undergoes a period-doubling bifurcation cascade, leading to regimes of collective chaos.

Finally, it is worth mentioning that analogous phenomena of noise-induced macroscopic bifurcations have been studied in the context of continuous-time dynamical systems. In particular, the attention has been focused on excitable systems, where the firing of the single systems induced by the addition of noise is amplified by the presence of coupling and gives rise to a macroscopic regular mean field dynamics [131, 178].

5.3 Order parameter expansion

In this section we will develop a method that allows us to describe the macroscopic regimes of large population of globally and strongly coupled noisy maps, numerically studied in section 5.2, in terms of few macroscopic degrees of freedom. This method is formally analogue to the order parameter expansion formulated in Chapter 3 for populations with parameter mismatch. An approximate (exact for maximal coupling) reduced system reproducing the time evolution of such macroscopic variables will be derived in general, given the single-element dynamics:

$$x_j \mapsto (1-K)\, f(x_j) + K\, \langle f(x) \rangle + \xi_j(t) \quad j = 1, \dots N, \tag{5.3.1}$$

and the noise distribution moments $m_q = \langle \xi^q \rangle$. This system is obtained by closing the infinite hierarchy of equations for the moments of the population distribution in the limit of strong coupling.

Since our aim is to find a map that is able to reproduce the behaviour of the mean field $X = \langle x_j \rangle$, its iterate is formally computed by averaging Eq. (5.3.1) over the population units. The individual dynamics can be expanded in series with respect to the distances $\epsilon_j := x_j - X$ between the population elements and the mean field, thus yielding:

$$f(x_j) = f(X) + \sum_{q=1}^{\infty} \frac{1}{q!}\, \mathcal{D}^q f(X)\, \epsilon_j^q. \tag{5.3.2}$$

where $\mathcal{D}^q f$ indicates the q-th derivative of the function f.

Substituting in the mean field definition, we get the following equation for the macroscopic dynamics:

$$X \mapsto \langle f(x) \rangle = f(X) + \sum_{q=1}^{\infty} \frac{1}{q!}\, \mathcal{D}^q f(X)\, \langle \epsilon^q \rangle \; + \langle \xi \rangle \; . \tag{5.3.3}$$

The mean field is thus coupled to other macroscopic variables, the moments of the population instantaneous pdf, that we will from now on call *order parameters*. This is not only to avoid confusion with the noise distribution moments, but also to stress that these are the degrees of freedom relevant for a macroscopic description. Moreover, as will be show in Chapter 7, in the more general case in which the elements are not identical, the same expansion leads to order parameters that do not coincide with the population's moments. The q-th order parameter is defined as:

$$\Omega_q := \langle \epsilon^q \rangle \qquad\qquad q \in \mathbb{N}. \tag{5.3.4}$$

The iterate of the displacements:

$$\epsilon_j \mapsto (1-K) \sum_{p=1}^{\infty} \frac{1}{p!}\, \mathcal{D}^p f(X)\, \left(\epsilon_j^p - \Omega_p\right) + \xi_j - \langle \xi \rangle$$

can now be used for computing the order parameters iterate:

$$\Omega_q \mapsto \sum_{i=0}^{q} \binom{q}{i} (1-K)^i \left\langle (\xi - \langle \xi \rangle)^{q-i} \left[\sum_{p=1}^{\infty} \frac{1}{p!} \mathcal{D}^p f(X) \left(\epsilon^p - \Omega_p\right) \right]^i \right\rangle .$$

These equations can be recast into a more explicit form by observing that, as a consequence of the fact that the displacements ϵ_j and the noise are uncorrelated variables, $\langle h(X,\epsilon)\, \xi^q \rangle = \langle h(X,\epsilon) \rangle \, \langle (\xi - \langle \xi \rangle)^q \rangle$.

Moreover, taking the limit $N \to \infty$, the equations for the order parameters become:

$$\Omega_q \mapsto m_q + \sum_{i=1}^{q} \binom{q}{i} (1-K)^i \, m_{q-i} \left\langle \left[\sum_{p=1}^{\infty} \frac{1}{p!} \mathcal{D}^p f(X) \left(\epsilon^p - \Omega_p\right) \right]^i \right\rangle , \qquad (5.3.5)$$

where $m_q = \langle (\xi - \langle \xi \rangle)^q \rangle$ is the q-th moment of the noise distribution.

It is worth noticing that in taking the limit of infinite population size, in the mean field equation Eq. (5.3.3) we have neglected a term that scales like $1/\sqrt{(}N)$, that also defines the dominant scaling in the equations hierarchy. This "macroscopic noise" term accounts for the fact that for sufficiently large population sizes the mean field follows the law of large numbers. However, for smaller populations one expects to observe anomalies in the scaling of the mean field fluctuations due to the fact that the order parameters are themselves undergoing finite-size fluctuations.

The important point now is that the order parameters iterates depend on powers of $(1-K)$. Considering the fact that we are interested in the strong coupling region, this means that the order parameter expansion can be approximated by its truncation and the macroscopic dynamics given in a closed form. This approximated closed system will be also referred to as *reduced system*. The behaviour of the population can thus be seen as a perturbation of the limit case of maximal coupling $K = 1$, when the order parameters are, as Figure 5.3 shows, simply the moments of the noise distribution.

Looking at Eq. (5.3.5), one can see that, if the map is a polynomial of order P and the expansion is truncated to order n in $(1-K)$, there are only $n\,P$ independent order parameters, by which the remaining infinite degrees of freedom are slaved. The iterate of Ω_q for $q > n\,P$ is indeed a function of the first $n\,P$ elements of the hierarchy.

Such a $n\,P$-dimensional map can be simplified further and reduced to a system of n equations independently of the degree of nonlinearity of the single-element dynamics. In order to demonstrate this, let us define the vector $\mathbf{\Gamma}$ containing the terms that multiply $(1-K)^i$ $(i < n\,P)$ in the following way:

$$\Gamma_i = \left\langle \left[\sum_{p=1}^{P} \frac{1}{p!} \mathcal{D}^p f(X) \left(\epsilon^p - \Omega_p\right) \right]^i \right\rangle \qquad i = 1, \ldots, n\,P.$$

Let us then call $\mathbf{\Omega}$ the vector collecting the first $n\,P$ order parameters and $\mathbf{m}$ that composed by the corresponding moments of the noise distribution.

Eqs. (5.3.5) can thus be written as:

$$\mathbf{\Omega} - \mathbf{m} \mapsto \mathcal{C}\,\mathbf{\Gamma}, \tag{5.3.6}$$

where $\mathcal{C}$ is a $n\,P \times n\,P$ matrix whose entries are:

$$\begin{cases} \mathcal{C}_{q,i} = \binom{q}{i} (1-K)^i \; m_{q-i} & q = 1, \ldots, n\,P \qquad i < \min\{q, n\} \\ \mathcal{C}_{q,q} = (1-K)^q & q < n \\ \mathcal{C}_{q,i} = 0 & \text{otherwise.} \end{cases}$$

The $n\,P$ dimensional truncation of the order parameter expansion will have a number of constants of motion equal to the dimension of $\ker(\mathcal{C})$. Hence, it can be reduced by means of a linear transformation to a system whose dimension equals the rank of $\mathcal{C}$.

It is easy to see that $\mathcal{C}$ has rank smaller or equal to n, since all the columns with index $i \in \{n+1, n\,P\}$ have only null entries. If the noise is chosen to have zero average, also the first column is null and the equations for the order parameters can be reduced to a system of $n-1$ maps.

Together with the equation for the mean field the reduced system to order n will be thus in general composed of n scalar maps.

5.4 Order parameter expansion: reduced systems to the zeroth and second order

As we demonstrated in the previous section, the reduction of the n-th order truncation of the order parameter expansion to a n-dimensional system can be made in general. Its actual computation can however be quite engaging, so that here we will discuss only the truncations to the first orders. In Chapter 6 we will derive case by case, when needed, the reduced systems to order higher than two.

The lowest order truncation is the zeroth-order:

$$X \mapsto f(X) + \sum_{q=1}^{\infty} \frac{1}{q!}\,\mathcal{D}^q f(X)\, m_q. \tag{5.4.1}$$

This equation describes exactly the mean field dynamics for maximal coupling and provides a first approximation for the dynamics at strong coupling. Being independent of K, it cannot describe the change in the bifurcation values when the coupling is lowered.

It is remarkable that Eq. (5.4.1) naturally contains the interplay between nonlinearities of the uncoupled map, represented by the derivatives of the single-element dynamics, and the features of the noise distribution, given by its moments.

In particular, it allows us to infer that, if the single-element dynamics is polynomial, only a finite number of the noise distribution moments m_q will influence the macroscopic dynamics. This induces a relation of equivalence onto the space of the distributions for stochastic term. These distributions can thus be divided into classes on the bases of the effect on the mean field. Chapter 6 will provide some explanatory example of this "universality classes".

If the noise distribution has zero average, as we have assumed, the first order truncation only yields the relation $\Omega_1 = 0$, so we have to go to the second order to get a further approximation of the macroscopic dynamics. Such a truncation corresponds to the Gaussian approximation of the population pdf, commonly used for closing cumulant expansions [178]. However, it must be noticed that this does not imply that the noise distribution can be characterised only by its variance. In this case, Eq. (5.3.6) furnishes a recurrence relation for the order parameters:

$$\Omega_{q+2} = m_{q+2} - \frac{(q+2)(q+1)}{q(q-1)} \frac{m_q}{m_{q-2}} (m_q - \Omega_q).$$

which allows us to express every order parameter as a function of Ω_2 through the computation of a telescopic series:

$$\Omega_q = m_q - \frac{q(q-1)}{2}\, m_{q-2}\, \left(\sigma^2 - \Omega_2\right). \tag{5.4.2}$$

One of the consequences of the last equation is that all the odd order parameters are constantly equal to the corresponding moment of the noise distribution.

Equation (5.3.5) can be rewritten, expliciting the squared term, as:

$$\begin{aligned} \Omega_q \mapsto \quad & m_q + \frac{q(q-1)}{2}\,(1-K)^2\, m_{q-2} \\ & \left\{ \sum_{p,r=1}^{\infty} \frac{1}{p!\, r!}\, \left[\mathcal{D}^p f(X)\right]\, \left[\mathcal{D}^r f(X)\right]\, \Omega_{p+r} - \left[\sum_{p=1}^{\infty} \frac{1}{p!}\, \mathcal{D}^p f(X)\, \Omega_p \right]^2 \right\}. \end{aligned}$$

Substituting in this last equation the recurrence Eq. (5.4.2), one gets the two-dimensional reduced system :

$$\begin{aligned} X \mapsto \quad & f(X) + \alpha_0(X) + \alpha_1(X)\, \Omega_2 \\ \Omega_2 \mapsto \quad & \sigma^2 + \,(1-K)^2 \left[\gamma_0(X) + \gamma_1(X)\, \Omega_2 + \gamma_2(X)\, \Omega_2^2 \right]. \end{aligned} \tag{5.4.3}$$

The coefficients:

$$\alpha_0(X) = \sum_{q=2}^{\infty} \frac{1}{q!}\, \mathcal{D}^q f(X) \left[m_q - \binom{q}{2} m_{q-2}\, \sigma^2 \right]$$

$$\alpha_1(X) = \frac{1}{2} \sum_{q=2}^{\infty} \frac{1}{(q-2)!}\, \mathcal{D}^q f(X)\, m_{q-2}$$

$$\gamma_0(X) = -\left[\alpha_0(x)\right]^2 + \beta_0(X) - \beta_1(X)\, \sigma^2$$

$$\gamma_1(X) = \beta_1(X) - 2\, \alpha_0(X)\, \alpha_1(X)$$

$$\gamma_2(X) = -\left[\alpha_1(X)\right]^2,$$

where:

$$\beta_0(X) = \sum_{q,p=1}^{\infty} \frac{1}{q!\, p!}\, \left[\mathcal{D}^q\, f(X)\right]\, \left[\mathcal{D}^p\, f(X)\right] m_{q+p}$$

and:

$$\beta_1(X) = \sum_{q,p=1}^{\infty} \frac{1}{q!\, p!}\, \left[\mathcal{D}^q\, f(X)\right]\, \left[\mathcal{D}^q\, f(X)\right] \binom{q+p}{2} m_{q+p-2}$$

depend on the nonlinearities of the single-element dynamics and on the moments of the noise distribution. If f is a polynomial of degree P, the highest moment of the noise distribution that occurs as a macroscopic parameter is m_{2P}, and the higher order moments are unimportant for this approximation level.

The order parameter expansion is complementary to the methods based on the moment expansion of the Perron-Frobenius operator (Fokker-Plank equation in case of ODEs) [41, 124], which are often formally simple but generally extremely hard to solve analytically. On the other hand, our expansion is analogous in spirit to the method proposed by Shimansky-Geier and coworkers [78, 90].

Chapter 6

Order parameters in populations of noisy maps

In Section 5.3 we have proposed a method to tackle the strong coupling collective regimes in populations of globally coupled maps. In the derivation of the macroscopic equations of motion we have made no assumption on the specific for of the single-element dynamics and of the noise distribution, except basic requirements of smoothness.

This chapter is dedicated to demonstrate that the proposed approach is actually useful for the description of the population dynamics. Moreover, we show that the analysis of the equations for the order parameters allows us to predict what features at the level of the individuals are relevant for a macroscopic description and why.

As a first step, we address the regimes of maximal coupling, where the macroscopic equations have been derived exactly. Here, we show that the observed collective regimes originate from the interplay between the nonlinearities of the single-element dynamics and the features of the noise distribution. On the one side, this means that discrepancies on the highest orders of the single-element dynamics can be detected only for sufficiently strong noise. On the other side, we show that the microscopic map determines which of the noise distribution statistics the mean field behaviour is sensitive to. These two facts suggest that even if only averaged observable are accessible, information about the features of the single-element dynamics can be gathered by purely macroscopic measurements.

If the coupling is less than maximal, the order parameter evolution derived in the previous chapter is only an approximation for the mean-field trajectory. Section 6.2 examines the accuracy of the different approximation levels and relates them to the hierarchical structure of the macroscopic attractor. The order parameters are shown to describe finer and finer details of the mean field dynamics as their degree increases. For a broad region of coupling strengths, however, the second order approximation provides a sufficiently accurate description of the mean field attractor, in accordance with the direct simulation of the population

dynamics.

Section 6.3 discusses the dimensionality of the macroscopic attractor. The question whether the mean field orbit belongs to a manifold of low (in general, finite) dimension in the infinite-dimensional phase space of the population has been so far addressed for weak coupling regimes, as reviewed in Chapter 2. In the region of high coupling, the apparent low dimensionality of the macroscopic attractor and of the codimension of its bifurcations seems to be in contrast with the infinite levels of details that can be obtained by opportunely magnifying its structure. We will show here that the Lyapunov dimension of the mean field dynamics is finite in the region of strong coupling we address. Indeed, the evolution operator for the population pdf possesses only one positive Lyapunov exponent, while the other exponents become infinitely negative as the coupling approaches its maximal value. On the other hand, the modulus of these negative exponents approaches zero, and correspondingly the Lyapunov dimensionality increases, when the coupling is weakened. It is thus possible that for very small noise intensity and weak coupling our description combines with that of Shibata and Kaneko [144]. In order to confirm this, however, further studies should be conducted on the region of intermediate couplings, where the complexity of the mean field dynamics poses nontrivial numerical problems. As long as the coupling is strong, the reduced system reproduces the first n larger Lyapunov exponents, where n is the truncation degree of the expansion. The fact that the Lyapunov dimension provides an accurate measure of the fractal dimension of the attractor depends on whether the Kaplan-Yorke conjecture is valid in this case, which does not seem to be true at least in the limit of vanishing noise intensity.

In order to explore different possible applications of the order parameter expansion, and to confirm its generality, we will examine the mean field behaviour for populations with different single-element dynamics. Sections 6.1 and 6.2 will deal with the logistic maps considered in the previous chapter as an example. Section 6.1 will address different microscopic behaviour (logistic and quartic maps) and different noise distribution (uniform and Gaussian noise).

The case in which the single-element dynamics is excitable is examined separately in Section 6.4. In particular, we will address the relation of the noise-induced macroscopic bifurcations with the phenomenon of coherence resonance. As reported in Section 2.5.1, the existence of a noise intensity that optimises the signal-to-noise ration has been extensively studied for this class of systems. Here, we show that looking at the time series of one population element, rather than on the average value, we can associate a similar property to the onset of macroscopic oscillations. In particular, the optimal noise intensities are in our case those of the periodic windows within a chaotic attractor. Since the excitable map we consider is not polynomial, we will need a second closure assumption on the intensity of the noise in order to get a low-dimensional description of the mean field dynamics. In this manner, we derive a reduced system that allow us to associate the intermittent spikes in the mean field dynamics to crisis of a chaotic saddle, that gives rise to a macroscopic chaotic attractor.

6.1 Maximal coupling

As already pointed out in section 5.4, the order parameter expansion provides exact results when $K = 1$. In this case, the reduced system is a scalar map whose functional form Eq. (5.4.1) is a linear combination of the derivatives of the single-element dynamics $f(x)$, with coefficients proportional to the moments of the noise distribution.

Two major consequences can be drawn from the observation of the mean field equation Eq. 5.4.1 for polynomial maps.

First, if the highest nonlinearity of the microscopic map is P, all noise distributions having the same first P moments will affect the macroscopic dynamics in the same manner. For instance, if the single-element dynamics is logistic, as in the examples presented in section 5.2, the bifurcation diagram shown in Figure 5.2 does not change if instead of uniform noise we use Gaussian noise with the same variance. In turn, this is exactly reproduced by the bifurcation diagram of the macroscopic map:

$$X \mapsto 1 - a\,\sigma^2 - a\,X^2, \tag{6.1.1}$$

displayed in Figure 6.1.

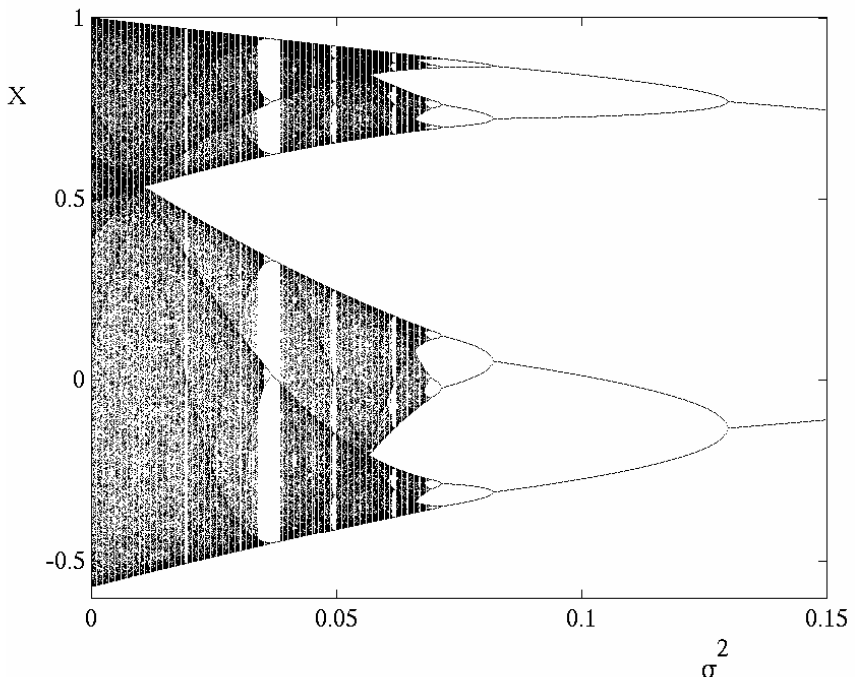

Figure 6.1: Bifurcation diagram of Eq. (6.1.1) for logistic maps ($a = 1.57$).

It is easily seen that Eq. (6.1.1) can be rescaled into the same form as the

microscopic logistic map, with the change of parameter:

$$a' = a\,(1 - a\,\sigma^2)$$

and of variable

$$X' = \frac{X}{(1 - a\,\sigma^2)}.$$

In this manner, the bifurcation diagram of Figure 5.2 can be mapped one-to-one into the usual Feigenbaum cascade for the single logistic map:

$$X' \mapsto 1 - a'\,X'^2$$

undergoing a change in the nonlinearity parameter. This leads us to interpret the qualitative changes in the collective dynamics as noise-induced macroscopic bifurcations.

A second aspect of the interplay between nonlinearities of the individual map and moments of the noise distribution is that the macroscopic effects of the microscopic stochasticity depend on the moments of the noise distribution of order less than the degree of the map. This means for instance that if the microscopic dynamics is ruled by a map with linearities higher than quadratic, uniform and Gaussian noise terms will induce qualitatively different bifurcation diagrams as the variance σ^2 is changed.

As an example, let us consider populations whose single-element dynamics is ruled by the quartic map:

$$x \mapsto 1 - a\,x^2 + b\,x^4. \tag{6.1.2}$$

The reduced system Eq. 5.4.1 read in this case :

$$X \mapsto 1 - a\,\sigma^2 + b\,m_4 - \left(a - 6\,b\,\sigma^2\right)\,X^2 + b\,X^4. \tag{6.1.3}$$

Figure 6.2 displays the diagrams of the macroscopic attractor for the cases of uniform and Gaussian noise distributions. The diagrams for the corresponding populations, not shown, coincide with those for Eq. 6.1.3 up to finite-size effects.

When the noise intensity is small, the bifurcations scenarios for the two populations are very similar, but their diversity becomes progressively more evident as the intensity increases. For strong noise, the population behaves chaotically or is stationary depending whether the noise distribution is uniform or Gaussian, respectively. This fact can be understood by looking at the macroscopic equations of motion. Contrary to the reduced system for the logistic map Eq. (6.1.1), that for the quartic map Eq. (6.1.2) shows a dependence on the fourth moment of the noise distribution. Since the kurtosis scales as σ^4, the two macroscopic descriptions diverge as the weight of the fourth moment grows.

Figure 6.2 also shows that the macroscopic dynamics is bistable for intermediate noise values and that the hysteresis region is slightly changed by the kind of noise that is applied. Similar hysteretical phenomena have been found in populations of globally coupled ODEs with independent noise [66] and with parameter mismatch (see Section 3.2).

Figure 6.2: Bifurcation diagrams of Eq. (5.4.3) for quartic maps ($a = 1.57$, $b = 0.1$) with different noise distributions: Gaussian (grey dots), uniform (black dots).

6.2 Strong coupling

When the coupling is less than maximal, any truncation of the order parameter expansion represents an approximation of the dynamics of the full infinite-dimensional system. Nonetheless, in this section we will show that this approximation not only accounts for the qualitative features of the collective dynamics, but also has a quantitative agreement with the simulations for the population's mean field. By capturing the hierarchical nature of the macroscopic chaotic attractor, the order parameter expansion allows us to describe the collective dynamics in increasing detail, the more macroscopic variables are taken into account.

This section will deal with the same population of logistic maps that has already been used in Section 5.2. The fact that this map has a quadratic nonlinearity would allow us to write explicitly any truncation of the order parameter expansion. In this work, we present only the truncation up to the fourth order. The successive orders can be retrieved with some algebra according to the procedure outlined in Section 5.3.

Let us now write explicitly the truncations of the order parameter expansion to the first relevant orders and see what kind of information they provide. We already derived the zeroth order reduced system Eq. (6.1.1). It is evident that such a scalar dynamical system cannot be a good approximation for the collective dynamics if the interaction strength is less than maximal, since it is independent on the coupling constant K.

Due to the fact that the noise has zero mean, the first order truncation does not provide any new dynamical feature, but only states that the mean field is mapped into the average of the iterates.

The truncation to the second order of Eq. (3.3.8) is a four-dimensional map. By exploiting the existence of two constants of motion, as illustrated in Section 5.3, this can be reduced to to the system of two equations:

$$\begin{cases} X \mapsto & 1 - a\, X^2 - a\, \Omega_2 \\ \Omega_2 \mapsto & \sigma^2 + (1-K)^2\, a^2 \left[m_4 - 6\sigma^4 + (4X^2 - \Omega_2 + 6\,\sigma^2)\, \Omega_2 \right]. \end{cases} \tag{6.2.1}$$

Figure 6.3: First period-doubling bifurcation lines for the full (dots), second order reduced system Eq. (6.2.1) (continuous line) and fourth order reduced system Eq. 6.2.4 (dashed line). The zeroth order approximation would give vertical lines corresponding to the bifurcation values for $K = 1$.

This macroscopic map depends on the coupling constant K, that plays the role of a population-level parameter for the macroscopic dynamics. Together with it, we find that the collective motion is influenced by other population-level parameters, that are the first four moments of the noise distribution.

The subsequent order parameters are either slaved to the first two or constant. The third, Ω_3 is trivially equal to the skewness m_3 of the noise distribution. When this is symmetric, as in the cases we have considered so far, it is thus constantly zero. The fourth order parameter depends linearly on the second:

$$\Omega_4 = m_4 + 6\,\sigma^2\left(\Omega_2 - \sigma^2\right), \tag{6.2.2}$$

where m_4 is the kurtosis of the noise distribution (in general, m_q stands for the q-th moment of the noise distribution). All the other order parameters are equal to the moments of corresponding degree. Again, this means that the odd order parameters all vanish for symmetric noise distributions.

Equations (6.2.2) are sufficient to capture the most salient features of the macroscopic dynamics. First of all, they reproduce the shift towards smaller noise intensities of the period doubling bifurcation cascade, which occurs when the coupling strength is weakened. Figure 6.3 indeed shows that the region where the macroscopic dynamics is chaotic shrinks when K is reduced, so that for low couplings a small amount of noise is sufficient to drive the collective dynamics to periodic regimes. This result is compatible with what was observed by Shibata, Chawanya and Kaneko [144] and by Li [89], although these authors focused their attention onto the region of weak coupling.

Figure 6.4: First return map of the population (black dots) and of the reduced system at second order Eq. (6.2.1) (grey dots), for $K = 0.4$ and $\sigma^2 = 0.001$. The dashed line is the invariant parabola on which the single-element dynamics is embedded, the solid line is the invariant parabola for the zeroth-order approximation Eq. (6.1.1).

Secondly, the introduction of a second order parameter captures the fact that, inside the chaotic region, the collective dynamics is no longer one-dimensional as

soon as K is strictly less than one. However, the need for introducing a second degree of freedom in the description of the mean field dynamics becomes evident only for sufficiently low coupling, where the folded structure of the first return map can be resolved over the blurring of the attractor due to finite-size effects. Figure 6.4 shows that such folding is captured with great accuracy by the second order truncation Eq. (6.2.1), while the zeroth-order, scalar Eq. (6.1.1) only provides a slight correction to the single-element map.

In spite of the fact that the second order truncation reproduces qualitatively and quantitatively the macroscopic dynamics of the population, this approximation is still insufficient for describing the asymmetry in the snapshot distribution that is introduced by the interplay between coupling and noise. The fact that for a coupling less than maximal the population is no longer symmetrically distributed around the mean field is evident from Figs. 5.6 and 5.7. Therefore, one would not expect the third order parameter to be strictly zero. This is indeed the case as, in general, the third moment of the snapshot distribution has a dynamics. However, this can be accounted for by a increasing the approximation level of the order parameter expansion.

The truncation to the third order can be compactly written as the reduced system:

$$\begin{cases} X \mapsto & 1 - a\,X^2 - a\,\Omega_2 \\ \Omega_2 \mapsto & \sigma^2 + (1-K)^2\,a^2\,\Sigma_2 \\ \Omega_3 \mapsto & -(1-K)^3\,a^3\,\Sigma_3 \end{cases} \tag{6.2.3}$$

where:

$$\begin{aligned} \Sigma_2 = \quad & m_4 - 6\,\sigma^4 + 6\,\sigma^2\,\Omega_2 - \Omega_2^2 + 4\,X^2\,\Omega_2 - 4\,X\,\Omega_3 \\ \Sigma_3 = \quad & m_6 - 15\,m_4\,\sigma^2 + \left(12\,m_4 - 72\,\sigma^4\right)\,X^2 + \left(12\,m_4 + 18\,\sigma^4\right)\,\Omega_2 + 72\,\sigma^2\,X^2\,\Omega_2 \\ & -18\,\sigma^2\,\Omega_2^2 - 12\,X^2\,\Omega_2^2 + 2\,\Omega_2^3 - 12\,X\,\Omega_2\,\Omega_3 + 8\,X^3\,\Omega_3. \end{aligned}$$

The following three order parameters are slaved to the first three macroscopic variables and they obey the relations:

$$\begin{aligned} \Omega_4 = \quad & m_4 + 6\,\sigma^2\left(\Omega_2 - \sigma^2\right) \\ \Omega_5 = \quad & 10\,\sigma^2\,\Omega_3 \\ \Omega_6 = \quad & m_6 + 15\,m_4\left(\Omega_2 - \sigma^2\right), \end{aligned}$$

while $\Omega_q = m_q$ holds for $q > 6$.

Figure 6.5: The third order parameter Ω_3 versus the second Ω_2 for the population of logistic maps (back dots) and for the third order reduced system Eq. (6.2.3) (grey dots). The continuous line is the invariant manifold which embeds the dynamics of the second order truncation Eq. (6.2.1) (light grey dots) and of the zeroth order truncation Eq. (6.1.1) (square).

In order to check that Eq. 6.2.3 actually captures additional properties of the macroscopic dynamics, we plot the third order parameter as a function of the second (Figure 6.5). In both the zeroth and the second order truncation, the third order parameter vanishes. The third order approximation, instead, reproduces the qualitative structure of the population behaviour, displaying an analogous folding.

By iterating these considerations, one can draw similar conclusions for the successive truncations.

As a last example, we project the macroscopic attractor onto the plane (Ω_2, Ω_4), as shown in Figure 6.6. In the zeroth order truncation, the two order parameters coincide with the noise distribution moments and thus identify only a point. Both the second and the third order truncations give for Ω_4 a dynamics that is embedded in the line defined by Eq. (6.2.2).

Let us now consider the truncation to the fourth order:

$$\begin{cases} X \mapsto & 1 - a\,X^2 - a\,\Omega_2 \\ \Omega_2 \mapsto & \sigma^2 + (1-K)^2\,a^2\,\Sigma_2 \\ \Omega_3 \mapsto & (1-K)^3\,a^3\,\Sigma_3 \\ \Omega_4 \mapsto & m_4 + 6\,\sigma^2\,(1-K)^2\,a^2\Sigma_2 + (1-K)^4\,a^4\,\Sigma_4 \end{cases} \tag{6.2.4}$$

Figure 6.6: The fourth order parameter Ω_4 versus the second Ω_2 for the population of logistic maps (back dots) and for the fourth order reduced system Eq. (6.2.4) (grey dots). The continuous line is the invariant manifold which embeds the dynamics of the second and third order truncation Eqs. (6.2.1) and (6.2.3) (light grey dots) and of the zeroth order truncation Eq. (6.1.1) (square).

where:

$$\begin{aligned}
\Sigma_2 = \quad & \Omega_4 - \Omega_2^2 + 4\,X^2\,\Omega_2 + 4\,X\,\Omega_3 \\
\Sigma_3 = \quad & \Omega_6 + 6\,X\,\left(\Omega_5 - 2\,\Omega_2\,\Omega_3\right) - 3\,\Omega_2\,\Omega_4 - 12\,X^2\,\left(\Omega_2^2 - \Omega^4\right) + 8\,X^3\,\Omega_3 + 2\Omega_2^3 \\
\Sigma_4 = \quad & \Omega_8 + 8\,X\,\left(3\,\Omega_2^2\,\Omega_3 - 2\,\Omega_2\,\Omega_5 + \Omega_7\right) + 24\,X^2\,\left(\Omega_2^3 - 2\,\Omega_2\,\Omega_4 + \Omega_6\right) \\
& -4\Omega_2\,\Omega_6 - 32X^3\,\left(\Omega_2\,\Omega_3 - \Omega_5\right) + 6\Omega_2^2\,\Omega_4 + 16X^4\,\Omega_4 - 3\Omega_2^4
\end{aligned}$$

and:

$$\begin{aligned}
\Omega_5 = \quad & 10\,\sigma^2\,\Omega_3 \\
\Omega_6 = \quad & m_6 + \left(m_4 - 6\,\sigma^4\right)\left(\Omega_2 - \sigma^2\right) + \sigma^2\,\left(\Omega_4 - m_4\right) \\
\Omega_7 = \quad & 35\,m_4\,\Omega_3 \\
\Omega_8 = \quad & m_8 + 28\,\left(m_6 - 15\,m_4\,\sigma^2\right)\left(\Omega_2 - \sigma^2\right) + 70\,m_4\,\left(\Omega_4 - m_4\right).
\end{aligned}$$

Figure 6.6 shows that the fourth order parameter, that at this approximation level is an independent variable, indeed has a dynamics very close to that of the population.

The order parameter expansion seems thus to capture the hierarchical organising structure of the macroscopic attractor, furnishing more and more details as the truncation order is increased.

In general, however, this fine structure of the emergent dynamics can be neglected in the exam of the mean field behaviour, which is not significantly altered by an improvement of the approximation level. This is testified by the fact that the first return map does not change significantly when the truncation order is increased. Indeed, the higher order approximations are nearly indistinguishable from the second-order one even in the region of low coupling and chaotic behaviour considered on this section (therefore, in Figure 6.4 we have only plotted the second order truncation). Analogously, the main trend of the period-doubling bifurcation lines is captured by Eq. (6.2.1), while further approximations only slightly improve the quantitative agreement with the bifurcation diagrams of the full system.

At first, the agreement between analytical and numerical results can be surprising, considering that an infinite number of terms have been neglected in the closure of the order parameter expansion. On the other hand, it is understandable that the reduced systems describes well the cyclic macroscopic regimes if one thinks in terms of the microscopic picture of the population: in a cyclic regime of period two, for instance, the snapshot pdf alternates between two well defined states. Consequently, its moments Ω_q will all evolve periodically with period two. The relative error that the n-th order reduced system introduces in the estimate of the values assumed by the moment m_q ($q > n$) is of the order of magnitude of $\binom{q}{n} m_n/m_q$, that remains limited. It is indeed noticeable that the second and fourth order truncations give essentially the same period-doubling bifurcation lines.

6.3 Dimensionality of the macroscopic dynamics

Although the need of introducing a second order parameter for the description of the mean field dynamics is evident from the existence of folding, it is not at all clear what the dimensionality of the macroscopic dynamics is and in how many dimensions it should be embedded.

A similar question has been previously addressed for the regimes of weak coupling, where the noise drastically affects the otherwise incoherent motion, introducing correlations among the population elements. When the noise intensity is increased, the mean field seems to "collapse" on a low-dimensional attractor, and the finite-size Lyapunov dimension decreases as $-\log \sigma^2$ [144]. As discussed by Shibata et al. [144, 143] and Cencini et al. [22, 108], such a low-dimensional collective dynamics is not in contradiction with the fact that microscopically all the oscillators are chaotic. To the contrary, it emerges naturally when the observation time scale is long enough, so that the evolution of a sufficiently big perturbation of a finite (though large) system is representative of the infinite-size limit perturbation response.

Following such an interpretation of macroscopic chaos, we claim that if the coupling is sufficiently strong, there exists a truncation of the order parameter expansion which is able to effectively reproduce the collective dynamics. The dimensionality of the reduced system increases when the coupling weakens, being

strictly one only in the limit case $K = 1$. For a fixed coupling, the macroscopic dynamics is effectively described by a sufficiently large number n of order parameters. In this approximation, the following $n\,P$ order parameters (where P is the degree of the microscopic map) are slaved to the principal ones, while all the others can be approximated by the noise distribution moments within the error of a macroscopic description.

In order to substantiate this claim, we will show that the Lyapunov exponents of the reduced system correspond to the larger Lyapunov exponents of the population. This allow us to compute the Lyapunov or Kaplan-Yorke dimension of the macroscopic attractor directly from the low-dimensional reduced system.

The largest Lyapunov exponents of the population are numerically computed in the thermodynamic limit, where the population is described by a continuous probability distribution function. Such a snapshot pdf evolves according to the nonlinear Perron-Frobenius operator [124, 144, 143]:

$$\rho_{t+1}(x) = \int G\left\{F_t(y) - x\right\}\ \rho_t(y)\, dy \tag{6.3.1}$$

where $\rho_t(x)$ is the population probability distribution at the time t, $G\{z$ is the distribution of the noise term and F_t is the iterate of the map:

$$F_t(y) = (1 - K)\ f(y) + K \int \rho(z)\, dz.$$

The dynamics defined in this way can be simulated numerically by choosing a sufficiently fine binning on the support of the pdf, that allows to represent the pdf by a vector on which the discretised form of the Perron-Frobenius operator acts.

The Lyapunov exponents are computed with the method of Benettin et al. [12], following the evolution of a step perturbation of the pdf, according to the formula:

$$\lambda_i = \frac{1}{T} \sum_{t=1}^{T} \log(\Delta_i^t), \tag{6.3.2}$$

where Δ_i^t is the ratio between the Euclidean norm of the i-th component of a vector basis at time $t-1$ and its corresponding component of the basis at time t. This last basis is recomputed at each time step, after a sufficiently long transient, by orthonormalizing the image of the basis of the tangent space at time $t-1$.

If the Jacobian of the map can be explicitly computed, as in the case of the reduced systems, the tangent space is spanned by the eigenvectors of the Jacobian. Otherwise, as in the case of the Perron-Frobenius operator, the convergence to the correct values of the Lyapunov exponents depends on the process of orthonormalization, that in the long run allows to separate directions with different expansion rates. However, this computation can be problematic in the cases in which there are directions converging very fast, that is for very negative Lyapunov exponents, since in just one time step all the vectors will flatten over the most expanding direction, thus reducing the accuracy of the orthonormalization outcome.

The *Lyapunov spectrum*, that is the set of all the Lyapunov exponents of the population, contains in principle an infinite number of exponents. By discretising the population we can compute a number of them equal to the length of the pdf vector. Here, we will consider only the four largest Lyapunov exponents, in order to compare them to those obtained for the reduced systems.

Figure 6.7 reproduces an example of eigenvectors (in the space of the pdfs) relative to the dominant Lyapunov exponents.

Figure 6.7: Eigenvectors relative to the four largest Lyapunov exponents for the population of noisy logistic maps ($K = 0.5$ and $\sigma^2 = 0.03$).

The algorithm for the computation of the population Lyapunov exponents allows us now to study how the Lyapunov spectrum is affected by changes in the population-level parameters. Figure 6.8 shows the four largest Lyapunov exponents for the population and for the reduced system truncated at the fourth order as a function of the coupling strength K and for fixed noise intensity.

Figure 6.8: Lyapunov exponents of the population (dots) and of the reduced system to fourth order (solid lines) as a function of the coupling strength, for fixed noise intensity $\sigma^2 = 0.03$.

One can clearly see that the reduced system captures the main features of the macroscopic dynamics, that is the existence of only one positive Lyapunov exponent (magnified in Figure 6.9). The quantitative agreement with the population is extremely good for the first two exponents. The discrepancy on the third and fourth exponent, evident for couplings close to the maximal one, are due to a degrading of the numerical accuracy when some directions are too strongly attractive. The quantitative correspondence between the population and the reduced system, especially as far as the third and fourth exponents are concerned, is also lost for too low values of the coupling, where the introduced approximation is likely to be insufficient to take every detail into account.

In the limit $K \to 1$ the maximum Lyapunov exponent tends to the value which can be analytically derived from the exact scalar map Eq. (5.4.1), while all the other directions are attracting more and more, the closer the coupling is to the maximal. The truncations of order greater than zero provide the successive exponents, each approximation level adding one new exponent, that is more negative than those retrieved with the previous order truncations. This can be seen in Figure 6.10, that displays the Lyapunov exponents of the reduced system at different truncation levels.

Figure 6.9: Maximal Lyapunov exponent of the population (dots) and of the reduced systems to second (solid line), third (dashed line) and fourth order (dotted lines) as a function of the coupling strength, for fixed noise intensity $\sigma^2 = 0.03$. The fourth order truncation provides a slightly better approximation for the lower values of the coupling in the displayed range.

Figure 6.10: Lyapunov exponents of the reduced system to second (solid lines), third (dashed lines) and fourth order (dotted lines) as a function of the coupling strength, for fixed noise intensity $\sigma^2 = 0.03$.

By extrapolating to the case of higher approximation levels, we can imagine

that increasing by one the truncation degree adds a further Lyapunuv exponent that is more negative than those of the lower degree approximation.

In view of the obtained quantitative and qualitative agreement with the Lyapunov exponents of the population, we conclude that, in spite of being just one of the possible projections of the population dynamics on a lower dimensional space, the order parameter expansion indeed captures the hierarchical structure of the macroscopic attractor.

The computation of the Lyapunov exponents also allows us to address the delicate question of how the macroscopic attractor dimension depends on the population parameters K and σ. The question whether the collective behaviour is truly low-dimensional, or it is instead always infinite-dimensional has been mainly faced in the context of weakly coupled noiseless maps. As reported in Chapter 2, this point is still actively discussed, and it seems that the existence of low-dimensional attractors depends on the structural stability of single-element dynamics [77, 107, 26, 108, 159]. Shibata, Chawanya and Kaneko, however, pointed out that it is sufficient to add a small amount of noise to reduce drastically the dimensionality of the collective motion, measured as the number of positive Lyapunov exponents of the spectrum of the Perron-Frobenius operator.

We approach here this question starting from maximal coupling rather than from zero coupling. In the region of strong coupling, the macroscopic dynamics remains, even in the chaotic regimes, relatively low dimensional, with only one positive Lyapunov exponent. In order to compare the dimension of the mean field attractor for the reduced system and the population, we will make use of the *Lyapunov dimension* or *Kaplan-Yorke dimension*:

$$D_L = j + \frac{\sum_{k=1}^{j} \lambda_k}{|\lambda_{j+1}|} \tag{6.3.3}$$

where j is the smallest integer such that, if the Lyapunov exponents λ_k are listed in descending order (so that $\lambda_1 \geq \lambda_2 \geq \dots$):

$$\sum_{k=1}^{j} \lambda_k \geq 0.$$

The *Kaplan-Yorke conjecture*, which states that the fractal dimension of a strange attractor is equal to D_L [120] appears to hold well for sufficiently nonsingular maps, and has been proved to be an upper estimate of the fractal dimension for a class of maps [52]. We thus expect to be able to use the Lyapunov dimension as a measure of the dimension of the macroscopic attractor. When the limiting case of perfect synchronisation is achieved, however, the Lyapunov dimension is not a good approximation for the fractal dimension of the attractor . Indeed, we know that in absence of noise, strong coupling leads the perfectly synchronous solution to be locally stable. This means that the mean field dynamics is identical to the scalar chaotic single-element dynamics, that has one positive Lyapunov exponent.

If the one-dimensional manifold that supports this attractor is embedded into a higher dimensional space, where the transverse directions are attractive, the Lyapunov dimension of the perfectly synchronised solution will be, according to the definition Eq. (6.3.3), strictly larger than one (and depend on the coupling strength K), unless the negative Lyapunov exponents transverse to the attractor are all infinitely large.

Figure 6.11 shows that the Lyapunov dimension of the reduced system has the same qualitative dependence on the population parameters as that of the population.

Figure 6.11: Lyapunov dimension of the macroscopic attractor for the population (dots) and the reduced system to the fourth order (solid line). The values of the Lyapunov dimension of the reduced systems of lower order overlap with those of the fourth order, except some small difference for low couplings, and therefore they are not displayed.

In particular, this dimension tends to one for $K \to 1$, that is where we have analytically concluded that the macroscopic attractor is strictly one-dimensional. Weakening the coupling strength, instead, one observes an increase in the attractor dimension, up to the point when the system exits the chaotic region, where the Lyapunov dimension drops to zero. Similarly, the intervals within the chaotic region in which the dimension of the macroscopic attractor is zero correspond to the windows of periodic behaviour that one can identify in the bifurcation diagram shown in Figure 5.8.

6.4 Excitable maps

From the results exposed in the previous section one could be tempted to conclude that, in general, the introduction of noise simplifies the mean field dynamics. In this Section we provide an example of a case in which noise drives the system from a "simple" collective behaviour, that is a fixed point, to a "complex" chaotic regime. We thus conclude that what is relevant is not the degree of complexity of the single-element dynamics, but rather the class of its close-by dynamical systems. The order parameter expansion again identifies the unfolding that tells which of such neighbouring dynamics can be reached by a change in the noise intensity.

It is well-known that excitable units subjected to random fluctuations exhibit regular behaviour for an optimal amount of noise. This phenomenon, called *coherence resonance* [125] has been widely studied for single noisy dynamical systems and manifests itself in the strong enhancement of the peak of the signal power spectrum when the noise attains an optimal level. When an external periodic signal is added to the autonomous system, moreover, one observes that the frequency enhanced by the presence of noise corresponds to that of the forcing term, in what is called *stochastic resonance*. For a brief review on the effect of noise on low-dimensional dynamical systems, see Section 2.5.1.

When populations of coupled low-dimensional dynamical systems are considered, one can observe phenomena that on the one side have the features of coherence resonance, since the single unit of the population is excited by the noise, and on the other side are related to stochastic resonance, due to the appearance of a macroscopic field that is fed back onto the local oscillators. These characteristics are common to the noise-induced phenomena recently described under the terms of "noise-induced phase transitions" [70, 78], "noise-induced global oscillations" [178, 90] ,"noise-enhanced (phase) synchronisation" [161, 111, 182], "noise-induced excitability" [163] "noise-induced coherence" [131], "system-size coherence resonance" [160], "noise-sustained pattern formation" [63, 19], "noise-sustained coherent oscillations" [183], "spatial coherence resonance" [20], or simply "coherence resonance" [91]. When the populations are composed of excitable units, it has been observed that an optimal noise intensity exists, at which the coherent firing of the population elements results in an enhanced regularity of the mean field dynamics. In case the population elements are locally coupled, this gives rise to spatial patterns.

Here, we will again focus on the case of global coupling and address the phenomenon of noise-induced coherence among excitable units from an alternative point of view, analogous to the approach introduced in [78, 178] for continuous time systems. The order parameter expansion allows us to interpret the results obtained for ODEs in a general framework, valid for any microscopic dynamics and any choice of the microscopic noise (although here we mostly consider noise with finite support, which seems to correspond better to physical, necessarily bounded, fluctuations). Besides providing information about how the nonlinearities of a generic system interact with the features of the noise, this approach also explains why similar responses are obtained for different white noises. This allows us to

relate the intermittent loss of synchronous behaviour, occurring close to the onset of global oscillations, to the crisis of a chaotic attractor.

To illustrate this claim, let us consider the population of excitable maps defined as:

$$f(x) = (\alpha\, x + \gamma\, x^3)\, e^{-\beta\, x^2} \tag{6.4.1}$$

(For other examples of excitable maps, see [161, 62]). The parameter α defines the slope of the map in the origin, and thus the eigenvalue of this fixed point. In order for the origin to be attractive, α will be chosen in the interval $(-1, 1)$. The rate of decay $\beta > 0$ of the map is related to the strength of the global attractivity of the region around the origin, and makes it a globally stable fixed point. The parameter $\gamma > 0$ measures the intensity of the excitation response and is the main determinant of the nature (periodic or chaotic) of a saddle orbit coexisting with the global attractor.

Figure 6.12: Excitable map defined by Eq. (6.4.1) with parameters $\alpha = 0.4$, $\beta = 1$, $\gamma = 8$. Besides $(0, 0)$, the map has two positive (and two negative, their symmetric with respect to the origin) fixed points. The origin is the only globally stable equilibrium, while those next to it are saddle points.

Figure 6.12 shows the map defined by Eq. (6.4.1) for the parameter values that will be used in the rest of this section. The dynamics has three fixed points in the positive orthant (five if also the negative fixed points are taken into account), one of which, the origin, is globally stable. If the system is initiated above the threshold value, set by the position of the intermediate saddle point, the excitation response drives the system away from the stable point and the following decay to the origin takes place through a chaotic transient.

It is thus to be expected that, when the noise intensity becomes sufficiently large, some maps can be excited over the threshold, thus triggering the excitation of the whole population. However, if only few elements are excited, the mean field nature of the coupling may let this perturbation either to die out or to spread to the whole population depending on the "excitability" of the microscopic systems.

Again, let us study the dynamics of the mean field as we change the noise intensity, measured by the standard deviation σ of a uniform noise distribution. As illustrated in Figure 6.13, where we plot the modulus of the mean field oscillations, when the stochastic terms become sufficiently large, the mean field is occasionally driven over the threshold, triggering intermittent bursts of collective activity. These intermittent bursts are associated with the boundary crisis of the chaotic attractor that the mean field dynamics attains for higher noise intensities. Indeed, when noise is increased further, the collective dynamics exits the chaotic region via a backward period-doubling cascade akin to what one observes for logistic maps.

Figure 6.13: Bifurcation diagram for a population of 2^{20} excitable maps, defined as Eq. (6.4.1) ($\alpha = 0.4$, $\beta = 1$, $\gamma = 8$), with additive uniform noise of standard deviation σ.

This deterministic collective behaviour, the result of averaging an infinite number of independent stochastic processes, acts like a drive to the dynamics of each noisy population element. Thus, looking at the power spectrum of a single element within the population, one finds that for small noise intensity a coherent

behaviour emerges according to the macroscopic transition to a nonvanishing mean field. Figs. 6.15 and 6.14 show the power spectrum obtained from the time series of one element within the population compared to that of the mean field.

Figure 6.14: Power spectra of one population element (dots), of the mean field (solid line). The excitable maps are defined as Eq. (6.4.1) with $K = 1$ and a) $\sigma = 0.3$, where the mean field dynamics is chaotic and b) $\sigma = 0.41$, in a periodic window within the chaotic region.

As long as the noise is weak enough, the single-element spectrum resembles that of the mean field. For a noise intensity such that the mean field dynamics is chaotic, the spectrum displays some broad structure (Figure 6.15(a)), while it becomes sharply peaked in the periodic windows within the macroscopic chaotic region (Figure 6.15(b)).

Figure 6.15: Power spectra of one population element (dots), of the mean field (solid line) of a population of excitable maps (Eq. (6.4.1) with $K = 1$) in two cyclic region of large coupling: a) period-two cycle ($\sigma = 0.5$); b) period-one cycle ($\sigma = 0.6$).

For large noise intensities, instead, the single element power spectrum flattens, reflecting the prevalence of the white noise term, while the mean field one has a sharp peak corresponding to the macroscopic periodic evolution (Figure 6.15).

In the case of excitable maps considered here, the closure of the order parameter expansion is more delicate than in the case of polynomial maps. Indeed, already the truncation to zeroth order Eq. (5.4.1) is a series containing an infinite number of terms, so that all the moments of the noise distribution in principle influence the macroscopic dynamics. However, in the relevant cases in which a macroscopic attractor exists for any noise value, that is when the series is convergent, one can approximate it to any accuracy by considering only a finite number of terms. The truncation obtained in this way will be valid for sufficiently low noise intensity.

Figure 6.16: Bifurcation diagram of a truncation of Eq. 5.4.1 to the eight order. This approximation is able to reproduce the bifurcation diagram of the population (Figure 6.13) up to noise intensities $\sigma < 0.7$. The interval where the approximation is quantitatively in agreement with the population simulation increases with the truncation order in σ. The deviation with respect to the bifurcation diagram of the population, present for large noise intensities, is due to the fact that the reduced system has been obtained by neglecting terms at high order in σ. These terms, negligible as long as the noise is weak, affect the macroscopic dynamics for higher intensities.

Let us first examine the case of maximal coupling and uniform noise distribution. Figure 6.16 shows that the bifurcation diagram of the population, displayed in Figure 6.13, is well reproduced, as long as the noise is sufficiently weak, by a truncation of the reduced system.

The reduced system accounts for the most important features of the macroscopic dynamics, such as the onset of macroscopic oscillations and the transition to collective periodic dynamics. In particular, one can interpret the intermittent

behaviour that is observed at the onset of the collective oscillations as due to the crisis of a chaotic attractor. This disappears through the collision with the origin, that is always a fixed point, though unstable, for the macroscopic dynamics. A straightforward consequence of such an analysis is that the observed intermittency is expected to be of type I.

Another question one can ask is at what noise intensity the non-equilibrium macroscopic dynamics sets on in the population. Since this transition to collective oscillations takes place for relatively low noise intensity, one can analytically obtain the noise intensity threshold σ^* by neglecting all the terms $O(\sigma^4)$ in the order parameter expansion. The continuous line in Figure 6.17 shows the analytical results obtained for the second order reduced system (truncation to the second order in σ of Eq. (5.4.3)):

$$\begin{aligned} X &\mapsto \quad f(X) + \frac{1}{2}\, d_2 f(X)\, \Omega_2 \\ \Omega_2 &\mapsto \quad \sigma^2 + (1-K)^2 \left\{ [\, d_x\, f(X)\,]^2\ \sigma^2 - \frac{1}{4}\, [\, d_{xx}\, f(X)\,]^2\ \Omega_2 \right\} \Omega_2, \end{aligned}$$

where $d_x\, f$ and $d_{xx}\, f$ are the first and second derivatives, respectively, of the excitable map Eq. (6.4.1).

Figure 6.17: Threshold noise intensity σ^* corresponding to the onset of collective oscillation in a population of excitable maps as a function of the parameter α and for three different coupling strengths: $K = 1$ ($\Box$); $K = 0.8$ ($\circ$); $K = 0.6$ ($*$).

This equations, truncated to the second order both in $(1-K)$ and in σ, account for the change in the excitation threshold as the linear stability of the origin, measured by the parameter α, is changed. The approximation works well as long as either the coupling strength is sufficiently large or $(1-\alpha)$ (that is, the excitation threshold for the individual map) is sufficiently small.

Chapter 7

Collective dynamics of populations with different kinds of microscopic disorder

The previous Chapters have presented several examples of collective behaviour in populations of globally and strongly coupled dynamical systems with microscopic disorder. Populations with such an interaction structure indeed constitute the simplest examples of systems with many interacting degrees of freedom, are at the same time a model for experimental systems where the coupling takes place through a medium, as in the case of yeast cells, or is sufficiently long ranged, as in the case of flashing fireflies. The introduction of microscopic disorder, either in the form of parameter mismatch (Chapters 3 and 4) or in the form of additive independent noise (Chapters 5 and 6) is meant to overcome the hypothesis that the population is composed by exactly identical elements. While this assumption is often justified for physical systems, it is definitely an oversimplification as far as biological populations are concerned. One question arising from the aforementioned analysis is if and when the effects of those different sources of microscopic disorder are equivalent.

This chapter will compare the emergent dynamics resulting from different ways of breaking the microscopic identity. At this scope, we address a population of scalar maps with an additive term that can be either randomly drawn at each time step (noise) or assigned once and for all (parameter mismatch) according to a given distribution.

We show here that, in general, the two sources of disorder have different macroscopic effects. These can be traced back to the population pdf, that has substantially different features in the two cases. Such microscopic properties of the population reflect on the assumptions introduced for obtaining a closed-form formulation for the macroscopic dynamics. For parameter mismatch, indeed, the closure assumption is related to the coherence of the motion, while in the case of

noise the important thing is that the population has infinite size.

The macroscopic equations derived in Chapter 5 for populations of noisy maps will be compared to the equations obtained through an order parameter expansion for the case of parameter mismatch. In this way, we reproduce the mean field behaviour of the two populations, showing that the difference between the two sources of disorder are mostly evident for intermediate couplings and for broad distributions of either noise or parameter diversity. The two macroscopic descriptions, instead, converge in the limit of maximal coupling.

This study allows to identify population-level characteristics that correspond to different microscopic features. Potentially, on this basis one could develop experimental techniques for enquiring the character of individual-level disorder from purely macroscopic observations.

The final section of this Chapter will summarise the results obtained in the first part of this thesis for strongly and globally coupled dynamical systems and discuss the perspectives and future possible applications of the order parameter expansion.

7.1 Different forms of disorder: parameter mismatch and noise

Parameter mismatch and noise are often regarded as two fundamental ways of modelling microscopic disorder. In the first case, the mismatch within the population is traced back to the existence of a time-independent distribution in the properties of the single-element dynamics. In the second case, the difference among individual behaviour is though of as changing in time due to some process that cannot be described at the chosen observation level, and that is generically equated to a stochastic term.

The persistence of the main features of the population dynamics after the introduction of a small amount of individual diversity is usually regarded as a proof for the robustness of a phenomenon, and, consequently, for its relevance in the description of real-world systems. Here, we propose to use the results derived in the previous Chapters to perform a systematic comparison between the effects of these two sources of disorder.

With this scope, we consider populations of globally coupled chaotic scalar maps with an additive independent term, that can be either constant (parameter mismatch), or sampled at each time step (noise). In both cases, this term is drawn according to the same assigned distribution with finite moments. This section will complement the results presented in Chapter 5 by examining the features of the collective behaviour and the dynamics of the population probability distribution for the case of parameter mismatch.

In the following, we discuss how the statistical proprieties of the two populations reflect on the order parameter expansions and show that the two different

reduced systems describe the effective dynamics of the population for strong coupling.

The equations describing the population with parameter mismatch have the same form as those with additive noise Eq. (5.2.1):

$$x_j \mapsto (1-K)\, f(x_j) + K\, \langle f(x) \rangle + p_j \quad j = 1, \dots N, \tag{7.1.1}$$

but the additive term $p_j \in \mathcal{R}$ is now assigned once and for all. According to the choice we made in Chapter 6, we consider a uniform disorder distribution with mean $p_0 = 0$, variance σ^2 and fourth moment m_4. The the parameters p_j will be taken equally spaced on the support of such a distribution.

Note that the global coupling term now has a different formulation from the form considered in Chapter 3, and thus the reduced system cannot be obtained directly from Eq. (3.3.8). However, arguments similar to those explained in Chapter 3, and in particular the assumption of coherence Eq. (3.3.4), can be used in order to close the order parameter expansion and derive the reduced system for Eq. (7.1.1).

By neglecting terms of order larger than one in $\epsilon_j = x_j - X$, we obtain the reduced system:

$$\begin{cases} X \mapsto & f(X) + \frac{1}{2} \left[d_x f(X) \right]^2 \Omega_2 \\ W \mapsto & \sigma^2 + (1-K)\, d_x f(X)\, W \\ \Omega_2 \mapsto & \sigma^2 + 2\,(1-K)\, d_x f(X)\, W + \\ & (1-K)^2 \left\{ \left[d_x f(X) \right]^2 \Omega_2 + \frac{1}{4} \left[d_{xx} f(X) \right]^2 \left(m_4 - \Omega_2^2 \right) \right\}. \end{cases} \tag{7.1.2}$$

The mean field is hence coupled to the variance of the snapshot distribution:

$$\Omega_2 = \langle p_j^2 \rangle.$$

The variance is in turn influenced by a third order parameter, that we named the shape parameter in Chapter 3:

$$W = \langle p_j\, \epsilon_j \rangle.$$

As in the other cases, the macroscopic parameters that naturally emerge in the expansion as macroscopically relevant are the coupling strength K and the moments, namely the variance σ^2 and fourth moment m_4, of the parameter distribution.

The simulations presented in this section refer to populations of logistic maps $f(x) = 1 - a\, x^2$, with $a = 1.57$ inside the chaotic region. In the case of parameter mismatch, the population is composed by $N = 128$ maps. Eq. 7.1.2 reads in this

case:

$$\begin{cases} X \mapsto & 1 - a\,X^2 - 2\,a\,\Omega_2 \\ W \mapsto & \sigma^2 - 2\,a\,(1-K)\,X\,W \\ \Omega_2 \mapsto & \sigma^2 - 4\,a\,(1-K)\,X\,W + a^2\,(1-K)^2\,\left[m_4 + \left(4\,X^2 - \Omega_2\right)\,\Omega_2\right] \end{cases} , \quad (7.1.3)$$

By comparing this order parameter expansion with the reduced system to second order derived in Sec. 6.2 for the case of noisy maps (Eq. (6.2.1)):

$$\begin{cases} X \mapsto & 1 - a\,X^2 - a\,\Omega_2 \\ \Omega_2 \mapsto & \sigma^2 + a^2\,(1-K)^2\left[m_4 - 6\sigma^4 + (4X^2 - \Omega_2 + 6\,\sigma^2)\,\Omega_2\right] \end{cases} , \quad (7.1.4)$$

we immediately notice that the approximation at second order in $(1-K)$ involves three order parameters in the case of parameter mismatch, but only two in the case of noise.

This two descriptions converge to the same equation if the coupling is maximal, when the shape parameter and the population variance for the population with parameter mismatch become uncoupled and coincide. From a microscopic point of view, this corresponds to the fact that the snapshot pdf is in both cases equal to the distribution of the disorder, that displaces it solidly with the mean field motion (that is, Fig. 5.3 provides a microscopic picture valid for both sources of disorder). The only difference is that in the case of parameter mismatch the oscillators maintain the order of their arrangement, while in the case of noise they randomly exchange their positions at each time step. A straightforward consequence of this is that even if the macroscopic dynamics is indistinguishable for infinite population size, in the case of noise it depends essentially on the number of elements composing the population, while this dependence is much weaker for parameter diversity. In the following, we discuss why this difference exists for every value of the coupling.

When the coupling is less than maximal, on the other hand, we expect to observe differences in the macroscopic regimes induced by parameter mismatch or by noise. These differences can be visualised by plotting in the plane (σ^2, K) the period doubling bifurcation lines (Fig. 7.1).

While for weaker couplings a low intensity of noise is sufficient to drive the system out of the chaotic region, the opposite happens if the microscopic disorder is due to a diversity in the parameters. Indeed, in this case the region where the mean field displays chaotic behaviour becomes larger the smaller K is. This property of the macroscopic dynamics is captured by the reduced system Eq. (7.1.2), whose bifurcation lines provide a good quantitative approximation of those determined by numerically simulating the population.

As mentioned above, another important difference between the two sources of microscopic disorder is the dependence of the collective dynamics on the population size. As pointed out in Sec. 5.3, the derivation of Eq. (7.1.4) is based on

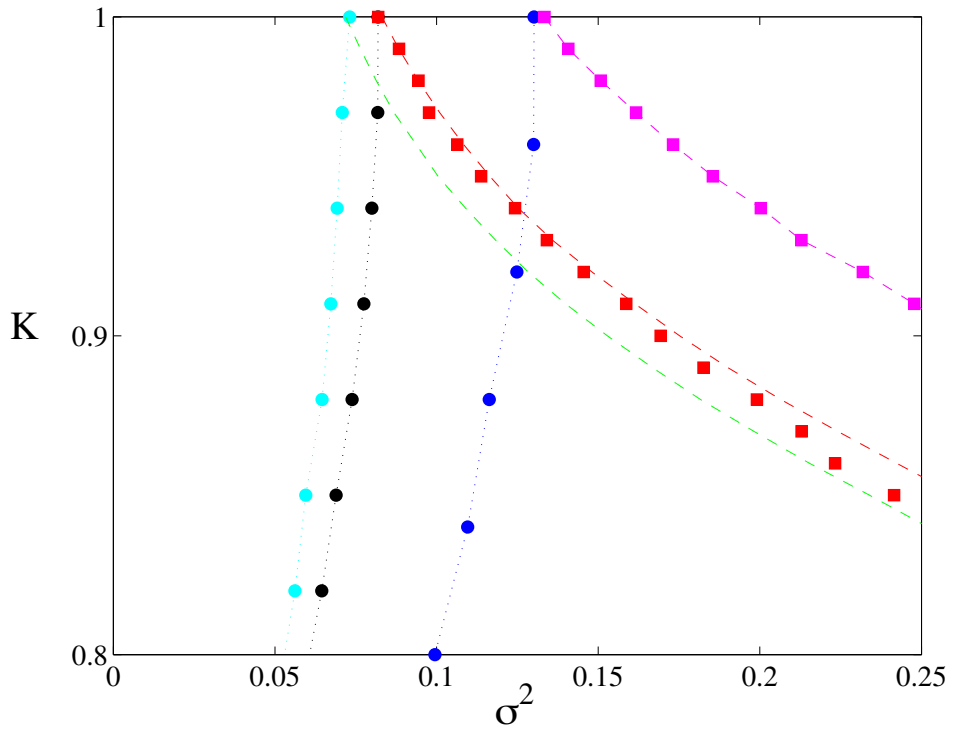

Figure 7.1: Period-doubling bifurcation lines for the population of noisy maps studied in Sec. 6.2 (full system, dots and reduced system to the second order Eq. (7.1.4), dotted lines) and for Eq. (7.1.1) (population of $N = 64$ logistic maps, squares, reduced system Eq. (7.1.2), dashed lines. The bifurcation parameters are the variance of the parameter/noise distribution σ^2 and the coupling strength K. In the up-right region of the diagram the mean field is stationary for both forms of disorder, while for still larger σ^2 the macroscopic dynamics diverges.

the assumption that the population is infinitely large, while the mean field of finite populations undergoes fluctuations that scale as $1/\sqrt{N}$. On the other hand, Eq. (7.1.4) has been derived without making any assumption on the system size. Hence, system size is expected to play a minor role for the qualitative features of the macroscopic dynamics.

The weak dependence on the system size of the mean field behaviour for populations with parameter mismatch, already pointed out for ODEs in Chapter 4 is confirmed by the numerical simulations and can be understood by looking at the characteristics of the snapshot distribution. Fig. 7.2 displays the instantaneous pdfs for the populations with parameter mismatch and additive noise in regimes where the mean field has a period-two attractor.

If the disorder is due to parameter mismatch, the shape of the instantaneous pdf is little affected by the number of points that identify its profile, along which

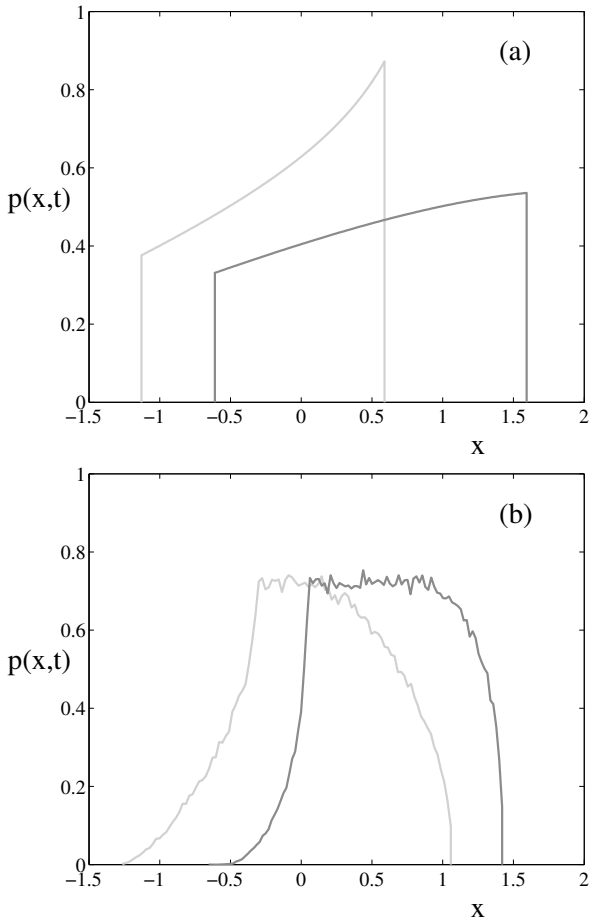

Figure 7.2: Snapshot pdf for a macroscopic period-two regime in populations of logistic maps with (a) parameter mismatch ($\sigma^2 = 0.6$, $K = 0.9$)and (b) additive noise ($\sigma^2 = 0.4$, $K = 0.7$).

the oscillators maintain their ordered configuration. If noise is present, on the other hand, reducing the population size alters the shape of the instantaneous pdf at every time step, broadening the pdf with respect to the infinite-size limit distribution, and, hence, affecting the mean field dynamics in an unpredictable way.

Another conclusion that can be drawn by looking at Fig. 7.2 is that the snapshot distribution reflects of the source of microscopic diversity that generates a given collective behaviour. Given a certain mean-field dynamics, thus, one should be able in principle to identify the character of the microscopic disorder by looking at the statistical properties of the instantaneous distribution.

This is even more evident if we compare the individual pdfs, obtained from the time series of an individual map within the populations with different nature of mi-

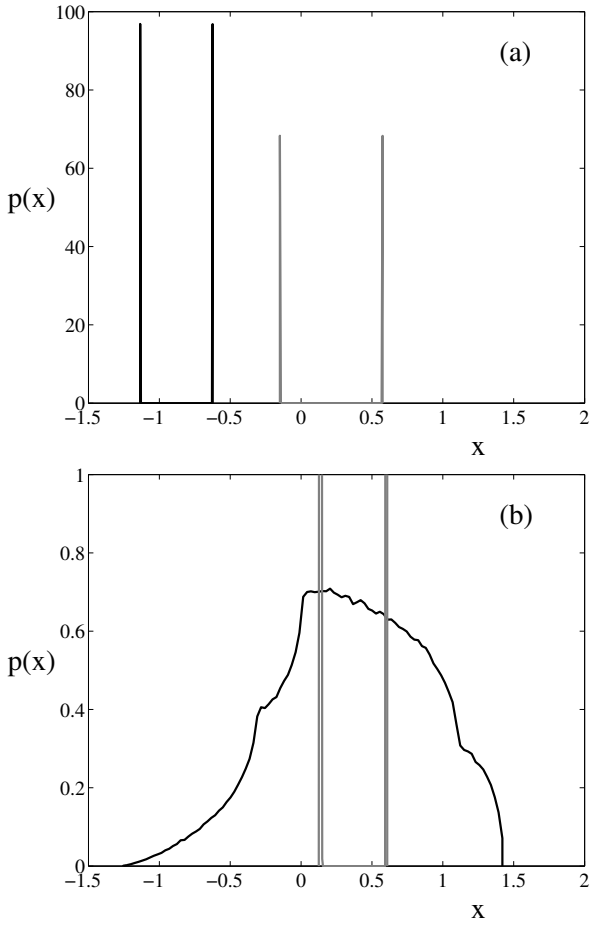

Figure 7.3: Mean field and individual pdfs for a macroscopic period-two regime in the populations of Fig. 7.2.

croscopic disorder. Figure 7.3 illustrates this in the case when the two populations possess qualitatively similar macroscopic regimes, that is they are both periodic of period two. Correspondingly, the mean field pdf consists in two Dirac's deltas centred on the values taken up by the cycle. Although the two populations cannot be distinguished at a macroscopic level, the difference is evident if one considers the individual pdfs.

In the case of parameter mismatch, the probability distribution of an individual time series is identical to the mean field pdf, but centred on shifted values. This is a consequence of the fact that one oscillator in the population maintains in time its position relative to the population average. When the disorder is due to noise, on the other hand, the individual pdf is broad, since the trajectory of one individual within the population is blurred by the stochastic term.

Having access to a macroscopic-level and a microscopic-level observable, such as the time series of the average and of one element within the population, these differences can be exploited for the investigation of what kind of disorder is the main determinant of the emergent population dynamics.

7.2 Conclusions and perspectives

The first part of this work is dedicated to the study of the collective behaviour in populations of globally and strongly coupled dynamical systems with microscopic disorder.

When all the population elements are exactly identical, the population has a perfectly synchronous motion. In this regime, the observable at the macroscopic level, i.e. the mean field, exactly mirrors the single-element dynamics. Such a one-to-one relation is broken if disorder is present at the level of the units composing the population. The macroscopic variable can indeed possess attractors different and even more complex with respect to the asymptotic behaviour of any of its components, if uncoupled.

The study conducted in the last five chapters is motivated by the search for a relation between microscopic and macroscopic dynamics that would take into account for the properties of the introduced disorder. Such a description should include, as a special case, the regime of perfect synchronisation and predict how are the macroscopically observable quantities affected by changes in the diversity among population elements.

In order to address this questions, we have developed an approach, that we have called order parameter expansion, for deriving approximate macroscopic equations of motion. In these equations, the mean field is coupled to some other averages over the population, the order parameters, playing the role of effective macroscopic degrees of freedom. Formally, the order parameter expansion is similar to the moment expansion of the operator for the evolution of the population pdf. However, there are two important differences. First, the fact of not dealing directly with the probability distribution functions, which would mean considering infinite population sizes, allows us to address the system-size dependence of the macroscopic regimes. Secondly, the relevant order parameters are determined on the basis of the microscopic features and need not to be necessarily the moments of the pdf, as in the case of the shape parameter for populations with parameter mismatch.

The possibility of reducing the order parameter expansion to a closed low-dimensional system relies mainly on the fact that the coupling among the population units is strong. When the coupling strength is reduced, the mean field attractor becomes more and more complex. In our perspective, this can be interpreted as an increase in the degrees of freedom that are macroscopically relevant.

Indeed, the description in terms of order parameters establishes a sort of threshold for the amount of details that one wants to include in a macroscopic description of the population. The degrees of freedom others than those included in this de-

scription act as perturbations onto the low-dimensional dynamics of the reduced system.

This is most evident in the case of noisy maps addressed in Chapters 5 and 6. The truncation to a given order will never account for all the details of the macroscopic attractor, that as soon as $K < 1$ appears to have an infinitely complex structure. However, this complex structure is hierarchically organised in a manner that is captured in the order parameter expansion. The mean field behaviour is influenced by the order parameters of higher degree as much as from any microscopic variable. This makes it difficult, for instance, to distinguish the fine structure of the attractor from the finite-size effects unless the coupling is sufficiently low.

It must be noticed that there is no unique criterion to determine a priori whether a given approximation level will provide a sufficiently accurate description of the population dynamics. This is due to the fact that the macroscopic dynamics can have an infinitely complex structure even if it remains low-dimensional (in the sense of the Lyapunov dimension, as discussed in Section 6.3). Thus, the truncation degree needs to be determined according to the measurements that one wants to perform on the population. However, the failure of a given approximation can be empirically detected if the Lyapunov dimension of the macroscopic system is maximal. For these parameter values it is then likely that the population dynamics has more effective degrees of freedom with respect to those of the given truncation.

In most of the cases considered here, the coupling strength was sufficiently strong to keep the dimensionality of the macroscopic dynamics sufficiently low for us to be able to describe the macroscopic bifurcations in terms of few order parameters. This does not hold any more in the region of low coupling and weak noise. Indeed, even if the addition of noise promptly reduces the dimensionality of the macroscopic attractor, the regimes occurring very close to the axis $\sigma = 0$ seem to become more and more complex as the coupling is weakened. Shibata and Kaneko [144] have shown that for extremely low coupling strengths noise provokes a transition from a noiseless incoherent regime, whose dimensionality is infinite, to low-dimensional motion. What happens for intermediate coupling strengths, where the dimensionality of the macroscopic attractor is likely to be finite but larger than what we can capture through the reduced systems studied here, still remains an open question. One would like to know, for instance, how the clustering regimes, present in the case of identical maps, are influenced by the addition of noise. In particular, it would be interesting to determine which of their properties are preserved once the noise is added, and which are instead lost.

Analogously, also for populations with parameter mismatch one can wonder whether the order parameter expansion is able to provide information on the mean field behaviour out of the regimes of strong coupling that guarantee the coherence of the population dynamics. Already in the simple case where the single-element dynamics is a limit cycle, intermediate coupling strengths generate extremely complex collective phenomena. There, the effective dimensionality of the macroscopic dynamics appears to be intermediate between the low-dimensional strong coupling regimes and the infinite-dimensional incoherent motion that one finds when the

coupling is weak.

While in the regimes of strong coupling one can exploit the existence of an effective low-dimensional attractor, for incoherence it is the knowledge of the statistical properties of the population that play a central role. This indeed permits to determine, at least formally, the stability of the pdf under the action of its self-consistent evolution operator. This approach is however of little help in the regimes of intermediate coupling, where the nonstationary population pdf possesses non-trivial properties.

In Section 4.1 we have shown that the order parameter expansion allows us to gain an insight on the type of macroscopic bifurcation that take place for intermediate couplings. A preliminary study has shown that some of the regimes for the population can be, qualitatively but not quantitatively, reproduced by a reduced system of few variables. The most interesting thing is that those macroscopic equations produce the same arrangement of these regimes relative to each other than what observed for the full system. This let us think that there could be special points of higher codimension playing the role of "organising centers" for the region of intermediate coupling strengths, and that could be identified in the population a well as in the reduced systems. In particular, the lower left corner of the region of amplitude death seems to be the essential in the understanding of the neighbouring complex regimes, and therefore deserves further study. Being this an equilibrium, one could try to use an order parameter expansion to investigate the unfolding of the macroscopic dynamics around this point.

Finally, the exam of the combined effect of noise and parameter mismatch could be performed in populations of scalar maps, that are sufficiently simple to allow an analytical approach. This study could then be used as a theoretical tool for the development of investigation methods aimed at the experimental characterisation of the sources of disorder acting in real systems.

Part II

Adaptation in a game theoretical perspective

Chapter 8

Introduction to evolutionary game theory

In the previous chapter we have considered populations composed, as every biological population, of individuals that are different from each other. This diversity in the dynamical feature of each element reflected on the possible behaviours that the population as a whole would display. The variability within the population was not itself subjected to a dynamics, but the individual characteristics are either fixed, as in the case of parameter mismatch, or changing randomly in time, in the case of noise. The studies that we presented in the first part of this elaborate are conducted by using a measure of the microscopic variability, the variance of the disorder distribution, as a control parameter.

However, in natural populations there is nothing like a parameter assigned once and for all if long time scales are considered. Darwin's statement that the frequencies of traits within population vary in time is the basis of the theory of evolution. A second fundamental point of such a theory is that this changes do not happen randomly, but they obey some rule that can be generically stated as "natural selection". The existence of variability in a certain trait within the population is most easily modelled subdividing it into groups of individuals who share the same trait. Each group is then assigned a frequency, that is the state variable whose dynamics will be addressed.

We want to stress that the concept of "adaptation" used in this thesis is related to the fact that, contrary to the aforementioned cases, the distribution of parameters within the population is subjected to changes, that let the groups adapt to each other. It is in this sense different from the idea beyond adaptive dynamics, where the traits act on and are influenced by the environment.

What are the most appropriate equations to account for the dynamics of traits within a population is still the debated, and indeed several approaches are commonly used depending on the nature of the organisms (e.g. viral, animal or human), on the time scale of the changes (i.e. micro and macro-evolution) and on

the level of description adopted (e.g. genetic or ecologic). Among other methods, evolutionary game theory provides a framework that is both sufficiently simple for the mathematical results to be intuitively meaningful and comprehensive of the classical game theory developed by Nash and Maynard Smith [64].

Evolutionary game theory deals with the changes in time of the frequency of strategies. By strategy, we design a character of one individual that describes its interaction with other population elements, whose outcome is summarised in a scalar value, the so-called payoff of the strategy. The game denotes the set of rules according to which the payoff is computed. As an example, let us consider the "game of the chicken" , also called "hawk-dove game" or "snowdrift game". As in the famous movie "Rebel without a cause", let us imagine a pair of teenagers driving their parent's cars towards a cliff. They have two choices, or strategies: either to jump out of the car, with the risk of becoming a "chicken" if the other has not jumped yet, or to stay in, and, in case, die a hero. Once scores are assigned to the three events (two possibilities are symmetric) that the two of them stay in the car, only one jumps, or both jump out, the game is defined and one can compute what is the probability with which choose one of the two strategies in order to optimise the outcome. Set aside James Dean, exactly the same formulation has been given by Maynard Smith and Pride for studying why ritual fighting is more common in species that bear heavy weapons than in apparently harmless ones. In this case, the two strategies are escalate a conflict (hawk) or retreat from it (dove). Game theory predicts that, if the players acted rationally (that is, they try to maximise their payoff), the frequency of hawks in a population (or the probability to escalate) should be equal to the ratio between the gain of winning over the other and the cost incurred from open fight. Hence, in the absence of a deterrent, it is most likely that individuals are ready to engage into a fight.

This way of describing the interaction among individuals neglects all its actual features other than the final results (for instance, it does not include the teenager remaining caught in the car's handle). This is based on the implicit assumption that the evolutionary dynamics time-scale, which makes the advantage of one strategy over the other visible, is much longer than that of the interaction. This allows us to assign a fitness value to a strategy even if it is not played just once, but in a number of successive rounds that take place within the span of one generation. In such a case of repeated games, the payoff is replaced by an average payoff and memory of the past actions acquires a central role.

The next section presents briefly the replicator equation for symmetric two-player games. We will stress that at the basis of its formulation there is random pair-wise encounter in a homogeneous population. This same principle led in the context of chemical kinetics to the law of mass action, and in the ecological context to the equations of Lotka-Volterra. From a mathematical viewpoint, this different models are equivalent and characterised by quadratic nonlinearities. As an explanatory example, we illustrate the evolutionary dynamics for the two-strategies one-shot games and for the rock-scissor-paper game.

Section 8.2 is dedicated to the issue of the evolution of altruistic behaviour. Starting from the prototypical game called the "prisoner's dilemma", we review the

theories proposed so far for explaining the emergence of cooperation in two-player games. These theories do not apply however in a social context, when individuals interact in groups rather than in pairs. A generalisation of the prisoner's dilemma to a multi-player game is the "public goods game", that we introduce in this section and address in more detail in Chapter 9, where we explicitly compute a replicator equation for its evolutionary dynamics.

8.1 The replicator equation

Two-player games are most conveniently described in terms of the *payoff matrix* $\mathcal{A} = \{a_{i,j}\}$, that collects the payoffs of the interaction of each pair of strategies present in the population. The element $a_{i,j}$ is the score that is assigned to the first player when he adopts strategy i and the second player strategy j. For symmetric games, assigning this value is enough to determine also the gain of the second player, that is given by the element $a_{j,i}$.

Calling x_i the frequency of strategy i in the population, the state vector $\mathbf{x} \in \mathcal{R}^n$ represents the composition of the population and $\mathbf{x}\,\mathcal{A}\,\mathbf{x}$ is the average payoff in the population. The frequencies have to obey the condition of normalisation $\sum_{i=1}^{n} x_i = 1$ and the must all be non negative. This means that their dynamics is embedded into a region of a $n-1$ dimensional hyperplane in $\mathbb{R}^n$, that is called the *simplex*. The edges of the simplex are the vectors e_i such that all the individuals have the same strategy.

Let us now make some assumptions that will allow us to write the dynamics of the state vector $\mathbf{x}$.

First, we assume that the players that will perform the game are randomly drawn from an infinite and homogeneous population, so that the probability of choosing an individual playing strategy i is equal to the frequency x_i of that strategy within the population. From this, it follows that the probability of choosing a pair of individuals one of which plays strategy i while the other plays strategy j is $x_i\,x_j$. This term is also what defines the law of mass action used in chemical kinetics, where the entries of the state vector $\mathbf{x}$ would be concentrations, and the Lotka-Volterra dynamics in ecology, where $\mathbf{x}$ would represent the species biomass. Note however that in this last case the state vector need not be of unitary norm, and therefore, as we shall see later, its dynamics is better compared with the restriction on the simplex of the other two cases.

A further consequence of considering infinite populations is that the frequencies can be considered as continuous variables in the interval $[0, 1]$, fact that is not true for any finite population. The evolutionary dynamics will be thus ruled by ordinary differential equations.

In order to define such ODEs, we must make some assumption about the mechanism by which a strategy is transmitted. If the strategy is a heritable character, we can for simplicity think that it is passed clonally by an individual to its offspring. Based on the idea that the individuals who have a better score also

dispose of more energy to invest in the transmission of their character and thus reproduce more, we assume that the rate of change of strategy i is given by:

$$\frac{\dot{x_i}}{x_i} = \sum_{j=1}^{n} a_{i,j}\, x_i\, x_j. \tag{8.1.1}$$

where $a_{i,j}$ is the payoff of strategy i against strategy j. Games defined by means of a payoff matrix $\mathcal{A}$, that are those where the fitness is a quadratic function of the frequencies, are called normal form games.

This equation takes into account the fact that, as we mentioned before, any i-player is likely to encounter individuals with other strategies according to their frequency. The rate equations Eq. (8.1.1) can be recast into the *replicator equation* for normal form games:

$$\dot{x_i} = x_i \left[(\mathcal{A}\,\mathbf{x})_i - \mathbf{x}\,\mathcal{A}\,\mathbf{x} \right]. \tag{8.1.2}$$

This is a particular case of the *replicator equation*:

$$\dot{x_i} = x_i \left[f_i(\mathbf{x}) - \bar{\mathbf{f}}(\mathbf{x}) \right] \tag{8.1.3}$$

that states in general that the transmission rate of strategy i is proportional to the difference between its fitness f_i and the average fitness $\bar{\mathbf{f}}$.

Equation (8.1.2) can also describe another situation, that occurs when the strategy is not genetically determined, but rather a socially transmitted behavioural rule [64]. In this case, the replicator dynamics takes place on short time-scales and the basic mechanism of transmission is imitation. Accordingly, one can interpret Eq. (8.1.1) as if the probability of player i assuming the partner's j behaviour was proportional to the difference in payoff $a_{i,j}$ between the two partners. The fact that the matrix $\mathcal{A}$ is now composed of payoff differences is equivalent to the case previously addressed, when its entries were the payoffs. This is due to the linear structure of the right-hand side of Eq. (8.1.2), that makes the equations invariant under the addition of any constant to the j-th column of $\mathcal{A}$.

The equation for the imitation dynamics can be cast into a more general form for pair-wise interactions, if we do not specify the form of the imitation rule, but call $f_{i,j}$ the probability that an i-player switches to j after having encountered a j-player. Hence, the frequency dynamics reads:

$$\dot{x_i} = x_i \sum_{j=1}^{n} \left[f_{i,j}(\mathbf{x}) - f_{j,i}(\mathbf{x}) \right] x_j. \tag{8.1.4}$$

Other kinds of imitation dynamics are commonly adopted even if the mathematical analysis of the corresponding equations can result more difficult than for the linear mechanism considered here.

In Chapter 9 we show that by adopting the same imitation mechanism or, equivalently, by assuming clonal transmission of the strategies, we can write explicitly the replicator equation for a case, the voluntary public goods game, where

the individuals meet in groups of size N. In this case, Eq. (8.1.3) is nonlinear of order $N+1$ and is nevertheless analytically solvable.

It can be shown that the replicator equation Eq. (8.1.2) is topologically equivalent to the Lotka-Volterra system in $n-1$ dimensions:

$$\dot{x_i} = x_i \left(r_i + \sum_{j=1}^{n-1} b_{i,j} x_j \right) . \tag{8.1.5}$$

This system is nongeneric and the replicator equation can as well display structurally unstable dynamics, as we show in the rock-scissor-paper game.

Before addressing the examples, it is worth to point out that the importance of the replicator equation lies on the possibility of linking its equilibria to the concepts, central in classical game theory, of Nash equilibrium, where the two payers both choose the best reply to the other, and of Evolutionary Stable Strategy (ESS), that is a strategy that resists to the invasion of the other available strategies [64].

Let us now consider a class of games that are played only once (one-shot) between two (symmetric) individuals, each of which can adopt one out of two strategies. Calling this possible strategies "cooperate" (**C**) and "defect" (**D**), the payoff matrix is the rank two matrix collecting the outcomes of the four possible matches:

	D	**C**
D	P	T
C	S	R

(8.1.6)

The first player then gets the "reward" R if he cooperates and so does the other; he gets the "sucker's payoff" S if he cooperates while the other defects; he gets the "temptation" T if he defects playing with a cooperative individual; and the "punishment" P if both players defect.

The replicator equation is in this case extremely simple and it describes the dynamics on the simplex, that in this case is the interval $[0,1]$. There are thus only three possibilities. Either one strategy dominates the other, so that one of the extrema of the interval is globally attractive, or there exist one interior point. In this last case, we have bistability or coexistence of the two strategies depending whether this interior point is unstable or stable, respectively.

Depending on the relative values of this payoffs one obtains dynamical systems with these different characteristics. In the aforementioned "game of the chicken", for instance, the relation among the payoffs is $P < S < R < T$. This is characterised by the fact that jumping out of the car before the other (S) is better than fall both down the cliff (P). In this case, there exist an interior equilibrium point, that corresponds to the ESS of coexistence found by Maynard Smith and Price.

A second prototypical example is the so-called *prisoner's dilemma*, that will be addressed in more detail in the forthcoming section. The game got its name

from the following hypothetical situation: imagine two criminals arrested under the suspicion of having committed a crime together. However, the police does not have sufficient proof in order to have them convicted. The two prisoners are isolated from each other, and the police visit each of them and offer a deal: the one who offers evidence against the other one will be freed. If none of them accepts the offer, they are in fact cooperating against the police, and both of them will get only a small punishment R because of lack of proof. They both gain. However, if one of them betrays the other one, by confessing to the police, the defector will gain more (T), since he is freed; the one who remained silent, on the other hand, will receive the full punishment S, since he did not help the police, and there is sufficient proof. If both betray, both will be punished (getting P), but less severely than if they had refused to talk.

This game is defined by the relation $S < P < R < T$ (note that contrary to the game of chicken, here the sucker's payoff is the worst possible outcome). The dilemma resides in the fact that, whatever does the partner, it is always convenient to defect (correspondingly, a population only composed by defectors is a global attractor for the replicator dynamics). On the other hand, the "altruistic" case in which both cooperate yields the best possible solution. In the following section, we will review the possible ways out of such a dilemma.

Let us consider one example where the players of a two-person, one shot game can choose among three strategies. the most famous example of such games is the so-called *rock-scissor-paper game*, where the three strategies playing rock **R**, playing scissor **S** and playing paper **P** are characterised by a relation of relative dominance. This means that **P** wins over **R**, **R** wins against **S** and in turn **S** wins against **P**. The payoff matrix for this game reads:

$$\begin{array}{c|ccc} & \mathbf{R} & \mathbf{S} & \mathbf{P} \\ \hline \mathbf{R} & 0 & 1 & -1 \\ \mathbf{S} & -1 & 0 & 1 \\ \mathbf{P} & 1 & -1 & 0 \end{array} \tag{8.1.7}$$

The replicator equations associated with the matrix (8.1.7) (and to those obtained substituting the ones with arbitrary positive values) have only one equilibrium at the interior of the simplex, that is in this case the triangle shown in Figure 8.1.

Such an equilibrium point is a center, that means that all the orbits, except form those lying on the boundary or on the equilibrium, are closed cycles. These cycles fill the whole simplex, so that the amplitude of the oscillations in the frequencies depends on the initial condition.

Although topologically unstable, this scenario is useful for modelling situations where there exist relations of dominance of rock-scissor-paper type. Among these, we find populations of lizards[148], bacteria [130], and humans [142]. In these,

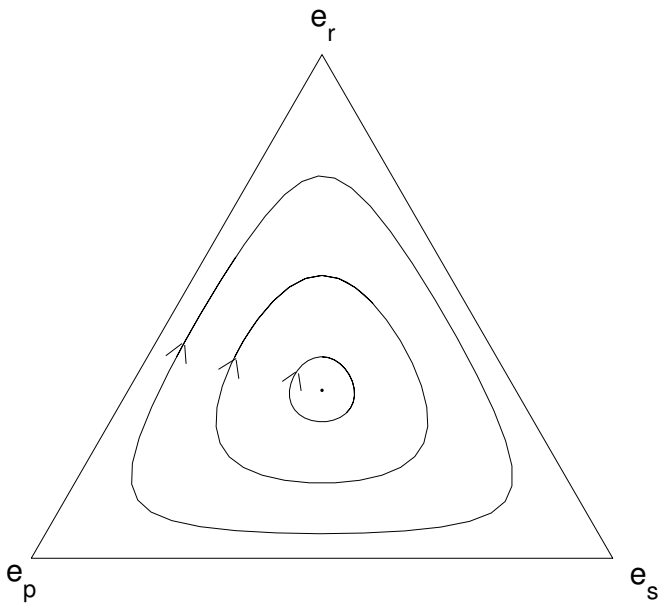

Figure 8.1: Phase portrait of a rock-scissor-paper game. The triangle represents the simplex $x + y + z = 1$, where x, y and z are the frequencies of the three strategies. The vertexes correspond to populations entirely composed by individuals playing with the same strategy and the direction of the motion along the edges is the condition that identifies the rock-scissor-paper type of dominance.

cases, however, people have looked for the dominance scheme among the strategies, that defines the dynamics on the edges of the simplex, rather than for the properties of the dynamics in its interior. Indeed, in many cases when one speaks of rock-scissor-paper type of game, the system has some generic behaviour, such as a limit cycle or a heteroclinic cycle (asymptotically approaching the boundary). In Chapter 9 in the case of public goods games we retrieve a dynamics that is of the same type of the original rock-scissor-paper game, that has the advantage of being Hamiltonian and has some useful averaging properties.

8.2 The evolution of cooperation

The existence of altruism, defined as a behaviour that reduces one own's fitness while increasing the fitness of another individual, in nature in general and in the human society more specifically, is a phenomenon that has long puzzled biologists. Indeed, the fact that altruistic behaviour is well established in many populations seems to be in contrast with the idea that natural selection lead less fit strategies to disappear.

Among the most striking examples of cooperation, we find the populations of social insects, such as bees, ants and termites, where nearly all the individuals refrain from reproduction in favour of the queen. Other examples are care-taking or help towards unrelated individuals, the signal calls for signalling the presence of a predator and inspection behaviour. In humans, many psychological and economic experiments have demonstrated that there seem to exist a momentum towards cooperation that induces people to adopt, at least in the simplified settings where this has been studied, a cooperative rather than egoistic attitude.

In the following, we present a review of the main theoretical explanations for the emergence of altruistic behaviour and eventually introduce the "public goods game" as a model for studying cooperation in social settings. Chapter 9 will then propose another mechanism able to explain the maintenance of sizable levels of cooperation in a mixed population.

8.2.1 Kin selection

Although the behaviour of social insects appears to be one of the most extreme cases of altruism, it can be well understood on the basis of genetic arguments. Indeed, what makes it convenient for a worker ant to favour the reproduction of an individual other than herself is that this individual, the queen, shares with her three quarters of her genes.

Hamilton suggested that what counted in the transmission of a character was that the gene pool of one individual was transmitted at best to the following generation, rather than the individual itself actually had offspring. He thus suggested to extend the concept of fitness considering how much a gene is represented in the following generation when not only the individual, but also his relatives, are taken into account [56]. By means of such "inclusive fitness", he was able to find a general criterion for cooperation to be favoured by natural selection, known as Hamilton's rule, that reads:

$$r > \frac{c}{b}. \tag{8.2.1}$$

This states that an altruistic act towards another individual is evolutionarily rewarding if the coefficient of relatedness r (equal to $3/4$ in social insects) is larger than the ratio between the cost of the altruistic act to the donor c and the benefit that this brings to the receiver b.

In spite of being recognised as the basic mechanism for the origin of eusociality, Hamilton's rule is of more difficult applicability in other contexts. The convenience of cooperation is indeed hindered by the fact that individuals have generally much lower coefficients of relatedness with respect to social insects. In most sexually reproducing species, this coefficients are always smaller than $1/2$ and rapidly decay in the genealogy, making it difficult to explain how could cooperation get established in groups larger than a family.

8.2.2 Group selection

Groups of cooperators fare better than groups of defectors, in spite of the fact that defectors always outperform cooperators within a group. This statement has led to the formulation of theories where natural selection acts at a level higher than the individual. The most famous among these is the theory, first formulated by Wilson, of group selection [171, 172], that has been debated now for several decades. Some of its ideas became recently intermingled with other theoretical approaches, especially those related to spatially extended populations and metapopulation theory, where (really or effectively) isolated subpopulations can be thought of as the groups (see, for instance, Van Baalen [164]).

8.2.3 Reciprocity

The idea that reciprocity had to be involved in the evolution of altruistic behaviour was first put forward by Trivers [162]. He suggested that an action that benefits the receiver more than it damage a donor can get established if the same individuals meet more than once, so that a cooperative attitude can result in a later reward.

This principle of direct reciprocity is the basis for one solution of the problem that had been posed to game theory by the prisoner's dilemma. Indeed, if the same players meet more than once, their choices can be influenced by the memory of the past behaviour of their partner or of his reaction to their own moves. The repetition of the game opens an enormous number of possibilities in the definition of the player's strategies, depending on how long term the memory of the players is. Therefore, it came as a surprise the fact that in a computer tournament organised in 1978 by Axelrod [9], where many different strategies were let compete, the one that performed best was based on just one-step memory. Such a strategy, named "tit-for-tat" consists in reply to defection with defection and to cooperation with cooperation. Accordingly, a tit-for-tat player will defect with defectors, but whenever he meets a cooperator he will be able to exploit the opportunity of joining in a common enterprise. On average, then, tit-for-tat players will gain more than defectors, who only gain if they meet a cooperator, and of cooperators, who are prone to be exploited by defectors. Indeed, evolutionary game theory can demonstrate that direct reciprocity leads to the establishment of cooperative behaviour if the prisoner's dilemma game is repeated for a sufficient number of times.

It later became evident that tit-for-tat is not the best strategy to choose if players make mistakes. Indeed, two players adopting this strategy and cooperating will shift to permanent defection if one of the two defects once. There exist anyway another strategy that does not have this property, but still allows to maintain cooperation between the players once this takes place once. This strategy is called "Pavlov" or "win-stay, lose-shift" [116]. As the name says, it consists in keeping on the strategy one has as long as it pays. Numerical simulations have shown that not only this strategy fares better than most of the memory-one strategies, but

also it cannot be invaded by any of them.

The assumption that the same pair of individuals played together a sufficient number of times to guarantee the advantage of reciprocity is sometimes too strong for social animals and humans in particular. Indeed, as stressed by Alexander [1], it is well possible that individuals reciprocate or not on the basis of the social status of their partner, that is acquired on the basis of its past actions. Nowak and Sigmund have proposed a model that implements indirect reciprocity by assigning each player a "social status" that increases when the player cooperates and decreases when he defects. This mechanism allows cooperators to channel their help towards other cooperators, leading to the formation of an effective group even in well-mixed population.

8.2.4 Public goods games

Public goods games, and more generally N-person games, are meant to model social rather than pair-wise interactions. Their central feature is the existence of a *public good* that is created by individual contributions at the advantage of every element of the population. For instance, shelter, protection and nourishment in social animals are often associated to a collective effort or to the investment into a common pool. If all individuals can exploit the public good at an equal rate, a "rational" player is faced the temptation not to contribute [57]. This paradox extends the prisoner's dilemma to a social context, and has been named "The tragedy of the commons" [58], "free rider problem" [162], "social dilemma" [149, 13] or "multiperson prisoner's dilemma" [140] depending on the context in which it arose.

According to the formalisation presented previously, we can imagine that each individual has two possible strategies: either cooperate, and hence ameliorate to the public good, or defect, and just take advantage of the other's contributions. We can define the *public goods game* in the following manner. Let cooperators invest c (the cost for an altruistic act) in a common pool and defectors invest 0. The common pool is multiplied by a factor $r > 1$ and than equally split among all the players, irrespective of their actual contribution. In a group formed by N players, n_c of which are cooperators, the payoff of a cooperator is:

$$P_c = r\,\frac{c\,n_c}{N} - c \tag{8.2.2}$$

and the payoff of a defector is:

$$P_d = r\,\frac{c\,n_c}{N}. \tag{8.2.3}$$

The social dilemma arises when $r < N$, where the return to a lonely cooperator is less than what he invested.

It is clear that for any composition of the group, the payoff of defectors is larger than that of cooperators. As in the case of the prisoner's dilemma, this means

that a rational player, who tries to optimise his own outcome, should always choose not to contribute to the common pool, thus forcing the group into a deadlock of mutual defection or economic stalemate.

In order to solve this paradox, Boyd and Richardson tried at first to apply the same recipe that had worked in the case of the prisoner's dilemma, i.e. reciprocity [18]. They showed that reciprocity was able to promote the establishment of cooperation only under conditions that become more and more restrictive as the size of the group of players, randomly chosen from a large population, increases. Indeed, retaliation does not work if many individuals are engaged in the game, because players intending to punish a defector can do so only by refraining from cooperation in subsequent rounds, thereby also punishing the cooperators in the group.

A second solution that was suggested is to let individuals the possibility of punishing, after each round of the game, the co-players who defected in that round. In this case, cooperation gets firmly established even if the punishment is costly to the punisher [17, 50] and players believe they will never meet again [47]. A similar result can be obtained if, instead of punish defectors, players are allowed to reward cooperators [101]. The effectiveness of punishment and reward has been experimentally demonstrated and seems to be a powerful mechanism to enforce cooperation in a population. However, in order such actions to be targeted towards the right individuals, it requires a large sharing of information among the players. Again, if the group is large or players are anonymous, this mechanism is unlikely to yield to the establishment of altruism.

Chapter 9 presents yet another mechanism by which sizable levels of cooperation get established in a well-mixed population. This mechanism works under full anonymity and is based on the simple principle that individuals may choose whether or not to take part to the game. Besides the two 'classical' strategies of cooperate and defect, we introduce a third strategy, that is adopted by individuals, named *loners*, who rely on some autarkic, constant, income. While the best payoff is obtained in a group composed only of cooperators, such a group is prone to being exploited by defectors, who would eventually take over the whole population leading to a solution of economic stalemate. In this situation, however, the payoff of every player would be less than the loner's income, so that a group of defectors is easily invaded by loners. Once most of the players opt for staying out of the game, it becomes convenient again to enter the social game as a cooperator, since the average group size is small enough to let the outcome of the game depend essentially on one individual contribution.

In this system, the three strategies oscillate in time, as cooperation is relaunched again and again. Although this does not lead to a firm establishment of cooperation once and for all in the population, it allows it to persist, thus providing the starting point for other selection mechanism to act. The simple hypothesis of voluntary participation works has a similar effect under very broad assumptions on the dynamics of the strategies (different imitation rules) and on the structure of the population (homogeneous, of finite size, spatially extended) [59, 155].

Moreover, a recent experimental investigation by Semmann et al. has showed

that such cycles occur when humans are asked to play the public goods game [142].

Chapter 9

Voluntary public goods games

9.1 Introduction

As reviewed in Chapter 8, most theories on the emergence of cooperation among selfish individuals are based on kin selection [56], group selection [172], reciprocal altruism [162] and altruistic punishment [16]. In all three models, cooperative behaviour is attained through basic mechanisms of discrimination enabling individuals to target their altruistic acts towards certain partners only.

In this chapter, we present another mechanism to achieve sizable levels of cooperation in a population. The following investigation is based on the public goods game [47, 71] which represents a natural extension of the prisoner's dilemma to an arbitrary number of players [18, 36, 60].

In a typical public goods game, an experimenter gives 20 Euros to each of eight players. The players may contribute part or all of their money to some common pool. The experimenter then triples this amount and divides it equally among the eight players, irrespective of the amount of their individual contribution. If all players contribute maximally, they will end up with 30 Euros each. But each individual is faced with the temptation to exploit, as a free rider, the contributions of the co-players. Hence, the dominating strategy is to invest nothing at all. If all players do this, they will not increase their initial capital. In this sense, the 'rational' equilibrium solution prescribed to 'homo oeconomicus' leads to economic stalemate. In actual experiments, players tend to invest a lot, however: typically, in the first round, they invest 10 Euros or more [47], while if the game is repeated the contributions rapidly fall in the absence of other mechanisms such as punishment or reward.

Public goods games are abundant in human and animal societies, and can be seen as basic examples of economic interactions (see e.g. [13, 43]).

9.2 The Model

We consider a large population of players. From time to time, N such players are chosen randomly. Within such a group, players can either contribute some fixed amount c or nothing at all. The return of the public good, i.e. the payoff to the players in the group, depends on the abundance of cooperators. If n_c denotes their number among the public goods players, the net payoff for cooperators P_c and defectors P_d is given by:

$$P_c = -c + rc\frac{n_c}{N}$$
$$P_d = rc\frac{n_c}{N},$$

where r denotes the interest rate on the common pool. For a public goods game deserving its name, we must have:

$$1 < r < N. \tag{9.2.1}$$

The first inequality states that if all do the same, they are better off cooperating than defecting; the second inequality states that each individual is better off defecting than cooperating. Selfish players will therefore always avoid the cost of cooperation c, i.e. a collective of selfish players will never cooperate. Defection is the dominating strategy. Hence both classical and evolutionary game theory predict that all players will defect, and obtain zero payoff.

We now extend the public goods game. In this optional public goods game, players can decide whether to participate in the public goods game or not. (For a similar approach in the prisoner's dilemma see [11, 117]). Individuals unwilling to join the public goods game are termed loners. These players prefer to rely on a small but fixed payoff $P_l = \sigma c$ with

$$0 < \sigma < r - 1, \tag{9.2.2}$$

such that the members in a group where all cooperate are better off than loners, but loners are better off than members in a group of defectors.

For the optional public goods game, there are thus three behavioural types in the population: (a) the loners unwilling to join the public goods game, (b) the cooperators ready to join the group and to contribute their effort, and (c) the defectors who join, but do not contribute. Assuming that groups form randomly, the payoffs for the different strategies P_c, P_d and P_l are then determined by the relative frequencies x, y and z of the three strategies.

9.3 The Equations of Motion

Evolutionary game theory assumes that a strategy's payoff determines the growth rate of its frequency within the population. More precisely, as explained in Chapter

8 [167, 141, 64], we postulate in our model that players using strategies $i = 1, ..., n$ occasionally compare their payoff with that of a randomly chosen 'model' member of the population, and adopt the strategy of their model with a probability proportional to the difference between the model's payoff and their own, if this is positive (and with probability 0 otherwise). In the continuous time model, the evolution of the frequencies x_i of the strategies i is given by

$$\dot{x_i} = \sum_j x_i x_j (P_i - P_j) \tag{9.3.1}$$

with $1 \leq i, j \leq n$, which reduces to the replicator equation

$$\dot{x_i} = x_i (P_i - \bar{P}) \tag{9.3.2}$$

where $\bar{P} = \sum x_j P_j$ is the average payoff in the population.

To be precise, we consider a very large, well-mixed population with three types of players: loners, cooperators and defectors. From time to time, sample groups of N players are randomly chosen and offered to participate in a single round public goods game. Note that in large populations, the probability that two players ever encounter again can be neglected. Depending on their type, players either refuse to participate or join the public goods game. In the latter case, they either defect, or cooperate. But, their strategies are specified beforehand, and do not depend on the composition of the sampled group. In particular, we do not consider conditional strategies of the type: cooperate if and only if the group contains more than two cooperators, or the like.

Each player is sampled a number of times, and obtains an average payoff which depends on his strategy as well as the composition of the entire population. This composition changes according to the replicator dynamics (see Eqs. 9.3.1 and (9.3.2)). The intuition behind the dynamics is that occasionally – and independently of the sampling of the public goods teams – a randomly chosen player A compares his payoff with that of another player B (also randomly chosen, within the entire population and not limited to the 'public goods' groups to which A belonged), and adopts the strategy of B, if it yields a higher payoff, with a probability proportional to the difference in their payoffs. Opportunities for updating, i.e. changing the strategy, are supposed to occur much less frequently than opportunities to play in a public goods group. We emphasise that there are other reasonable game dynamics, but for the replicator equation we can produce a full analysis.

For simplicity and without loss of generality, we set the cost c of cooperation equal to 1. The payoff for loners is then given by the constant

$$P_l = \sigma.$$

In order to compute the payoff values for cooperators and defectors, we first derive the probability that S of the N sampled individuals are actually willing to join the public goods game. In the case $S = 1$ (no co-player shows up) we assume

that the player has no other option than to play as a loner, and obtains payoff σ. This happens with probability z^{N-1}. For a given player willing to join the public goods game, the probability of finding, among the $N-1$ other players in the sample, $S-1$ co-players joining the group ($S>1$), is

$$\binom{N-1}{S-1}(1-z)^{S-1}\,z^{N-S}.$$

The probability that m of these players are cooperators, and $S-1-m$ defectors, is

$$\left(\frac{x}{x+y}\right)^m\left(\frac{y}{x+y}\right)^{S-1-m}\binom{S-1}{m}.$$

In that case, the payoff for defectors is $r\cdot m/S$. Hence the expected payoff for a defector in a group of S players ($S=2,...,N$) is

$$\frac{r}{S}\sum_{m=0}^{S-1} m\left(\frac{x}{x+y}\right)^m\left(\frac{y}{x+y}\right)^{S-1-m}\binom{S-1}{m}=\frac{r\,(S-1)}{S}\,\frac{x}{x+y}.$$

Thus,

$$\begin{aligned}P_d &= \sigma\,z^{N-1}+r\,\frac{x}{1-z}\sum_{S=1}^{N}\binom{N-1}{S-1}(1-z)^{S-1}\,z^{N-S}\left(1-\frac{1}{S}\right)\\ &= \sigma\,z^{N-1}+r\,\frac{x}{1-z}\left[1-\sum_{S=1}^{N}\binom{N-1}{S-1}(1-z)^{S-1}\,z^{N-S}\,\frac{1}{S}\right]\end{aligned}$$

and using $\binom{N-1}{S-1}=\binom{N}{S}\frac{S}{N}$ leads to

$$P_d=\sigma\,z^{N-1}+r\,\frac{x}{1-z}\left(1-\frac{1-z^N}{N\,(1-z)}\right). \tag{9.3.3}$$

In a group with $S-1$ co-players playing the public goods game, switching from cooperation to defection yields $1-r/S$. Hence,

$$P_d-P_c=\sum_{S=2}^{N}\left(1-\frac{r}{S}\right)\binom{N-1}{S-1}(1-z)^{S-1}\,z^{N-S}.$$

Using the same arguments as before, we obtain

$$P_d-P_c=1+(r-1)\,z^{N-1}-\frac{r}{N}\frac{1-z^N}{1-z}=:F(z). \tag{9.3.4}$$

The advantage of defectors over cooperators depends only on the fraction of individuals actually willing to play i.e. on the fraction of loners z. At the same time, it is independent of the loner's payoff σ. Figure 9.1 displays the payoff difference between defectors and cooperators as a function of the fraction of loners.

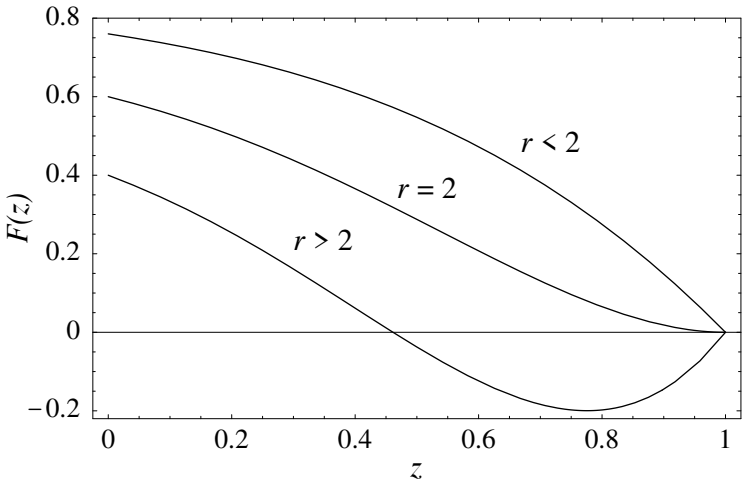

Figure 9.1: The difference between the payoff of cooperators P_c and defectors P_d is a function of the fraction of loners z: $F(z) = P_d - P_c$. If almost everybody is participating in the public goods game ($z \to 0$) then $F(z) > 0$ holds and it pays to defect. However, for interest rates $r > 2$, if the proportion z of loners increases, it eventually pays to cooperate ($F(z) < 0$) and the social dilemma disappears – at least for a while. $F(z)$ has either no or a unique root in the interval $(0, 1)$.

The sign of $P_d - P_c$ determines whether it pays to switch from cooperation to defection or vice versa, $F(z) = 0$ being the equilibrium condition. We claim that for $r \leq 2$, F has no root, and for $r > 2$ exactly one root $\hat{z}$ in the interval $(0, 1)$. In order to show this, we consider the function $G(z) = F(z)(1-z)$ which has the same roots as $F(z)$ in $(0, 1)$ and note that (a) $G(0) = 1 - r/N > 0$, (b) $G(1) = 0$, (c) $G(z) \asymp (2-r)(N-1)(1-z)^2$ for $z \to 1$, such that in a neighbourhood of $z = 1$ $G(z)$ is negative for $r > 2$, and (d) $G''(z) = z^{N-3}(N-1)((N-2)(r-1)-z(Nr-N-r))$ changes sign at most once in $(0, 1)$. Thus, for $r > 2$ (which by Eq. (9.2.1) implies $N > 2$) there exists a threshold value of the loners frequency $\hat{z}$ above which cooperators fare better than defectors.

Hence, in a population where loners are abundant, the average payoff of cooperators is higher than the average payoff of defectors, in spite of the fact that within each group it is the second strategy that yields a better outcome. This is an instance of the so-called Simpson's paradox. For instance, consider two groups A and B, with $N = 10$ and $r = 5$. Assume that A consists of eight cooperators and two defectors. The cooperators obtain 3 Euros and the defectors 4 Euros. Group B contains two cooperators and eight defectors. Cooperators get nothing and defectors 1 Euro. In both groups, defectors earn one Euro more than cooperators. Yet on average, defectors get only 1.6 Euros while cooperators earn 2.4 Euros. Whenever the payoff values allow Simpson's paradox to operate in the small groups made possible through the loner's option, rock-scissors-paper dynamics can be expected. The assumption that payoff is linear in the number n_c of cooperators

is used only for the sake of simplicity, and because this is the traditional way to model public goods games.

The average population payoff $\bar{P}$ can now be rewritten using the condition $y = 1 - x - z$:

$$\begin{aligned} \bar{P} &= x\,P_c + y\,P_d + z\,P_l = x\,(P_c - P_d) + z\,(\sigma - P_d) + P_d \\ &= -x\,(P_d - P_c) + (1-z)\,(P_d - \sigma) + \sigma \end{aligned}$$

Substituting Eqs. 9.3.3 and (9.3.4) then yields

$$\bar{P} = \sigma - [\,(1-z)\,\sigma - (r-1)\,x]\,\left(1 - z^{N-1}\right). \tag{9.3.5}$$

9.4 The Dynamics

Let us now analyse the replicator dynamics. The corners of the simplex $S_3 = \{(x,y,z) : x,y,z \geq 0, x+y+z = 1\}$, i.e. the vectors $\mathbf{e}_i$ of the standard basis ($i = c,d,l$ in a straightforward notation), are obviously fixed points. There are no other fixed points on the boundary of S_3. In fact, the edge $\mathbf{e}_c\mathbf{e}_d$ consists of an orbit leading from $\mathbf{e}_c$ (cooperators only) to $\mathbf{e}_d$ (defectors only), the edge $\mathbf{e}_d\mathbf{e}_l$ is an orbit leading to the state consisting of loners only, and the orbit $\mathbf{e}_l\mathbf{e}_c$ closes this heteroclinic cycle of rock-scissors-paper type on the boundary.

In order to analyse the dynamics in the interior, it is useful to show that the replicator equation, defined on the simplex S_3, can be rewritten in the form of a Hamiltonian system, and thus admits an invariant of motion. Indeed, defining as a new variable $f = x/(x+y)$, i.e. the fraction of cooperators among the individuals actually participating in the public goods game, we obtain

$$\dot{f} = \frac{y\,\dot{x} - x\,\dot{y}}{(x+y)^2} = \frac{x\,y}{(x+y)^2}\,(P_c - P_d).$$

This, as well as substituting Eq. (9.3.5) into the replicator equation $\dot{z} = z\,(\sigma - \bar{P})$, yields

$$\dot{f} = -f\,(1-f)\,F(z) \tag{9.4.1}$$

$$\dot{z} = [\sigma - f\,(r-1)]\;z\,(1-z)\,(1-z^{N-1}) \tag{9.4.2}$$

with (f,z) on the unit square $(0,1)^2$. Dividing the right hand side by the function $f\;(1-f)\;z\,(1-z)\;\left(1-z^{N-1}\right)$, which is positive on the unit square, corresponds to a change in velocity which does not affect the orbits. This yields

$$\dot{f} = \frac{-F(z)}{z\,(1-z)\;(1-z^{N-1})} =: -g(z)$$

$$\dot{z} = \frac{\sigma - f\,(r-1)}{f\;(1-f)} =: l\,(f)\,.$$

Introducing $H := G + L$, where $G(z)$ and $L(f)$ are primitives of $g(z)$ and $l(f)$:

$$G(z) = \left(1 - \frac{r}{N}\right) \log z + \left(\frac{r}{2} - 1\right) \log(1 - z) + R(z) \tag{9.4.3}$$

$$L(f) = \sigma \log f + (r - 1 - \sigma) \log (1 - f) \tag{9.4.4}$$

with $R(z)$ bounded on $[0, 1]$, we obtain the Hamiltonian system

$$\begin{aligned} \dot{f} &= -\frac{\partial H}{\partial z} \\ \dot{z} &= \frac{\partial H}{\partial f}. \end{aligned}$$

The actual dynamics of the system depends on whether the condition $P_d = P_c$ can be satisfied in the interior S_3, and hence on the interest rate r. For $r \leq 2$ there are no fixed points except the corners and all trajectories in int S_3 are homoclinic orbits of $\mathbf{e}_l$. Thus, if some noise (due for instance to mistakes or mutations by which cooperation is introduced by chance in the population) the system will display intermittently brief bursts of cooperation, but always ends up with no one willing to participate in the public goods game, as shown in figure 9.2.

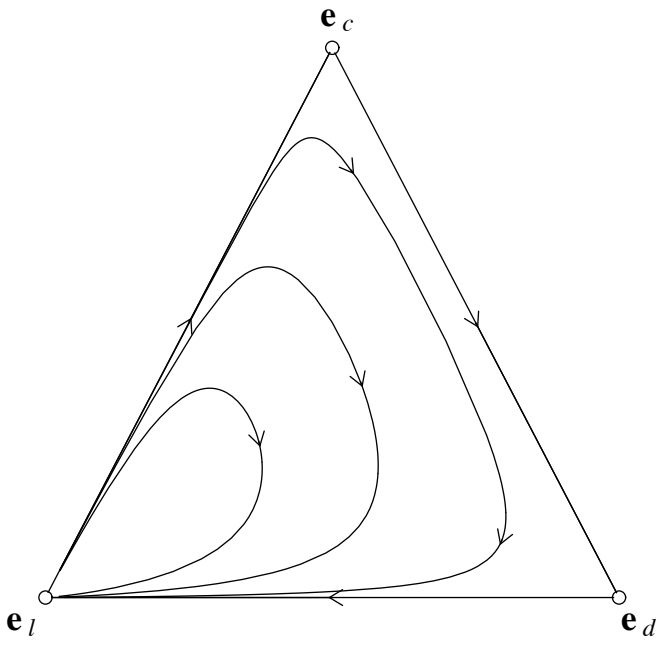

Figure 9.2: The three corners $\mathbf{e}_c, \mathbf{e}_d, \mathbf{e}_l$ of S_3 are saddle points (but $\mathbf{e}_l$ is not hyperbolic) and the boundary bd S_3 represents a rock-scissors-paper type heteroclinic cycle. For small interest rates, $r < 2$, no fixed point exists in int S_3 and all orbits converge to $\mathbf{e}_l$. But $\mathbf{e}_l$ is not Lyapunov stable. Parameters: $N = 5, r = 1.8, \sigma = 0.5$.

For $r > 2$, Eq. (9.2.2) implies that there exists a unique fixed point $\mathbf{Q} = (\hat{x}, \hat{y}, \hat{z})$ in $\operatorname{int} S_3$ such that $F(\hat{z}) = 0$ and:

$$\hat{x} = \frac{\sigma}{r-1}\,(1-\hat{z}) \tag{9.4.5}$$

as well as

$$\hat{y} = \left(1 - \frac{\sigma}{r-1}\right)(1-\hat{z}) \tag{9.4.6}$$

which follows from $P_d = P_l$. Due to the fact that the system is conservative, and the Hamiltonian H attains a strict (global) maximum at $(\frac{\sigma}{r-1}, \hat{z})$, the interior equilibrium $\mathbf{Q}$ is a center, i.e., it is neutrally stable and surrounded by closed orbits (see figure 9.3).

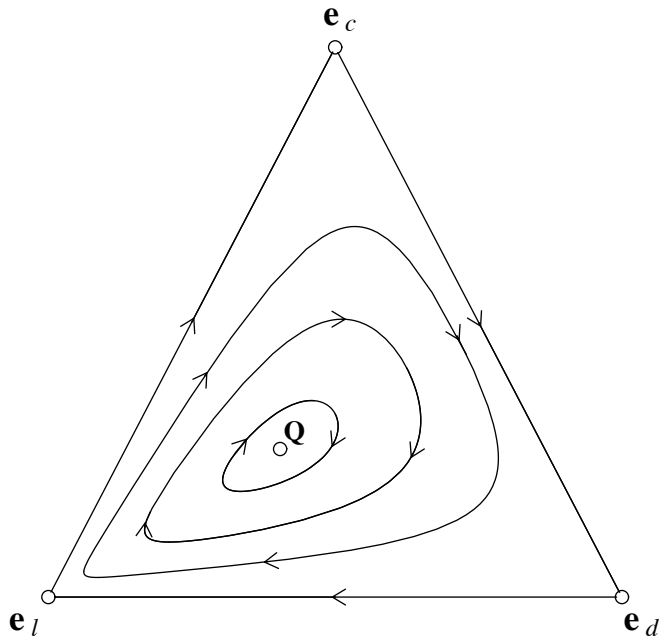

Figure 9.3: For $r > 2$, the three corners $\mathbf{e}_c, \mathbf{e}_d, \mathbf{e}_l$ are again saddle points and $\operatorname{bd} S_3$ represents a heteroclinic cycle. In $\operatorname{int} S_3$ a single fixed point $\mathbf{Q}$ appears. It is a center surrounded by closed orbits (see text). Parameters: $N = 5, r = 3, \sigma = 1$.

Actually *all* interior orbits are closed: Eq. (9.4.3) shows that $G(z) \to -\infty$ for $z \to 0, 1$ if $2 < r < N$, and Eq. (9.4.4) implies that $L(f) \to -\infty$ as $f \to 0, 1$ if $\sigma < r - 1$. Therefore $H \to -\infty$ uniformly near the boundary of $[0,1]^2$ and hence all level sets of H are closed curves. In particular, no interior orbit converges to the nonhyperbolic equilibrium $\mathbf{e}_l$.

Variations of the three parameters N, r, σ allow to position $\mathbf{Q}$ anywhere in the interior of the simplex (see figure 9.5). Note that in general all three parameters

must be adjusted to place **Q** in a particular location. According to Eqs. 9.4.5 and (9.4.6), the fixed point **Q** lies on the line

$$x = \frac{\sigma}{r - 1 - \sigma}\, y \tag{9.4.7}$$

independent of the group size N. For increasing N, **Q** moves towards the corner $\mathbf{e}_l$ and in the limit $N \to \infty$ homoclinic orbits issuing from and leading to $\mathbf{e}_l$ are obtained.

For the limiting cases $r = N$, $\sigma = r - 1$ and $\sigma = 0$, **Q** approaches the edges $\mathbf{e}_c\mathbf{e}_d$, $\mathbf{e}_l\mathbf{e}_c$ or $\mathbf{e}_l\mathbf{e}_d$, respectively. In particular, for $r = N$, cooperation becomes stable in the sense that, while the state can fluctuate along the edge $z = 0$ by random drift, any small fluctuation introducing the missing loners will be offset in such a way that the loners vanish again and the number of cooperators is larger than previously (see figure 9.4).

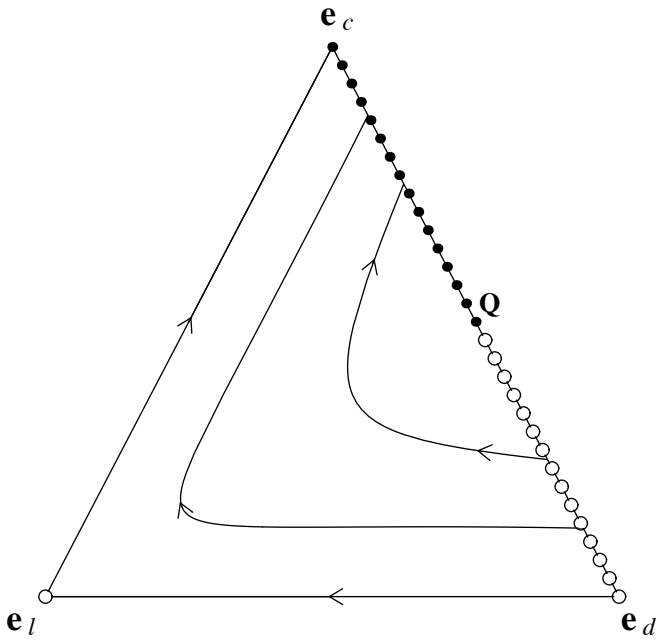

Figure 9.4: In the limiting case $r = N$, the edge $\mathbf{e}_c\mathbf{e}_d$ is a line of fixed points, stable on $\mathbf{e}_c\mathbf{Q}$ (closed circles) and unstable on $\mathbf{Q}\mathbf{e}_d$ (open circles). Random drift and occasional appearances of the missing loner strategy will eventually drive the system close to the corner $\mathbf{e}_c$ with almost everybody cooperating. Parameters: $N = 3, r = 3, \sigma = 1$.

Although the time averages of the state variables over an orbit of period T, defined as $\bar{v} = \frac{1}{T}\int_0^T v\, dt$, depend on the initial conditions, the following relations hold for every orbit. First, the average fraction of cooperators among playing

individuals corresponds to its value at the equilibrium point **Q**:

$$\frac{\bar{x}}{\bar{x}+\bar{y}} = \frac{\sigma}{r-1}. \tag{9.4.8}$$

This means that the time average lies on the solid line in figure 9.5 which connects **Q** and $\mathbf{e}_l$. Second, the average of the fraction of cooperators among participants in public goods games $\bar{f}$ corresponds to the fraction of the averages:

$$\bar{f} = \frac{\sigma}{r-1}. \tag{9.4.9}$$

Surprisingly, perhaps, increasing r always favours defection, i.e. it decreases the fraction f of cooperators among those actually engaging in the public goods game.

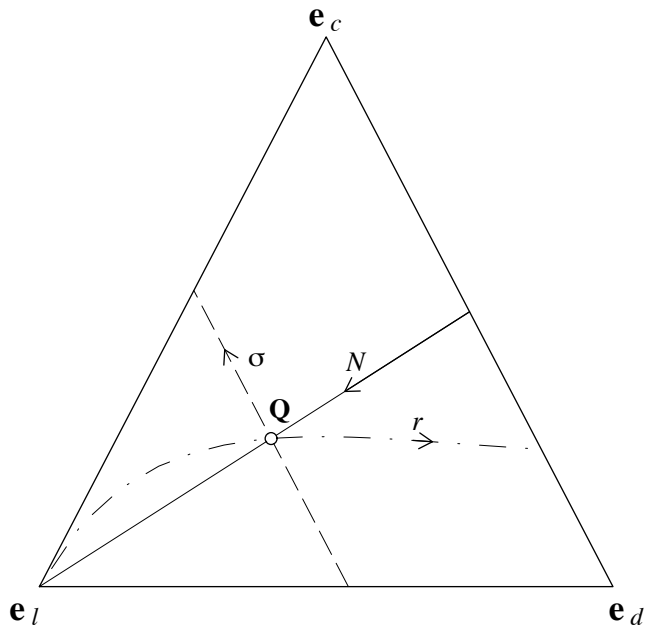

Figure 9.5: The position of the center **Q** in S_3 depends on the values of the parameters N, r and σ. The intersection of the three lines corresponds to $N = 5, r = 3, \sigma = 1$. Each line indicates the displacement of the center when varying a single parameter. Increasing the number of potential participants N shifts the center along the solid line in the direction indicated by the arrow, i.e. towards the corner $\mathbf{e}_l$. Similarly, increasing σ shifts the center upwards on the dashed line $z = \hat{z}$ and increasing r moves the center to the right, along the dash-dotted line. For $r \to 2$, the center approaches the corner $\mathbf{e}_l$.

According to numerical calculations, the time average lies on the line segment $\mathbf{Q}\mathbf{e}_l$ and converges to $\mathbf{e}_l$ as the closed orbit approaches the boundary of S_3. We can offer only a heuristic explanation of this observation: The closer the periodic orbit is to the boundary the more time it will spend near the degenerate equilibrium $\mathbf{e}_l$

(both eigenvalues zero) where motion is much slower than close to the hyperbolic equilibria $\mathbf{e}_c$ and $\mathbf{e}_d$.

Let us show how Eq. (9.4.8) is deduced by integrating Eq. (9.4.2). Remembering that, by definition, $x = f(1-z)$, and dividing both sides of Eq. (9.4.2) by $z\,(1-z^{N-1})$, we get:

$$\int_0^T \left[\sigma\,(1-z) - (r-1)\,x\right]\,dt = \int_0^T \frac{\dot{z}\,dt}{z\,(1-z^{N-1})} = p(z)\Big|_{z(0)}^{z(T)}$$

$p(z)$ being a primitive of $\left[z\left(1-z^{N-1}\right)\right]^{-1}$. Since the orbits are closed, the last term vanishes and the proportionality between $\bar{x}$ and $1-\bar{z}$, i.e. $\bar{x}+\bar{y}$ follows. The time average (9.4.9) follows in the same way after dividing Eq. (9.4.2) by $z\,(1-z)\,\left(1-z^{N-1}\right)$.

Due to the properties of the replicator equation, the time averages of the payoffs for the three different strategies are equal and reduce to the payoff of loners σ:

$$\bar{P}_c = \bar{P}_d = \bar{P}_l = \sigma.$$

Thus, in the long run, no one does better or worse than the loners.

9.5 Discussion

The oscillations, and thus the recurrent increase in cooperation, are due to the fact that a public goods game needs not always be a social dilemma. In a public goods game, those players who are defecting are always better off than those players who are cooperating. Nevertheless, if the group size S of participating players is less than the interest rate r, it pays the individual player to switch from defection to cooperation. If players have the option of an asocial 'fallback solution', they can refuse to join the public goods game. If enough players refuse to join, the group becomes so small that the game is no longer a social dilemma. But then, the higher payoff obtained by the cooperators in the public goods game causes more players to join, and larger groups of public goods players create the temptation to defect, i.e. the social dilemma. This requires $r > 2$, a condition which is similar to the condition that in the Prisoner's dilemma game, the benefit exceeds twice the cost: this condition is essential for the stability of the Pavlov strategy [115]. It may be argued that this condition can also be found in Hamilton's rule for kinship selection. Here, the cost-to-benefit ratio should exceed the degree of relatedness between donor and recipient, but under 'normal' conditions (no inbreeding, etc) this relatedness is at most 1/2.

The proposed model for an optional public goods game represents one of the rare cases where a highly non-linear system of replicator equations can be fully analysed by purely analytical means. For small interest rates, $r \leq 2$, homoclinic orbits are observed starting in and returning to $\mathbf{e}_l$, i.e. the state where no one participates in the public goods game. For $r > 2$ a fixed point occurs in the interior

of the simplex S_3. By reducing the replicator equations to a Hamiltonian system, we see that $\mathbf{Q}$ is actually a center and that in $\operatorname{int} S_3$ only closed orbits appear. From this follow various conditions on the time averages of the frequencies and payoffs of the three strategies. For example, the average ratio of cooperators and defectors corresponds to the ratio of the averages and is independent of the initial configuration and the group size N. It turns out to be impossible to increase cooperation by increasing the interest rate r – on the contrary, it favours defection and lowers $\bar{x}/\bar{y}$. In order to promote cooperation, one should rather increase the loner's payoff σ or reduce the group size N. Note that in the latter case $\bar{x}/\bar{y}$ still increases even when keeping the profits for each invested dollar constant ($r/N = const$). The fact that cooperation is favoured in smaller groups agrees with other theoretical as well as experimental results [15, 18, 100, 61].

We stress that the dynamics obtained in this simple and, we believe, natural model is highly degenerate: it has a center, an invariant of motion, a heteroclinic cycle, a nonhyperbolic fixed point, and an even number of Nash equilibria. All these properties are nongeneric under the usual assumptions. But as we show in [59], a wide variety of adaptive mechanisms, corresponding to many different types of evolutionary game dynamics, lead to persistent oscillations in the frequencies of the three strategies.

The option to drop out from a public goods game, i.e. a social and economic enterprise, avoids deadlocks in states of mutual defection and economic stalemate. As a prerequisite, the possible gain – i.e. the 'interest' r – has to be quite large. The enterprise must offer a considerable advantage. In simple societies, such situations may occur in big game hunting or in war. Small groups of volunteers are known to be efficient for difficult tasks. This must have been known to military people for ages. We only quote Marbot, an officer of Napoleon: 'To face immense perils, volunteers are infinitely preferable to bodies of men under orders.' Success attracts larger groups of participants, but growth may inherently spell decline. This mechanism leads to oscillations in the composition of the population. However, the average effect on the individual's payoff is just the same as if this possibility did not exist and all members of the population were loners.

Following the mechanism proposed in this chapter, the existence of rock-scissor-paper type of dominance and of a cyclic dynamics in optional public goods games has been experimentally investigated by Milinsky and coworkers [142]. Such experiments are performed by letting groups of first-year students interact by means of a computer (in order to maintain anonymity), according to rules of the games that are publicly explained. The rewards are actually paid at the end of the game. Milinsky and coworkers demonstrated that the dynamics predicted by the theoretical model actually takes place in such an experimental setting: as expected, in populations mainly composed by cooperators, defectors spread; in a population mainly composed by defectors, are the loners who take over; finally, when the groups of those who take part into the game are small, it is on average convenient to cooperate (Simpson's paradox) and thus the altruistic strategy gets affirmed. In their study, these authors performed a qualitative and quantitative comparison

with the model, finding that although the dynamics of the game corresponded to the predictions, thus leading to the persistence of cooperation in the population, the average frequencies and payoffs were slightly but significantly different from those predicted in the model. Indeed, people tend to be less risk-averse than one would expect from purely rational behaviour, thus suggesting that, not surprisingly, other factors play a role in the decision-making. The agreement between experimental and theoretical results is however remarkable, since the populations performing the game were extremely small and the choices of the individuals are likely to be determined by more complex rules than those used in the model. Indeed, in this chapter we have assumed infinite population size and a specific form of imitation dynamics by which the probability of switching to a strategy linearly depends on its advantage with respect to the average payoff.

The robustness of the mechanism has been moreover shown by considering different kinds of imitation dynamics (best response, where people adopt the strategy that fares better), by admitting mistakes and random choices, or by changing the topology of the interaction (individuals arranged on a lattice) [59, 155].

In the aforementioned experiment, the model has been used for the study of behavioural dynamics, that is transmitted culturally and not genetically. In this sense, it can be also used to inquire items like inspecting behaviour in minnows, that form small groups in order to get closer to their predator, a pike, and establish its degree of dangerousness. In this case, one can interpret the animals belonging to such a group as the players, with cooperators that stand closer to the predator and defectors lying back, but getting the same information. The rest of the shoal can get only second-hand notice of an imminent attack, but do not incur the risk of being eaten and can therfore be thought of as a group of loners.

However, if the replicator equation is interpreted in the traditional sense as describing the evolution of genetically determined traits under the action of natural selection, we can think of applying the results presented in this chapter also to other natural populations. Particularly suited for this kind of studies are populations of bacteria, due to their fast life cycle and to their almost exclusively clonal reproduction. An example that seem to be particularly suited is that of Pseudomonas fluorescens, where three strains can coexist: the ancestral smooth bacteria, that reproduce in the bulk of the culture medium; the wrinkly spreader, that colonises the air-liquid interface avoiding the anoxic conditions that develop in the growth medium; a cheating strain that proliferates in the biofilm created by the wrinkly spreaders without contributing to the colony building. The formation of biofilms has been experimentally studied as an example of transition from unicellular to multicellular societies [130]. However, the fact that cheaters induce the colony to collapse and thus to dive deep in the culture medium, where the ancestral smooth strain is likely to have a competitive advantage, is still to be explored and might lead to oscillations in the frequencies of the different strains.

Appendix A

English summary

COLLECTIVE DYNAMICS IN POPULATIONS WITH MICROSCOPIC VARIABILITY

The collective behaviour resulting from the interaction of individuals with similar features (molecules, cells, organisms or species) often displays a function or meaning at a higher level of description. For instance, in order for the heart to beat it is not sufficient that each single cell contracts, but the contraction of the muscle cells must occur in a coordinated manner throughout the tissue. Although not yet clearly related to a function, synchronisation of the metabolic activity of yeast cells suspensions provide a further example of a system allowing for controlled experimental investigations of how microscopic features determine population dynamics. On another level, the oscillations in the behavioural strategies induced by evolutionary or imitation dynamics also pose the problem of linking the microscopic rules to the performance of such strategies in a population.

The present thesis aims at gaining insight into how the dynamical properties at a high observation level (where the population is described by means of statistics) are related to the laws ruling the evolution and interaction of the individuals. This scope is pursued in the context of two theoretical frameworks: that of globally coupled oscillators, to which the first part of the thesis is dedicated, and that of evolutionary game theory, addressed in the second part.

When the population is composed of similar units it is often assumed that each individual can be described by the same dynamical system. In this manner, one can focus on the complexity of the collective regimes that occur due to the existence of a large number of microscopic degrees of freedom. On the other hand, diversity is characteristic of real and, notably, in biological populations. The first part of this thesis is dedicated to the development of an analytical approach for addressing the influence of disorder on the collective dynamics of globally coupled dynamical systems. This work has been inspired by the experiments on cell sus-

pensions performed at the Department of Chemistry, University of Copenhagen and developed in collaboration with Francesco d'Ovidio, Hugues Chaté and Erik Mosekilde. The primary idea is to examine to what extent one can deduce information about individual dynamics from observation of global variables.

In the second part of the thesis, I deal with populations that are divided into classes with different features (strategies), and where individuals change class according to assigned microscopic rules (defining a game). In the context of evolutionary game theory, I address a case in which players interact in groups rather than in pairs. Specifically, I provide a microscopic foundation to the dynamics of cooperation in the voluntary public goods game, widely used as a prototype for the study of social interactions. This part of the work was conducted in collaboration with Karl Sigmund, Christoph Hauert and Joseph Hofbauer at the Institute of Mathematics, University of Vienna.

Chapter 1 provides an overview on the themes addressed in the thesis and explain how the presentation is structured. In particular, it focuses on the concept of 'population' and on the two approaches for modelling population dynamics that will be adopted in this work.

The first part of the thesis is dedicated to the disorder-induced changes in the collective behaviour of dynamical systems with global strong coupling.

Chapter 2 reviews the established results on populations of globally coupled oscillators. First, it presents the collective regimes for populations composed of identical units. Then, it addresses the macroscopic dynamics of populations with microscopic disorder, introducing in particular the available results on synchronisation theory and on noise-induced coherence.

In *Chapter 3* disorder is introduced by distributing the parameters, in what is meant to model a permanent diversity among individuals belonging to the same population. I first describe the phenomena that we want to address and then introduce our theoretical approach, the order parameter expansion. This method systematically derives macroscopic equations for the effective population dynamics from the single-element dynamics and the features of the microscopic disorder. The equations of motion for few macroscopic degrees of freedom, obtained by perturbing the regime of identical synchronisation, mimic the average dynamics of the population. In the specific case of parameter mismatch studied in this and the following chapter, the diversity-induced changes in the collective behaviour are accounted for by a system of two macroscopic variables, or order parameters. In this system, the coupling constant and the variance of the parameter distribution assume naturally the role of population-level parameters, and this independently of the number of interacting individuals. Here, I perform the computation of such reduced system for general population, pointing out the closure assumptions and their limits of validity.

The proposed method is then applied in *Chapter 4* to different populations of globally and strongly coupled dynamical systems that differ in their microscopic structure. We consider here populations of limit cycle oscillators (Hopf normal

forms) with frequency mismatch, globally coupled complex Ginzburg-Landau oscillators and chaotic oscillators with time scale mismatch. We relate the mismatch-induced qualitative changes in the coherent collective dynamics to the bifurcations of the macroscopic dynamical system derived in the previous chapter. In particular, this approach allows us to determine under which conditions the collective oscillations are suppressed by the interplay between mismatch and coupling (oscillator death).

Chapter 5 considers systems where disorder is modelled by the addition of an independent stochastic term to the individual dynamical system. In particular, the presentation focuses on the collective behaviour of large populations of globally and strongly coupled noisy maps. A first phenomenological part is dedicated to the description of the noise-induced macroscopic regimes, where the average state variables displays a deterministic motion. These collective regimes can be studied by examining the structure of the macroscopic attractor, that undergoes qualitative changes as the noise intensity is varied. This part is followed by the derivation, again on the basis of an order parameter expansion technique, of systems of macroscopic equations, the closure assumption being in this case that of strong coupling. The scalar nature of the single-element dynamics permits in this case a more accurate study of the information provided by different approximation levels.

Chapter 6 demonstrates that the reduced systems derived in the previous chapter capture the hierarchical structure of the macroscopic attractor of noisy chaotic maps and describe it at different levels of detail. Their analysis reveals how the nonlinearities of each single population element interact with the properties of the noise distribution, progressively unfolding the synchronous dynamics as the noise intensity is increased. In particular, this chapter shows how the order parameter dynamics can provide an insight into the determination of the macroscopic attractor's dimensionality. As a second application of our theoretical results, we address collective noise-induced oscillations in globally coupled excitable maps and relate the deterministic macroscopic dynamics to the properties of the individual power spectra.

Chapter 7 compares the macroscopic effects of the two aforementioned sources of disorder in a population of chaotic maps. The analogies and differences in the collective regimes induced by parameter mismatch and noise are reproduced by appropriately defined order parameter expansions and related to the different statistical properties of the population. The final section, then, concludes the first part of the thesis by discussing the foreseeable applications of the theoretical results to experiments and to populations with other microscopic structures.

The second part of the thesis considers the evolutionary dynamics of behavioural traits. In this case, the population is dividend into classes, each of which composed by players behaving according to the same strategy. The relative weight of such classes changes according to rules that determine how individuals respond to a given composition of the population. A mathematical description of such a dynamics is given in evolutionary game theory by means of the so-called

replicator equation, that constitute a model both for the evolution through natural selection and for the behavioural dynamics based on imitation.

Chapter 8 introduces the basic tools of evolutionary game theory. We explain the concepts of strategy, game and the replicator equation by means of two-person symmetric one-shot games. The issue of the evolution of altruism is then addressed. We review the most important existing theories able to explain the establishment of cooperative behaviour in populations, stressing under what conditions they can be applied to biological populations. In particular, we define the public goods game and discuss reciprocity and punishment in the context of N-players games.

In Chapter 9 we develop a mean-field approach (through the formulation of the appropriate replicator equation) for N-player, public goods game. We show that while the selfish strategy is evolutionary stable if the game is compulsory, the assumption of optional participation is sufficient for the population to attain sizable levels of cooperation. The dynamics results in oscillations of the rock-scissor-paper type, leading to a so-called red queen mechanism for the evolution of the different strategies.

Appendix B

Dansk resumé

KOLLEKTIV DYNAMIK I POPULATIONER MED MIKROSKOPISK VARIABILITET

Vekselvirkningen mellem elementer (molekyler, celler, individer eller arter), der hver for sig udviser komplicerede ikke-lineære dynamiske fænomener, giver ofte anledning til meningsfyldte processor eller strukturer på at højere aggregeringsniveau. Eksempelvis afhænger hjertets udpumpning af blod til kredsløbet af en koordineret aktivitet af de myriader af muskelceller, der sidder i hjertevægen. Det er ikke nok, at muskelcellerne hver for sig trækker sig sammen.

I nyrerne kan man på tilsvarende vis iagttage, hvorledes vekselvirkningen mellem tætsiddende funktionelle enheder (nefroner) giver anledning til kollektive fænomener (synkronisering af svingningerne i blodtilstrømningen til de enkelte nefroner), som kan have afgørende betydning for den overordnede regulering af nyrernes funktion. En sådan synkronisering kan iagttages både ved normalt blodtryk, hvor der er regulære svingninger i nefronernes blodforsyning, og ved forhøjet blodtryk, hvor svingningen kan blive kaotiske. I andre tilfælde (feks. ved forskellige former for tremor) er det velkendt, at den sygelige tilstand hænger sammen med en uhensigtsmæssig synkronisering af aktiviteten hos bestemte grupper af hjerneceller, og en mulig behandling består i at ødelægge synkroniseringen ved hjælp af signaler fra en elektrode, der indplanteres i hjernen.

Kapitel 1 giver en introduktion til projektet. Jeg har taget udgangspunkt i to konkrete problemstillinger, der optræder (i) i forbindelse med fortolkningen af eksperimentelle resultater for en population af gærceller i opslemning og (ii) i forbindelse med beskrivelsen af de svingninger i strategi, der kan opstå i forbindelse med imitation og udvikling af samarbejde i økologiske og samfundsmæssige systemer. For begge problemstillinger er hovedspørgsmålet, hvorledes de mikroskopiske processer afspejles i den makroskopiske dynamik.

Under bestemte betingelser (udsultning) udviser de enkelte gærceller oscilla-

tioner i deres metabolisme. Gærcellerne vekselvirker med hinanden via de produkter de frigiver til opslemningen, og eksperimenter udført ved Institut for Kemi, Københavns Universitet har vist, at denne vekselvirkning kan give anledning til vedvarende oscillationer i opslemningens makroskopiske variable.

Som antydet ovenfor er spørgsmålet derfor, om man ved undersøgelsen af de makroskopiske oscillationer og deres respons på forskellige forstyrrelser kan udlede noget om de intercellulære vekselvirknigner og/eller om de intracellulære processer. Et eksempel på de problemer, der optræder i denne forbindelse er, at et fravær af makroskopisk observerbare oscillationer kan skyldes, enten at cellerne via deres vekselvirkning undertrykker hinandens oscillationer, eller at de oscillerende celler er ude af fase, således at oscillationerne i middel ophæver hinanden.

Det omvendte spørgsmål, om man kan beregne populationernes makroskopiske egenskaber på grundlag af de enkelte elementers dynamik og formen af deres kobling, er naturligvis også relevant. Dette spørgsmål udtrykker på mange måder den grundlæggende problemstilling inden for det relativt nye fagområde der betegnes "komplekse systemer". Ved behandlingen af disse spørgsmål er det naturligvis vigtigt at tage hensyn til de fænomener, der kan modvirke cellernes synkronisering, herunder en variation af cellernes parametre (fexs. af frekvensen af de internt genererede oscillationer) samt støjen i de cellulære processer.

I afhandlingens anden halvdel beskæftiger jeg mig med populationer, som kan opdeles i klasser med forskellige egenskaber (strategier), og hvor individerne kan skifte klasse i overensstemmelse med specifikke mikroskopiske regler. I relation til en spilteoretisk beskrivelse af imitiations- og udviklingsprocesser beskæftiger jeg mig med en situation, hvor deltagerne samarbejder i grupper. Nærmere beskrevet forsøger jeg at etablere den mikroskopiske basis for teorien om samarbejde om udnyttelsen af et fælles gode. Denne del af arbejdet er udført i sammen med Karl Sigmund m.fl. ved Institute of Mathematics, University of Vienna.

Kapitel 2 giver et overblik over de kendte resultater for populationer af globalt koblede ulineære oscillatorer. Global kobling betyder, at hver enkelt oscillator vekselvirker med alle de øvrige oscillatorer eller, anderledes udtrykt, at den enkelte oscillator vekselvirker med et middelfelt genereret af de øvrige oscillatorer. Det må betragtes som en god model af en opslemning af gærceller, når opslemningen omrøres. Den globale kobling opfattes også som en god model af visse fænomener i hjernen, idet den enkelte nervecelle typisk har kontakt til mange andre nerveceller. Kapitlet præsenterer først de kollektive områder for populationer af ens oscillatorer. Dernæst beskrives den makroskopiske dynamik for populationer med mikroskopisk uorden. I denne forbindelse skitseres bl.a. den eksisterende teori for synkronisering og for støj-genereret kohærens.

Kapitel 3 beskriver den teoretiske fremgangsmåde, som jeg har valgt at benytte i den første halvdel af rapporten. Denne fremgangsmåde, en ordensparameter udvikling, giver mulighed for på systematisk vis at udlede makroskopiske ligninger af voksende orden på grundlag af de enkelte oscillatorers dynamik og den mikroskopiske uorden. Med ganske få makroskopiske frihedsgrader kan de opstillede ligninger reproducere resultaterne af detaljerede computerberegninger af et meget stort antal koblede ulineære oscillatorer. Reelt kan de ændringer i den makroskopiske dy-

namik, som parameterforskelle mellem oscillatorerne giver anledning til, beskrives ved to makroskopiske variable. I det makroskopiske system er koblingens styrke og spredning i parametervariationen naturlige parameter. Kapitlet afsluttes med en redegørelse for metodens konsistensbetingelser og grænserne for dens anvendelsesområde.

Kapitel 4 demonstrerer den udviklede metode på forskellige populationer af globalt og stærkt koblede dynamiske systemer. Specielt analyseres populationer af regulære grænsecykel-oscillatorer, globalt koblede Ginzburg-Landau oscillatorer, og kaotiske oscillatorer med variation i den karakteristiske frekvens. Jeg viser, hvorledes de kvalitative ændringer, der optræder i den kollektive dynamik, når spredningen i oscillatorernes parameterfordeling øges, kan relateres til bifurkationer i det etablerede makroskopiske dynamiske system. Denne fremgangsmåde tillader mig bl.a. at beskrive, hvorledes de kollektive oscillationer undertrykkes gennem koblingen af oscillatorer med forskellige parametre. Specielt viser jeg, hvorledes man kan beskrive denne såkaldte oscillatordød i generelle termer, der gælder feks. for både Rössler og Lorenz oscillatorer.

Kapitel 5 beskriver populationer af koblede oscillatorer, hvor den mikroskopiske uorden optræder i form af uafhængige støjprocesser i de enkelte oscillatorer. Hovedvægten lægges her på systemer af koblede éndimensionale afbildninger. Kapitlet indledes med en fænomenologisk beskrivelse af, hvorledes den støj kan inducere områder med deterministiske makroskopisk dynamik. I denne forbindelse følger vi strukturen af den makroskopiske attraktor, når den mikroskopiske støj gradvis øges. Den fænomenologiske diskussion følges op af en ordensparameter udvikling af de makroskopiske bevægelsesligninger ved tilstedeværelsen af støj, og det vises hvorledes den éndimensionale struktur af den enkelte oscillator tillader os at beskrive den information, der opnås i forskellige udviklingsordner.

Kapitel 6 viser i detaljer, hvorledes ulineariteten i den enkelte oscillators dynamik vekselvirker med forskellige former for støj, og hvorledes ordensparameter udviklingen gradvis afslører den hierarkiske struktur af den makroskopiske attractor. I dette kapitel viser jeg også, hvorledes ordensparameter udviklingen kan give information om den makroskopiske attraktors dimension. Det er et åbent og meget kontroversielt spørgsmål i teorien for koblede ikke-lineære oscillatorer. Som en anden anvendelse af de teoretiske resultater diskuterer jeg, hvorledes støjen kan inducere kollektive oscillationer i populationer af eksciterbare afbildninger. Også her sammenholdes den makroskopiske dynamik beregnet via computersimuleringer af et stort antal oscillatorer med de teoretisk beregnede bifurkationsdiagrammer.

Kapitel 7 sammenligner den makroskopiske effekt af de to forskellige kilder til mikroskopisk uorden via parameterforskelle og støj. Kapitlet afsluttes med en beskrivelse af de mulige anvendelser af de opnåede resultater, dels i forbindelse med tolkningen af eksperimentelle resultater og dels i forbindelse med koblingen af andre typer af ikke-lineære dynamiske systemer.

Kapitel 8 har til formål at introducere nogle af de grundlæggende begreber (strategi, spil, replikatorligninger m.v.) i den spilteoretiske beskrivelse af udviklingsprocesser. I denne beskrivelse udgør de enkelte spil den mikroskopiske dynamik og udviklingsprocesserne repræsenterer den resulterende makroskopiske

dynamik. Kapitlet gennemgår også nogle af de vigtigste resultater, der er opnået i forsøg på at opstille en mikroskopisk forklaring på udviklingen af altruisme i biologiske systemer. Specielt lægger jeg vægt på at klargøre, under hvilke betingelser de forskellige resultater er opnået. Endelig defineres det såkaldte fælles-gode spil, og betydningen af gensidighed og straf i forbindelse med N-deltager spil diskuteres.

Via etableringen af en passende replikaktorligning udvikler jeg i Kapitel 9 en middelfeltsbeskrivelse af et fælles-gode spil med N deltagere. Det vises, hvorledes den selviske strategi er udviklingsmæssig stabil, så længe deltagelse i spillet er obligatorisk. Hvis en deltager imidlertid kan trække sig ud af spillet i en periode for siden at genoptage det, bliver udviklingen af et betydeligt element af samarbejde i populationen mulig.

Bibliography

[1] R. D. Alexander. *Darwinism and human affairs*. University of Washington Press, Seattle, 1979.

[2] V. Andrade, R. L. Davidchack, and Y. Lay. Noise scaling of phase synchronization of chaos. *Phys.Rev. E*, 61:3230–3233, 2000.

[3] V. S. Anishchenko (editor), A. B. Neiman, T. E. Vadivasova, L. Schimansky-Geier, and Vladimir Astakhov. *Nonlinear Dynamics of Chaotic and Stochastic Systems*. Springer, Berlin, 2002.

[4] C. Anteneodo, S. E. de S. Pinto, A. Batista, and R. L. Viana. Analytical results for coupled map lattices with long-range interactions. cond-mat/0308014.

[5] J. Ariaratnam and S. H. Strogatz. Phase diagram for the Winfree model of coupled nonlinear oscillators. *Phys. Rev. Lett.*, 86:4278–4281, 2001.

[6] D. G. Aronson, G. B. Ermentrout, and N. Kopell. Amplitude response of coupled oscillators. *Physica D*, 41:403–449, 1990.

[7] F. Atay. Distributed delays facilitate amplitude death of coupled oscillators. *Phys. Rev. Lett.*, 91:094101, 2003.

[8] F. Atay. Total and partial amplitude death in networks of diffusively coupled oscillators. *Physica D*, 183:1–18, 2003.

[9] R. Axelrod and W. D. Hamilton. The evolution of cooperation. *Science*, 211:1390, 1981.

[10] K. Bar-Eli. On the stability of coupled chemical oscillators. *Physica D*, 14:242–252, 1985.

[11] J. Batali and P. Kitcher. Evolution of altruism in optional and compulsory games. *J. theor. Biol.*, 175:161, 1995.

[12] G. Benettin, L. Galgani, A. Giorgilli, and J-M. Strelcyn. Lyapunov characteristic exponents for smooth dynamical systems and for hamiltonian systems: a method for computing all of them. part 1: Theory. *Meccanica*, page 9, 0.

[13] K. G. Binmore. *Playing fair: game theory and the social contract.* MIT Press, Cambridge, 1994.

[14] B. Blasius, A. Huppert, and L. Stone. Complex dynamics and phase synchronization in spatially extended ecological systems. *Nature*, 399:354–359, 1999.

[15] P. Bonacich, G. H. Sure, J. P. Kahan, and R. J. Meeker. Cooperation and group size in the n-person prisoner's dilemma. *J. Conflict Resolut.*, 20:687, 1976.

[16] R. Boyd, H. Gintis, S. Bowels, and P. J. Richardson. The evolution of altruistic punishment. *PNAS*, 100:3531, 2003.

[17] R. Boyd and P. J. Richardson. Punishment allows the evolution of cooperation (or anything else) in sizable groups. *Ethol. Sociobiol.*, 13:171, 1992.

[18] R. Boyd and P. J. Richerdson. The evolution of reciprocity in sizeable groups. *J. Theor. Biol.*, 132:337, 1988.

[19] J. Buceta, M. Ibañes, J. M. Sancho, and K. Lindenberg. Noise-driven mechanism for pattern formation. cond-mat/0211181.

[20] O. Carillo, M. A. Santos, J. García-Ojalvo, and J. M. Sancho. Spatial coherence resonance near pattern-forming instabilities. cond-mat/0306256.

[21] B. Cazelles, S. Bottani, and L. Stone. Unexpected coherence and conservation. *Proc. R. Soc. Lond. B*, 268:2595, 2001.

[22] M. Cencini, M. Falcioni, D. Vergni, and A. Vulpiani. Macroscopic chaos in globally coupled maps. *Physica D*, 130:58, 1999.

[23] M. Chabanol, V. Hakim, and W. Rappel. Collective chaos and noise in the globally coupled complex Ginzburg-Landau equation. *Physica D*, 103:273–293, 1997.

[24] H. Chaté. Spatiotemporal intermitttency regimes of the one-dimensional complex ginzburg-landau equation. *Nonlinearity*, 7:185, 1994.

[25] H. Chaté and P. Manneville. Evidence of collective behaviour in cellular automata. *Europhys. Lett.*, 14:409, 1991.

[26] T. Chawanya and S. Morita. On the bifurcation structure of the mean-field fluctuations in the globally coupled tent map systems. *Physica D*, 116:44–70, 1998.

[27] M. C. Ciocci, A. Litvak-Hinenzon, and H. W. Broer. Survey on dissipative kam-theory including quasi-periodic bifurcation theory based on lectures by Henk Boer. In J. Montaldi and T. Ratiu, editors, *Peyresq Lectures in Geometric Mechanics and Symmetry*, volume 1. Cambridge University Press, 2003.

[28] J. D. Crawford and K.T.R. Davies. Synchronization of globally coupled phase oscillators: singularities and scaling for general couplings. *Physica D*, 125:1–46, 1999.

[29] J. P. Crutchfield, J. D. Farmer, and B. A. Huberman. Fluctuations and simple chaotic dynamics. *Phys. Rep.*, 92:45, 1982.

[30] H. Daido. Lower critical dimension for populations of oscillators with randomly distributed frequencies: a renormalization-group analysis. *Phys. Rev. Lett.*, 61:231–234, 1988.

[31] H. Daido. Intrinsic fluctuations and a phase transition in a class of large populations of interacting oscillators. *J. Stat. Phys.*, 60:753–800, 1990.

[32] H. Daido. Order function theory of macroscopic phase-locking in globally and weakly coupled limit-cycle oscillators. *Int. of J. Bifurcation and Chaos*, 61:231–234, 1997.

[33] S. Danø. *Functional dynamics: The relations between function and dynamics studied in yeast cells and bacterial colonies.* PhD thesis, H. C. Ørsted institute, University of Copenhagen, Denmark, 2003.

[34] S. Danø, F. Hynne, S. De Monte, F. d'Ovidio, P. G. Sørensen, and H. Westerhoff. Synchronization of glycolytic oscillations in a yeast cell population. *Faraday Discuss.*, 120:261–275, 2001.

[35] S. Danø, P. G. Sørensen, and F. Hynne. Sustained oscillations in living cells. *Nature*, 402:320–322, 1999.

[36] R. M. Dawes. Social dilemmas. *Ann. Rev. Psychol.*, 31:169, 1980.

[37] S. De Monte and F. d'Ovidio. Dynamics of order parameters for globally coupled oscillators. *Europhys. Lett.*, 58:21, 2002.

[38] S. De Monte, F. d'Ovidio, H. Chaté, and E. Mosekide. Effects of microscopic disorder on the collective dynamics of globally coupled maps. in preparation.

[39] S. De Monte, F. d'Ovidio, H. Chaté, and E. Mosekide. Noise-induced macroscopic bifurcationa in globally-coupled chaotic units. *Phys. Rev. Lett.*, to appear.

[40] S. De Monte, F. d'Ovidio, and E. Mosekilde. Coherent regimes of globally coupled dynamical systems. *Phys. Rev. Lett.*, 90:054102, 2003.

[41] R. C. Desai and R. Zwanzig. Statistical mechanics of a nonlinear stochastic model. *J. Stat. Phys.*, 19:1–24, 1978.

[42] F. d'Ovidio. *Modelling biological systems with coupled oscillators.* PhD thesis, Dept. of Physics, The Technical University of Denmark, Denmark, 2002.

[43] L. A. Dugatkin. *Cooperation among animals: an evolutionary perspective.* Oxford University Press, Oxford, 1997.

[44] D. J. D. Earn, S. A. Levin, and P. Rohani. Coherence and conservation. *Science*, 290:1360–1363, 2000.

[45] G. B. Ermentrout. Oscillator death in populations of "all to all" coupled oscillators. *Physica D*, 41:219–231, 1990.

[46] G. B. Ermentrout and W. C. Troy. The uniqueness and stability of the rest state for strongly coupled oscillators. *SIAM J. Math. Anal.*, 20:1436–1446, 1989.

[47] E. Fehr and S. Gächter. Altruistic punishment in humans. *Nature*, 415:137, 2002.

[48] L. Gammaitoni, P. Hänggi, P. Jung, and F. Marchesoni. Stochastic resonance. *Rev. Mod. Phys.*, 70:223, 1998.

[49] H. Gang, T. Ditzinger, C.Z. Ning, and H. Haken. Stochastic resonance without external periodic force. *Phys. Rev. Lett.*, 71:0031, 1993.

[50] H. Gintis. Strong reciprocity and human sociality. *J. Theor. Biol.*, 206:169, 2000.

[51] L. Glass. Synchronization and rhythmic processes in physiology. *Nature*, 410:277–284, 2001.

[52] P. Grassberger and I. Procaccia. Measuring the strangeness of strange attractors. *Physica D*, 9:189, 1983.

[53] P. Hadley, M. R. Beasley, and K. Wiesenfeld. Phase locking of Josephson-junction series arrays. *Phys. Rev. B*, 38:8712–8719, 1988.

[54] H. Haken. *Synergetics, an introduction.* Springer, New York, 1977.

[55] V. Hakim and Wouter-Jan Rappel. Dynamics of globally coupled complex Ginzburg-Landau equation. *Phys. Rev. A*, 46:R7347–R7350, 2000.

[56] W. D. Hamilton. The evolution of altruistic behaviour. *Am. Nat.*, 97:354, 1963.

[57] W. D. Hamilton. *Biosocial anthropology.* Malaby, London, 1975.

[58] G. Hardin. The tragedy of the commons. *Science*, 162:1243, 1968.

[59] C. Hauert, S. De Monte, J. Hofbauer, and K. Sigmund. Volunteering as a red queen mechanism for cooperation in public goods games. *Science*, 296:1129, 2002.

[60] C. Hauert and H. G. Schuster. Effects of increasing the number of players and memory size in the iterated prisoner's dilemma: a numerical approach. *Proc. R. Soc. Lond. B*, 264:513, 1997.

[61] C. Hauert and H. G. Schuster. Extending the iterated prisoner's dilemma without synchrony. *J. Theor. Biol.*, 192:155, 1998.

[62] Y. Hayakawa and Y. Sawada. Learning-induced synchronization of a globally coupled excitable map system. *Phys. Rev. E*, 61:5091–5097, 2000.

[63] H. Hempel, L. Schimansky-Geier, and J. García-Ojalvo. Noise-sustained pulsating patterns and global oscillations in subexcitable media. *Phys. Rev. Lett.*, 82:3713, 1999.

[64] J. Hofbauer and K. Sigmund. *Evolutionary games and population dynamcis*. Cambridge Univ. Press, Cambridge, 1998.

[65] N. H. Holstein-Rathlou, K. Yip, O. V. Sosnovtseva, and E. Mosekilde. Synchronization phenomena in nephron-nephron dynamics. *Chaos*, 11:417–426, 2001.

[66] H. Hong and M.Y. Choi. Phase synchronization and noise-induced resonance in systems of coupled oscillators. *Phys. Rev. E*, 62:6462–6468, 2000.

[67] H. Hong, M.Y. Choi, K. Park, B.-G. Yoon, and K.-S. Soh. Synchronization and resonance in a driven system of coupled oscillators. *Phys. Rev. E*, 60:4014, 1999.

[68] F. Hynne, S. Danø, and P. G. Sørensen. Full-scale model of glycolysis in Saccharomyces Cerevisiae. *Biophys. Chem.*, 94:121–163, 2001.

[69] F. Hynne, P. G. Sørensen, and K. J. Nielsen. Quenching of chemical oscillations: General theory. *J. Chem. Phys.*, 92:1747, 1990.

[70] M. Ibañes, J. García-Ojalvo, R. Toral, and J.M. Sancho. Noise-induced scenario for inverted phase diagrams. *Phys. Rev. Lett.*, 87:020601, 2001.

[71] J. H. Kagel and A. E. Roth. *The handbook of experimental economics*. Princeton University Press, Princeton, 1995.

[72] K. Kaneko. Prevalence of Milnor attractors and chaotic itineracy in 'high'-dimensional dynamical systems. cond-mat/0302038.

[73] K. Kaneko. Chaotic but regular posi-nega switch among coded attractors by cluster-size variation. *Phys. Rev. Lett.*, 63:219, 1989.

[74] K. Kaneko. Clustering, coding, switching, hierarchical ordering and control in a network of chaotic elements. *Physica D*, 41:137–172, 1990.

[75] K. Kaneko. Globally coupled chaos violates the law of large numbers but not the central-limit theorem. *Phys. Rev. Lett.*, 65:1391, 1990.

[76] K. Kaneko. Mean field fluctuation of a network of chaotic elements. *Physica D*, 55:368–384, 1992.

[77] K. Kaneko. Remarks on the mean field dynamics of networks of chaotic elements. *Physica D*, 86:158, 1995.

[78] R. Kawai, X. Sailer, and L. Shimansky-Geier. Macroscopic limit cycle through noise-induced phase transition. In L. Schimansky-Geier, D. Abbott, A. Neiman, and C. Van den Breok, editors, *Proceedings of SPIE "Noise in complex systems and stochastic dynamic"*, volume 5114, 2003.

[79] B. Kerr, M.A. Riley, M.W. Feldman, and B.J.M. Bohannan. Local dispersion promotes biodiversity in real-life game of rock-paper-scissors. *Nature*, 418:171, 2002.

[80] I. Z. Kiss, J. L. Hudson, G. J. Escalera Santos, and P. Parmananda. Experiments on coherence resonance: noisy precursors to hopf bifurcations. *Phys. Rev. E*, 67:035201, 2003.

[81] I. Z. Kiss, W. Wang, and J. Hudson. Populations of coupled electrochemical scillators. *Chaos*, 12:252, 2002.

[82] I. Z. Kiss, Y. Zhai, and J. L. Hudson. Collective dynamics of chaotic chemical oscillators and the law of large numbers. *Phys. Rev. Lett.*, 88:238301, 2002.

[83] I. Z. Kiss, Y. Zhai, and J. L. Hudson. Emerging coherence in a population of chemical oscillators. *Science*, 296:1676, 2002.

[84] Y. Kuramoto. Self-entrainment of a population of coupled non-linear oscillators. In H. Araki, editor, *International Symposium on Mathematical Problems in Theoretical Physics*, volume 39 of *Lecture Notes in Physics*, pages 420–422. Springer, New York, 1975.

[85] Y. Kuramoto. *Chemical Oscillations, Waves and Turbulence*. Springer, Berlin, 1984.

[86] A. Lemaître and H. Chaté. Macroscopic model for collective behavior of chaotic map lattices. *Europhys. Lett.*, 46:565–570, 1999.

[87] A. Lemaître, H. Chaté, and P. Manneville. Cluster expansion for collective behavior in discrete-space dynamical systems. *Phys. Rev. Lett.*, 77:486–489, 1996.

[88] A. Lemaître, H. Chaté, and P. Manneville. Conditional mean field for chaotic coupled map lattices. *Europhys. Lett.*, 39:377–382, 1997.

[89] J-H Li. Simplest collective motion caused by external noise for globally coupled maps. *Physica D*, 190:129, 2004.

[90] B. Lindner, J. García-Ojalvo, and L. Schimansky-Geier A. Neiman. Effects of noise in excitable systems. *Phys. Rep.*, 392:321, 2004.

[91] Z. Liu and Y-C. Lai. Coherence resonance in coupled chaotic oscillators. *Phys. Rev. Lett.*, 86:4737, 2001.

[92] Yu. L. Maistrenko, V. L. Maistrenko, O. Popovych, and E. Mosekilde. Role of absorbing area in chaotic synchronization. *Phys. Rev. Lett.*, 80:1638, 1998.

[93] Yu. L. Maistrenko, V. L. Maistrenko, O. Popovych, and E. Mosekilde. Transverse instability and riddled basins in a system of two coupled logistic maps. *Phys. Rev. E*, 57:2713, 1998.

[94] Yu. L. Maistrenko, V. L. Maistrenko, O. Popovych, and E. Mosekilde. Desynchronization of chaos in coupled logistic maps. *Phys. Rev. E*, 60:2817–2830, 1999.

[95] S. C. Manrubia and A. S. Mikhailov. Very long transients in globally coupled maps. *Europhys. Lett.*, 50:580, 2000.

[96] A. Maritan and J.R. Banavar. Chaos, noise, and synchronization. *Phys. Rev. Lett.*, 72:1451–1454, 1994.

[97] M. S. O. Massunaga and M. Bahiana. Synchronization in large populations of limit cycle oscillators with long-range interaction. *Physica D*, 168-169:136–141, 2002.

[98] P. C. Matthews, R. E. Mirollo, and S. H. Strogatz. Dynamics of a large system of coupled nonlinear oscillators. *Physica D*, 52:293–331, 1991.

[99] P. C. Matthews and S. H. Strogatz. Phase diagram for the collective behavior of limit-cycle oscillators. *Phys. Rev. Lett.*, 65:1701–1704, 1990.

[100] M. Milinski, D. Pfluger, D. Külling, and R. Kettler. Do sticklebacks cooperate repeatedly in reciprocal pairs? *Behav. Ecol. Sociobiol.*, 27:17, 1990.

[101] M. Milinski, D. Semmann, and H.-J. Krambeck. Reputation helps solve the 'tragedy of the commons'. *Nature*, 415:424, 2002.

[102] J. Milnor. On the concept of attractor. *Commun. Math. Phys.*, 99:177, 1995.

[103] R. E. Mirollo and S. H. Strogatz. Amplitude death in an array of limit cycle oscillators. *Journ. Stat. Phys.*, 60:245–262, 1990.

[104] S. Morita and T. Chawanya. Collective motions in globally coupled tent maps with stochastic updating. *Phys. Rev. E*, 65:046201, 2002.

[105] E. Moro and A. Sánchez. Noise effects on synchronized globally coupled oscilators. *Europhys. Lett.*, 44:409–415, 1998.

[106] E. Mosekilde, Y. Maistrenko, and D. Postnov. *Chaotic Synchronization: Applications to Living Systems*. World Scientific, Singapore, 2002.

[107] N. Nakagawa and T. S. Komatsu. Collective motion occurs inevitably in a class of populations of globally coupled chaotic elements. *Phys. Rev. E*, 57:1570, 1998.

[108] N. Nakagawa and T. S. Komatzu. Confined chaotic behaviour in collective motion for populations of globally coupled chotic elements. *Phys. Rev. E*, 59:1675, 1999.

[109] Z. Néda, E. Ravasz, Y. Brechet, T. Vicsek, and A.-L. Barabási. The sound of many hands clapping. *Nature*, 403:849, 2000.

[110] Z. Néda, E. Ravasz, T. Vicsek, Y. Brechet, and A. L. Barabási. Physics of the rhythmic applause. *Phys. Rev. E*, 61:6987, 2000.

[111] A. Neiman, L. Schimansky-Geier, A. Cornell-Bell, and F. Moss. Noise-enhanced phase synchronization in excitable media. *Phys. Rev. Lett.*, 83:4896–4899, 1999.

[112] Z. Neufeld, I. Kiss, C. Zhou, and J. Kurths. Synchronization and oscillator death in oscillatory media with stirring. *Phys. Rev. Lett.*, 91:084101, 2003.

[113] S. Nichols and K. Wiesenfeld. Mutually destructive fluctuations in globally coupled arrays. *Phys. Rev. E*, 49:1865–1868, 1994.

[114] K. Nielsen, P. G. Sørensen, F. Hynne, and H.-G. Busse. Sustained oscillations in glycolysis: an experimental and theoretical study of chaotic and complex periodic behaviour and of quenching of simple oscillations. *J. Theor. Biol.*, 186:303–306, 1999.

[115] M. A. Novak and K. Sigmund. Invasion dynamics of the finitely repeated prisoner's dilemma. *Games and Economic Behavior*, 11:364, 1995.

[116] M. A. Nowak and K. Sigmund. Win-stay, lose-shift outperforms tit-for-tat. *Nature*, 364:56, 1993.

[117] J. H. Orbell and R. M. Dawes. Social welfare, cooperators' advantage, and the option of not playing the game. *American Soc. Rev.*, 58:787, 1993.

[118] G. V. Osipov, B. Hu, C. Zhou, M. V. Ivanchenko, and J. Kurths. Three types of phase synchronization in coupled chaotic oscillators. *Phys. Rev. Lett.*, 91:024101, 2003.

[119] G.V. Osipov, A. S. Pikovsky, M. G. Rosenblum, and J. Kurths. Phase synchronization effects in a lattice of nonidentical Rössler oscillators. *Phys. Rev. E*, 55:2353–2361, 1997.

[120] E. Ott. *Chaos in dynamical systems*. Cambridge University Press, 1993.

[121] E. Ott, E. D. Yorke, and J. D. Yorke. A scaling law: how an attractor's volume depends on the noise level. *Physica D*, 16:62, 1985.

[122] L. Pecora, T. L. Carroll, G. A. Johnson, and D.J Mar. Fundamentals of synchronization in chaotic systems, concepts and applications. *Chaos*, 7:520, 1997.

[123] A. Pikovsky. Comment on Chaos, noise and synchronization. *Phys. Rev. Lett.*, 73:2931, 1994.

[124] A. Pikovsky and J. Kurths. Do globally coupled maps really violate the law of large numbers? *Phys. Rev. Lett.*, 72:1644–1646, 1994.

[125] A. Pikovsky and J. Kuths. Coherence resonance in a noise-driven excitable system. *Phys. Rev. Lett.*, 78:775, 1997.

[126] A. Pikovsky and Yu. Maistrenko, editors. *Synchronization: Theory and application*, Dordrecht/Boston/London, 2003. Kuwler.

[127] A. Pikovsky, M. Rosenblum, and J. Kurths. *Synchronization-A Universal Concept in Nonlinear Science*. Cambridge University Press, Cambridge, 2001.

[128] A. Pikovsky, A. Zaikin, and M. A. de la Casa. System size resonance in coupled noisy systems and in the ising model. *Phys. Rev. Lett.*, 88:050601, 2002.

[129] A. S. Pikovsky, M. G. Rosenblum, and J. Kurths. Synchronization in a population of globally coupled chaotic oscillators. *Europhys. Lett.*, 34:165–179, 1996.

[130] P. B. Rainey and K. Rainey. Evolution of cooperation and conflict in experimental bacterial populations. *Nature*, 425:72, 2003.

[131] W. Rappel and A. Karma. Noise-induced coherence in neural networks. *Phys. Rev. Lett.*, 77:3256–3259, 1996.

[132] D. V. Ramana Reddy and A. Sen ans G. L. Johnston. Tiime delay induced death in coupled limit cycle oscillators. *Phys. Rev. Lett.*, 80:5109, 1998.

[133] M. G. Rosenblum, A. Pikovsky, and J. Kurths. Phase synchronization of chaotic oscillators. *Phys. Rev. Lett.*, 76:1804, 1996.

[134] M. G. Rosenblum, A. Pikovsky, and J. Kurths. From phase to lag synchronization in coupled chaotic oscillators. *Phys. Rev. Lett.*, 78:4193, 1997.

[135] L.L. Rubchinsky, M.M. Sushik, and G.V. Osipov. Patterns in networks of oscillators formed via synchronization and oscillator death. *Math. Comp. in Sim.*, 58:443–467, 2002.

[136] N. Rulkov. Regularization of synchronized chaotic bursts. *Phys. Rev. Lett.*, 86:183, 2001.

[137] N. F. Rulkov, M. M. Sushchik, and S. Tsimring. Generalized synchronization of chaos in directionally coupled chaotic systems. *Phys. Rev. E*, 51:980, 1995.

[138] Sakaguchi, H., Shinomoto, S., and Y. Kuramoto. Local and global self-entrainments in oscillator lattices. *Prog. Theor. Phys.*, 77:1005–1010, 1987.

[139] M. San Miguel and R. Toral. Stochastic effects in physical systems. In *Instabilities and Nonequilibrium Structures VI*. Kluwer Academic Publishers, 2000.

[140] T. C. Schelling. *Micromotives and macrobehaviour*. Norton, New York, 1978.

[141] K. Schlag. Why imitate, and if so, how? A bounded rational approach to multi-armed bandits. *J. Econ. Theor.*, 78:130, 0.

[142] D. Semmann, H-J Krambeck, and M. Milinski. Volunteering leads to rock-paper-scissor dynamics in a public goods game. *Nature*, 425:390, 2003.

[143] T. Shibata. Collective chaos, 1999. PhD. thesis, University of Tokio.

[144] T. Shibata, T. Chawanya, and K. Kaneko. Noisless collective motion out of noisy chaos. *Phys. Rev. Lett.*, 82:4424–4427, 1999.

[145] M. Shiino and M. Frankovicz. Synchronization of infinitely many coupled limit-cycle type oscillators. *Physics Letters A*, 136:103–108, 1989.

[146] T. Shimada and S. Tsukada. Periodicity manifestations in the non-locally coupled maps. *Physica D*, 168-169:126–135, 200.

[147] C. G. Shroer, E. Ott, and J. A. Yorke. Effect of noise on nonhyperbolic chaotic attractors. *Phys. Rev. Lett.*, 81:1397, 1998.

[148] B. Sinervo and C. M. Lively. The rock-paper-scissors game and the evolution of alternative male strategies. *Nature*, 380:240, 1996.

[149] J. Maynard Smith and E. Szathmáry. *The major transitions in evolution*. Freeman, Oxford, UK, 1995.

[150] Y. Soen, N. Cohen, D. Lipson, and E. Braun. Emergence of spontaneous rhythm disorders in self-assembled networks of heart cells. *Phys. Rev. Lett.*, 82:3556, 1999.

[151] H. Sompolinsky, D. Golomb, and D. Kleinfeld. Cooperative dynamics in visual processing. *Phys. Rev. A*, 43:6990–7011, 1991.

[152] O. Sosnovtseva, A.I. Fomin, D.E. Postnov, and V.S. Anishchenko. Clustering of noise-induced oscillations. *Phys. Rev. E*, 64:026204, 2001.

[153] S. H. Strogatz. From Kuramoto to Crawford: exploring the onset of synchronization in populations of coupled oscillators. *Physica D*, 143:1–20, 2000.

[154] S. H. Strogatz. *Sync: The emerging science of spontaneous order*. Hyperion, New York, 2003.

[155] G. Szabó and C. Hauert. Phase transitions and volunteering in spatial public goods games. *Phys. Rev. Lett.*, 89:118101, 2002.

[156] P. Tass, M. G. Rosenblum, J. Weule, J. Kurths, A. Pikovsky, J. Volkmann, A. Schnitzler, and H.-J. Freund. Detection of $n : m$ phase locking from noisy data: application to magnetoencelography. *Phys. Rev. Lett.*, 81:3291, 1998.

[157] J. Teramae and Y. Kuramoto. Strong desynchronizing effects of weak noise in globally coupled systems. *Phys. Rev. E*, 63:036210, 2001.

[158] B. Teusink, J. Diderich C. Larsson, P. Richard, K. van Dam, L. Gustafsson, and H. V. Westerhoff. Synchronized heat flux oscillations in yeast cell populations. *J. Biol. Chem.*, 271:24442–24448, 1996.

[159] D. Topaj, W.K. Kye, and A. Pikovsky. Transition to coherence in populations of coupled chaotic oscillators: a linear response approach. *Phys. Rev. Lett.*, 87:074101, 2001.

[160] R. Toral, C. R. Mirasso, and J. D. Gunton. System size resonance in coupled FitzHugh-Nagumo models. *Europh. Lett.*, 61:162, 2003.

[161] R. Toral, C. R. Mirasso, E. Hernández-García, and O Piro. Analytical and numerical studies of noise-induced synchronization of chaotic systems. *Chaos*, 11:665–673, 2001.

[162] R. L. Trivers. The evolution of reciprocal altruism. *Q. Rev. Biol.*, 46:35, 1971.

[163] E. Ullner, A. Zaikin, J. García-Ojalvo, and J. Kurths. Noise-induced excitability in oscillatory media. *Phys. Rev. Lett.*, 91:180601, 2003.

[164] M. Van Baalen and D. A. Rand. The unit of selection in viscous populations and the evolution of altruism. *J. Theor. Biol.*, 193:631, 1998.

[165] G. De Vries, A. Sherman, and H. Zhu. Diffusively coupled bursters: effects of cell heterogeneity. *Bull. Math. Biol.*, 60:1167–1200, 1998.

[166] W. Wang, I. Z. Kiss, and J. L. Hudson. Experiments on arrays of globally coupled chaotic electrochemical oscillators: synchronization and clustering. *Chaos*, 10:248, 2000.

[167] J. W. Weibull. *Evolutionary Game Theory*. MIT Press, Cambridge, Mass., 1995.

[168] N. Wiener. *Cybernetics, 2nd Edition*. MIT Press, Cambridge MA, 1961.

[169] K. Wiesenfeld. Amplification by globally coupled arrays: Coherence and symmetry. *Phys. Rev. A*, 44:3543–3551, 1991.

[170] K. Wiesenfeld, P. Colet, and S. H. Strogatz. Synchronization transitions in a disordered Josephson series array. *Phys. Rev. Lett.*, 76:404–407, 1999.

[171] D. S. Wilson. Structured demes and the evolution of group advantagous traits. *Am. Nat.*, 111:157, 1977.

[172] D. S. Wilson and E. Sober. Reintroducing group selection to the human behavioral sciences. *Behav. Brain Sci.*, 17:585, 1994.

[173] A. T. Winfree. Biological rhythms and the behavior of populations of coupled oscillators. *J. Theor. Biol.*, 16:15–42, 1967.

[174] A. T. Winfree. *The Geometry of Biological Time*. Springer, New York, 1980.

[175] A. T. Winfree. *The Geometry of Biological Time, 2nd edition*. Springer, New York, 2001.

[176] J. Wolf and R. Heinrich. Effect of cellular interaction on glycolytic oscillations in yeast: a theoretical investigation. *Biochem. J.*, 345:321–334, 2000.

[177] Y. Yamaguchi and H. Shimizu. Theory of self-synchronization in the presence of native frequency distribution and external noise. *Physica D*, 11:212–226, 1984.

[178] M. A. Zaks, A. B. Neiman, S. Feisel, and L. Schimansky-Geier. Noise-controlled oscillations and their bifurcations in coupled phase oscillators. *Phys. Rev. E*, 68:0066206, 2003.

[179] M. A. Zaks, E-H. Park, M. G. Rosenblum, and J. Kurths. Alternating locking ratios in imperfect phase synchronization. *Phys. Rev. Lett.*, 82:4228, 1999.

[180] D. Zanette and A. S. Mikhailov. Dynamical clustering in large populations of Rössler oscillators under the action of noise. *Phys. Rev. E*, 62:R7571–R7574, 2000.

[181] Y. Zhai, I. Z. Kiss, and J. L. Hudson. Amplitude death through a hopf bifurcation in coupled electrochemical oscillators: Experiments and simulations. *Phys. Rev. E*, 69:026208, 2004.

[182] C. Zhou, J. Kurths, I.Z. Kiss, and J.L. Hudson. Noise-enhanced phase synchronization of chaotic oscillators. *Phys. Rev. Lett.*, 89:014101, 2002.

[183] C. Zhou, J. Kurths, Z. Neufeld, and I. Kiss. Noise-sustained coherent oscillations of excitable media in a chaotic flow. *Phys. Rev. Lett.*, 91:150601, 2003.

Index